SCUOLA NORMALE SUPERIORE

CLASSE DI SCIENZE MATEMATICHE E NATURALI

CORSO DI PERFEZIONAMENTO IN NEUROBIOLOGIA

Tesi di Perfezionamento

Understanding Pain Construction from Nociception through a Novel Mutation in Nerve Growth Factor

Candidato

Giovanna Testa

Relatori

Prof. Antonino Cattaneo

Prof.ssa Simona Capsoni

CONTENTS

ABSTRACT

Pain is an important physiological function, whose primary role is to preserve an organism's integrity. Disruption of the nociception transduction chain results in the inability to perceive pain. Among these "painlessness" pathologies, Hereditary Sensory and Autonomic Neuropathy type V (HSAN V) is caused by the 661C>T transition in the *ngf* gene, resulting in the R100W missense mutation in mature Nerve Growth Factor (NGF), in keeping with the key role of this neurotrophin in the development of nociceptors and in their function in the adult . Homozygous HSAN V patients display indifference to noxious stimuli but, no cognitive deficits. In contrast, heterozygous carriers do not show an overt clinical phenotype and have been identified only through pedigree and genetic screening. Considering the particular features of HSAN V patients, I hypothesized that the R100W mutation might cause a dissociation between the actions of NGF on the central and peripheral nervous systems. To test this hypothesis and understand the mechanisms underlying the HSAN V phenotype, I generated a transgenic mouse line harboring the human 661C>T mutation in the human *ngf* gene. Homozygous $NGF^{R100W/R100W}$ mice were born normal, but failed to reach the first month of age. This early lethality could be due to reduced NGF bioavailability and, indeed, was rescued by continuous treatment, during development and the early postnatal life, with wild type NGF. In contrast, heterozygous $NGF^{R100W/m}$ mice grew normally but displayed impaired nociception, despite Dorsal Root Ganglia (DRGs) neurons being morphologically normal. On the other hand, skin innervation was reduced. The NGF^{R100W} protein showed reduced capability to activate pain-specific signalling, paralleling its reduced ability to induce mechanical allodynia. Surprisingly, $NGF^{R100W/m}$ mice, unlike heterozygous $mNGF^{+/-}$ mice, showed no learning nor memory deficits, despite a reduction in secretion and brain levels of NGF. These results prove the hypothesized dissociation between the peripheral and central actions of NGF, prompting me to investigate if the R100W mutation might affect brain elaboration of pain. To address this issue, I used the fear conditioning test and found that $NGF^{R100W/m}$ mice, despite normal nociceptive responses to a painful conditioning stimulus, showed a deficit in learned fear. Strikingly, their innate fear responses were normal. This was accompanied by a reduced activation of brain regions involved in pain processing and in the generation of task-related motor responses. I also found a decreased density of CGRP-positive fibers in the amygdala, which can provide a mechanistic explanation of the reduced fear response. On the other hand, the expression of endogenous analgesic peptides, namely β-endorphin and

oxytocin, was decreased in $NGF^{R100W/m}$ mice, suggesting a different set point of the homeostatic pain/analgesia system, as a consequence of a prolonged reduction of afferent pain signals. Consistent with these findings in mice, data collected in humans showed that heterozygous R100W carriers, despite having a normal pain threshold, had a decreased urgency to react to a painful stimulus, along with impaired ability to integrate sensory information with behavioral task requirements. Functional magnetic resonance imaging (fMRI) revealed, in accordance with mouse data, an altered processing of painful stimuli in brain areas involved in pain processing. These findings demonstrate an uncoupling of nociceptive signals from their central elaboration, leading to altered interpretation and meaning attributed to painful stimuli in human HSAN V carriers and heterozygous $NGF^{R100W/m}$ mice.

In addition to clarify the role of NGF in transduction of nociceptive inputs, these data also demonstrate that NGF is at the center of a regulation system linking peripheral nociception to the brain processes responsible for constructing painful perceptions and pain-related memories. Moreover, the peculiar effects of NGF^{R100W} could be exploited to open new avenues for treating conditions of chronic pain.

1. INTRODUCTION

1.1 The concept of "nociception"

1.1.1 Defining pain, the first step in understanding nociception

What is pain?

Researchers working on pain admit their difficulty when trying to define pain or refuse to come up with a simple definition.

In his physiology book published in 1900, Charles Sherrington defined pain as "*the psychical adjunct of a protective reflex*". His definition proposed an important separation between the protective reflex component and the sensory perception of pain (Sherrington, 1906). We generally define pain as the protective reflex that involves also a psychical adjunct, but the two processes are separate. Protective reflexes are present in all animals and were defined by Sherrington as the neural processes serving nociception (Sherrington, 1906). This last term refers to the process by which the nervous system detects and transmits injury-related information; it does not imply conscious perception of pain. On the other hand, the "psychical adjunct" term refers to a mental process of pain perception that depends on our social, religious and scientific beliefs. But what is the nature of this psychical adjunct?

In 1909, James MacKenzie defined pain as "*a disagreeable sensation which everyone has experienced and which we all recognize*". Later, Thomas Lewis wrote: "*pain is known to us by experience and described by illustration*". Both Lewis and MacKenzie thought that the only way to assess pain is through communication with other human beings.

However, Sherrington's definition is applicable only to "good pain", i.e., the pain that protects us from injury. Pain can be considered an alarm system, as Descartes first described it in the *Traité de l'Homme*, published in 1664, in which pain is represented as a line that links the stimulus – fire – with the brain (**Fig.1.1**).

Figure 1.1 Pain as an alarm system. The picture is from Descartes' *Traité de l'Homme*, (published in 1664, adapted from Cervero, Understanding Pain, MIT Press, 2012).

Descartes's vision of pain has been very influential on modern pain research. He proposed that fire excites the terminations of sensory fibers in the foot and that this information is transmitted to the brain, where an alarm is triggered in the form of an unpleasant sensation of pain. Thus, a "sensor" (or better, a "nociceptor") pulls the cord and the pain bell rings in the brain.

In addition to good pain that is helpful and protective, an "evil pain" exists, that is, pain associated with disease. An example is the "phantom limb syndrome", characterized by feeling pain sensations in a limb that no longer exists as a result of amputation. Similarly, chronic pain, which has no biological value as it persists after the nociceptive stimulus and beyond normal tissue healing time.

Is pain different from the five senses? Aristotle, in his *De Anima*, regarded as senses only the perceptions that could be associated with a specific sense organ. According to him, pain is not linked to a particular sense organ that gives us information regarding the external world, but is associated with an extreme stimulation of any other sense. Aristotle did not focus on the sensory and protective aspects of pain, concentrating instead on the emotional and behavioral components of pain and pleasure; indeed, he wrote "*we measure our actions by the rule of pleasure and pain"*. He considered pleasure and pain as engines of all our action and he called them "*the passions of the soul*". The Aristotelian view of pain, as a behavioral drive triggered by extreme stimulation of any sense organ, is very different from Descartes's idea of an alarm signal (Cervero, 2012). Actually, current knowledge of pain mechanisms is a synthesis of these two theories: pain is indeed a powerful alarm signal that protects us, but pain is also a passion of our soul, an emotion that drives our behavior, and in some cases a destructive curse. Pain is a conscious experience, an

interpretation of the nociceptive input influenced by memories, emotional, pathological, cognitive and genetic factors. Pain is not related linearly to the nociceptive input, neither it is simply connected to vital protective functions. This is particularly true in the chronic pain state.

Pain is, therefore, a highly subjective experience, as illustrated by the accepted definition given from the International Association for the Study of Pain (Treede, 2018) "*an unpleasant sensory and emotional experience associated with actual or potential tissue damage, or described in terms of such damage*". This definition covers all the various aspects of pain.

1.1.2 Theories on pain perception

The dawn of the 17th century saw the postulation of four major theories to describe the perception of pain: specificity, intensity, pattern and gate control theories.

Intensity theory defines pain as a sensory experience occurring when a stimulus is stronger than usual (Moayedi and Davis, 2013). This theory has been ruled out by evidence for specialization of primary sensory neurons. In addition, the pattern theory, proposed by Weddell and Sinclair, posited that the response to stimuli is produced by impulses travelling in various spatio-temporal patterns, with no dedicated transmission pathways. The pain, according to the pattern theory, is produced by an intense stimulation of non-specific fibers. This theory ignored the specialized properties of fibers, such as the threshold to different stimulus intensities; for this reason it was criticized by scientists.

On the contrary, the specificity theory postulated that dedicated pathways carry specific stimuli. For example, noxious stimuli are carried to the brain by pain-sensing afferents (later named nociceptors), while non noxious stimuli are encoded by mechanoreceptors. A representation of these connections had already been elaborated by René Descartes. This theory was further supported by the identification of cutaneous organs, such as the Meissner and Pacinian corpuscles, or Merkel cells.

Finally, the Gate Control theory of pain (GCT), proposed by Wall and Melzach in 1965, is based on the presence of gates in dorsal horn of the spinal cord, which are composed of inhibitory neurons that receive afferents from A and C fibers. According to this theory, noxious stimuli, carried by pain transducing fibers, open the gate, inhibiting the interneurons and leading to pain perception, whereas the A fibers excite the interneurons, thus suppressing the output of the projection neurons (Melzack and Wall, 1965). Interestingly,

the existence of a gate between the brain and nerves, open by ‹*A sensory cue driven by nerves, "tubular structures"*›, had also been postulated by Descartes in 1664 (Perl, 2007).

1.1.3 Measuring Pain

Many physicians and insurance companies would like to have an instrument, a *dolorimeter*, to accurately measure if a person is in pain, and how much of it he or she feels. Indeed, we have thermometers and sphygmomanometers to measure signs of disease, but no devices to quantify the level of pain.

One of the tools that partially accomplish this goal is the *visual analogue scale* (VAS), that is a continuous scale comprised of a horizontal (HVAS) or vertical (VVAS) line, usually 10 centimeters long. The clinician simply asks the patient to rate the pain, with 0 meaning no pain and 10 meaning the worst pain imaginable. Another tool, developed by Ronald Melzack, is the McGill Pain Questionnaire (Melzack, 1975), that is based on the selection by the patient of the adjectives that best describe his or her pain. For instance, inflammatory pain is often described as pulsating and neuropathic pain as burning. Thus, both the VAS and the McGill Pain Questionnaire are based on patients' verbal reports.

In the 20th century, thanks to introduction of bioelectrical signal recordings, it was possible to show that an electrical stimulus in the nerve evoked a series of electrical waves. Using a cathode-ray oscilloscope, Hebert Gasser and Joseph Erlanger recorded electrical changes of nerve potential. This technique allowed them to describe the compound action potential of peripheral nerves, i.e., an electrical signal that was generated by the summation of the action potentials of the single fibers composing the nerve (Raju, 1999). In accordance with the latency of appearance of the compound potential with respect to the stimulus, the fibers were named A, for the fastest, and C, for the slowest type.

A further development of this approach, is the recording of electrical signals generated by the brain when the subject experiences a specific pain condition. This can be achieved by using the electroencephalogram to sample the electrical activity of different brain sites (with good spatial specificity), and can be coupled to stimulation of the body periphery (e.g., the skin of a limb) to measure the corresponding "evoked potential" (Chen and Rappelsberger, 1994; Ploner et al., 2017). It should be noted, however, that these electrophysiological recordings often do not allow to discriminate between a deficit caused by abnormal pain perception or by other underlying neurological diseases.

Brain imaging, namely functional Magnetic Resonance Imaging (*fMRI*), allows to analyze brain activation during pain or emotional states associated with pain condition (Valet et al., 2004). The ultimate purpose of these studies is to assess objectively, by looking a brain map, if a person is in pain, and how strong his or her pain sensation is (Morton et al., 2016).

Studying pain is difficult due to the wide variety of factors (context, cognitive condition, mood etc.) that influence this perception. However, substantial help can come from the development of experimental paradigms based on measuring spontaneous and evoked pain behaviors in animal models that clearly reproduce specific acute and chronic human pain conditions (Schwei et al., 1999; Blackburn-Munro, 2004). These models can also take into account the genetic background, gender and age of the animal, thus leading to results that can be translated to the human context (Mogil and Belknap, 1997). These studies allow, for instance, to understand how nociceptors react to various forms of stimulation and how the brain responds to a pain- producing process and to identify the molecular mechanisms involved in the pain reaction.

1.2 Sensory transduction in pain

1.2.1 Primary sensory neurons, the first step in nociception

The cell bodies of primary afferent nociceptive fibers are located within the Dorsal Root Ganglia (DRGs). These cells are pseudo-unipolar neurons containing one process branching into different target regions (e.g., a specific skin receptive field), and an axon terminating in specific laminae of the spinal cord. Sensory neurons are, generally, electrically silent and transmit action potentials only upon stimulation. Indeed, their activity does not *per se* lead to pain perception. This requires peripheral information to reach higher center and normally depends on the frequency of action potentials in primary afferents, on temporal summation of pre- and postsynaptic signals, and is modulated by central influences.

Sensory neurons are classified into Aβ, Aδ and C-fibers, according to the propagation speed of impulses. The speed of transmission depends from the diameter of axons and on their myelination (Zotterman, 1939). Aβ fibers are thickly myelinated and have a fast conduction velocity (16-100 m/s). Aδ-fibers (diameter 1-5 µm) are also myelinated and have a conduction velocity of 5-30 m/s. C-fibers have a small diameter (0.2-1.5 µm) and unmyelinated axons, bundled in fascicles surrounded by Schwann cells. They have a conduction velocity of 0.4-1.5 m/s. In addition, electrophysiological studies based on mechanical

stimulation of DRG neurons, have shown the existence of low-threshold and high-threshold sensory neurons (Iggo, 1985). Almost all Aβ-fibers and subsets of Aδ and C-fibers show low mechanical threshold to stimulation with von-Frey filaments, suggesting a role in detecting innocuous mechanical stimuli, whereas most Aδ and C-fibers have high mechanical threshold and respond to noxious mechanical or thermal stimuli (Zotterman, 1939; Koerber and Woodbury, 2002; Zimmermann et al., 2009).

Generally, A-fibers mediate the initial pain sensation, that is described as lancinating; the following, longer lasting pain is caused by the activation of C fibers (**Fig.1.2**). In correlation with the corresponding conduction velocities, these pain sensations are often referred to as "fast" and "slow".

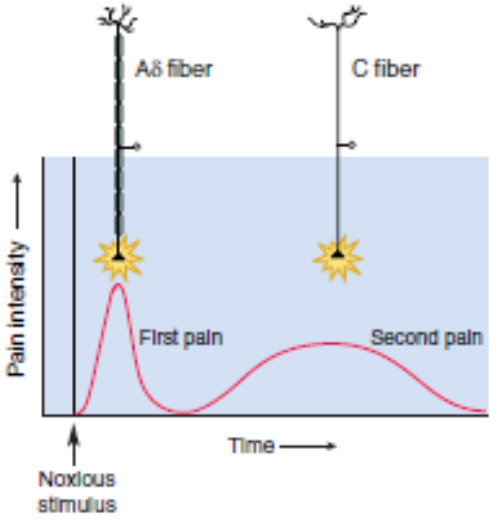

Figure 1.2 First and second pain (adapted from (Bear, Neuroscience, IV edition, Wolters Kluwer, 2015).

1.2.2 Development of primary sensory neurons

Sensory neurons originate from trunk neural crest cells (NCCs) and their neurogenesis occurs in waves. The first wave is characterized by migration of neural crest cells that form large-diameter touch and movement neurons The second wave occurs after DRGs coalesce, producing small nociceptive, as well as large touch and movement neurons. A third wave of neurogenesis generates primarily nociceptive (expressing the TrkA receptor) neurons from neural crest-derived boundary cap cells (Maro et al., 2004). The first two waves of NCC differentiation are regulated by *Neurogenin 1* (*Ngn1*) (Ma et al., 1999) and *Neurogenin 2* (*Ngn2*) (Fode et al., 1998). Indeed, analyses of individual *Ngn1* and *Ngn2* mouse mutant embryos show that *Ngn2* is expressed in early migratory NCCs, whereas *Ngn1* by coalesced DRGs (Ma et

al., 1999; Marmigere and Ernfors, 2007). *Ngn1* seems to play an important role in the formation of small-diameter nociceptive ($TrkA^+$) neurons and a minor involvement in the formation of large-diameter mechanoceptive ($TrkB^+$) and proprioceptive ($TrkC^+$) neurons. In contrast, *Ngn2* plays a transient role in the formation of large-diameter mechanoceptive ($TrkB^+$) and proprioceptive ($TrkC^+$) neurons. Furthermore, $Ngn2^+$ cells contribute to a small fraction of nociceptive ($TrkA^+$) neurons (Zirlinger et al., 2002). During development, many factors influence the early stage of DRG differentiation. One of these is the POU-domain transcription factor *Brn3a*, that is expressed in differentiating sensory neurons and is important for the correct development and/or survival of proprioceptive, nociceptive and mechanoceptive neurons (McEvilly et al., 1996). Brn3a binds to regulatory elements of the *ntrk1* gene, which encodes for the Nerve Growth Factor (NGF) receptor TrkA (Ma et al., 2003) and is expressed in all nociceptors during development. The expression of TrkA requires another transcription factor, *Klf7* (Lei et al., 2005). After neurogenesis has completed, most DRG neurons maintain the expression of TrkA, become responsive to NGF (White et al., 1996), and some of them start to express Calcitonin Gene-Related Peptide (CGRP). A distinct, albeit small, population of $TrkA^-$ neurons expresses the Ret receptor as early as E14; these $TrkA^-/Ret^+$ cells are classified as the "early Ret" population (Molliver et al., 1997). The majority of Ret^+ neurons, however, emerge from $TrkA^+$ neurons during the late embryonic period. This population of neurons begins to express Ret around E16 and gradually extinguishes TrkA expression after birth, and is classified as the "nonpeptidergic" population (Molliver and Snider, 1997). Thus, although TrkA is expressed in most DRG neurons during development, only a subset of them, $CGRP^+$ peptidergic neurons, continue to express TrkA into adulthood. The segregation of peptidergic and nonpeptidergic populations is complete between 2 and 3 weeks after birth.

Another factor that plays an essential role in the differentiation of nonpeptidergic neurons is *Runx1* (Chen et al., 2006; Kramer et al., 2006; Yoshikawa et al., 2007). NGF regulates expression of *Runx1* that, in turn, supports the expression of Ret and of a large cohort of genes characteristic of nonpeptidergic neurons (Luo et al., 2007). In this population of neurons, the transcription factor *MafA* plays an important role in the differentiation of low-threshold mechanoreceptors (LTMR). At birth, the *MafA/Ret* population can be divided into three subsets: Ret^+, $Ret^+/TrkB^+$ and $Ret^+/TrkC^+$. The specification of subsets of TrkB-expressing mechanoreceptor neurons requires *Shox2* (Scott et al., 2011), that drives the development of

early $Ret^+/TrkB^+$ population into two different subtypes: (i) neurons expressing $TrkB^+$ only become D-hair mechanoreceptor; (ii) the Ret^+ and $TrkB^+$ subset of neurons might represent a class of Aβ-LTMRs, such as Meissner's corpuscles afferents (Abdo et al., 2011).

Finally, the maintenance of $TrkC^+$ proprioceptive neurons depends on expression of *Runx3* around embryonic day E14.5 (Levanon et al., 2002). The $Ret^+/TrkC^+$ subset of neurons is required for the development of Pacinian corpuscles and circumferential endings (Bai et al., 2015) (**Fig.1.3**).

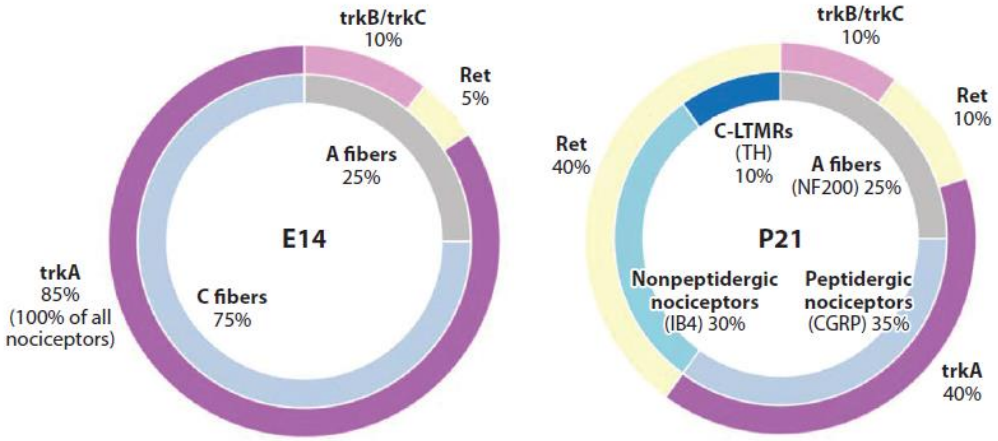

Figure 1.3 DRG neuron subtypes and receptor distribution in embryonic (*left*) and early postnatal (*right*) development (adapted from Denk et al., 2017).

Each subset of sensory neurons displays different combinations of receptors and ion channels. Usoskin and colleagues (Usoskin et al., 2015) (**Fig.1.4**), using single-cell sequencing technique, characterized the marker profile of each subset of sensory neurons. This study supports the idea that specific sensation modalities can be either generated through the selective activation of a specific neuronal type, or encoded by the integration of the activities of different neuronal types. This latter hypothesis suggests the intriguing idea that a combinatorial code might be present, in close analogy to other sensory modalities, such as color vision or olfaction.

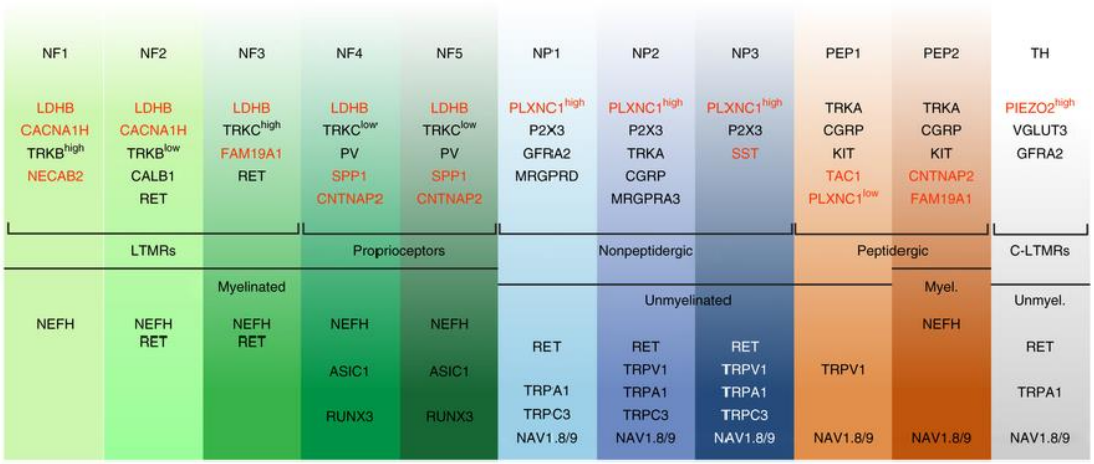

Figure 1.4 Classification of sensory neuron subtypes (adapted from Usoskin et al., 2015).

1.2.3 Mechanoreceptors

Mechanoreceptors represent a class of neurons that detect innocuous mechanical forces acting on tissues and do not elicit the sensation of pain. Mechanoception is the basis of physiological processes such as the senses of touch, balance and hearing. Mechanoreceptors can be classified according the threshold as low-threshold mechanoreceptors (LTMRs) and high-threshold mechanoreceptors (HTMRs) and are distributed in the skin, tendons, muscles, joints and viscera.

LTMRs include Aδ D-hair fibers that innervate hairs in the skin and detect hair movement, and Aβ-fibers that terminate on Merkel cells, Pacinian corpuscles and hair follicles and detect texture, vibration and light pressure. Finally, LTMRs also include C-fibers that terminate as free nerve endings and are associated with "tickling" sensations. LTMRs are activated by innocuous mechanical stimuli and they can be distinguished in rapidly adapting (RA; 3-6ms) and slowly adapting (SA; 200-300 ms) based on their rates of adaptation to sustained mechanical stimuli (Mountcastle, 1957). Meissner corpuscles, Pacinian corpuscles and longitudinal lanceolate endings are RA mechanoreceptors (Iggo and Ogawa, 1977), whereas, Merkel discs are the principal SA mechanoreceptors in rodents and monkeys (Pare et al., 2002).

The mammalian skin comprises hairy and glabrous parts. Glabrous skin is found on the hands and feet; it is specialized for discriminative touch, thus allowing object recognition, along with feedback to the central nervous system to mediate proper grip control, reaching and locomotion. The glabrous skin contains four types of LTMRs with fast conduction velocity (Aβ LTMRs), with distinct terminal morphologies and tuning properties

I. Aβ SA1-LTMRs innervate Merkel cells in the basal epidermis and report the static nature of touch stimuli;

II. Aβ SA2-LTMRs terminate in Ruffini corpuscles in the dermis and are sensitive to skin stretch;

III. Aβ RA1-LTMRs innervate Meissner corpuscles in dermal papillae and are sensitive to movement across the skin;

IV. Aβ RA2-LTMRs terminate in Pacinian corpuscles deep in dermis and are tuned to high-frequency vibration. (**Fig1.5**).

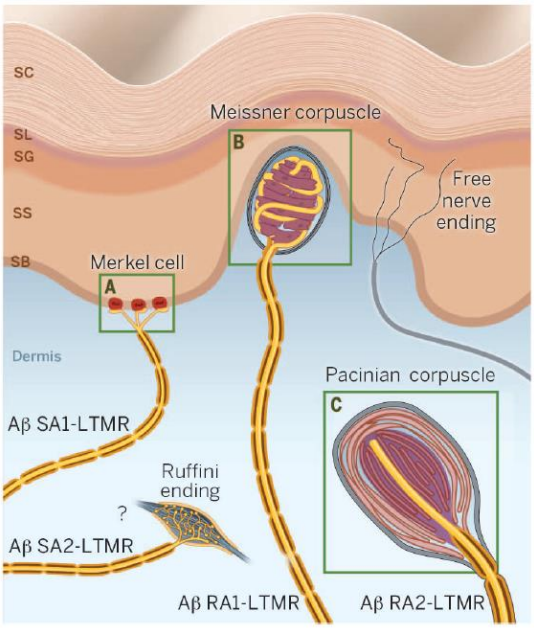

Figure 1.5 LTMR innervation of glabrous skin (adapted from Zimmerman et al., 2014).

Hairy skin covers more than 90% of the body surface and has a discriminative touch role, albeit with lower spatial acuity respect to glabrous skin. Hairy skin is composed of three main hair follicle subtypes: guard, zig-zag and awl/auchene which are innervated by different combination of LTMRs. Zig-Zag hair follicles are the most numerous and are associated with C and Aδ-LTMR lanceolate endings. The Awl/auchene type is innervated by C-, Aδ- and Aβ-LTMR longitudinal lanceolate endings, representing roughly 23% of total follicles. Guard hairs represent around 1% of the follicles and receive Aβ SA1-LTMR longitudinal lanceolate endings that innervate structures named “touch domes” (Li et al., 2011).

Different combinations of LTMRs, in association with hair follicles, confer a high specialization and complexity to hairy skin. In general, mechanotransduction influences many important processes, such as

embryonic development and sensory perception, and deregulation of mechanosensitivity, for example an aberrant sensitivity to mechanical forces, leads to peripheral neuropathies.

1.2.4 Proprioceptors

While cutaneous mechanoreceptors provide information about external stimuli, another important class of receptors is formed by proprioceptors ("receptors for self"), providing information about mechanical forces arising within the body itself, in particular from the musculoskeletal system. Proprioceptors have large diameter (13-20 μm), myelinated axons and support a conduction velocity of 80-120 m/s; their main role is to give detailed and continuous information about the position of the limbs and other body parts in space. Similar to other sensory neurons, the cell bodies of proprioceptors are located in DRGs, and their projections reach lamina V of the dorsal horn of the spinal cord. In particular, group Ia and II afferent axons innervate muscle spindles, whereas group Ib afferents innervate Golgi tendon organs. Group Ia afferent axons centrally ramify in the intermediate zone of the spinal cord and terminate in the motor nucleus of the ventral horn, whereas group Ib and II afferent axons project to the intermediate zone.

Strong evidence suggests that, in DRG neurons, the transcription factor Runx3 is necessary for the specification of $TrkC^+$ proprioceptive neurons (Inoue et al., 2002; Levanon et al., 2002; Chen et al., 2006). Indeed, in Runx3-deficient mice, $TrkC^+$ neurons of DRGs do not survive enough to extend their axons to reach target cells, resulting in lack of connectivity and ataxia (Inoue et al., 2002; Levanon et al., 2002). Moreover, a mutation in the *Egr3* (early growth response 3) gene impairs group Ia/II muscle spindle activation, eliminating one class of proprioceptive feedback. Analysis of walking and swimming behaviors in this mouse model demonstrated that altered proprioceptive sensory feedback causes degradation of the correct locomotor pattern (Akay et al., 2014).

1.2.5 Nociceptors: sensing pain

The word nociceptor comes from the Latin *nocere* "to hurt". Nociceptors are thus defined as sensors that respond to types and intensities of energy that can produce possible damage and injury to the body. Activation of nociceptors can lead to a conscious experience of pain: nociception and pain are vital for our life, but they do not always come together. Pain is the feeling, or the perception of sensations arising from a part of the body; whereas, nociception is the sensory process providing signals that trigger pain.

Nociceptors are present in many organs of the periphery, including skin, bone, muscle, most internal organs, blood vessels and heart. They are absent from the brain, except for the meninges. Unlike the specialized somatosensory receptors for light touch and pressure, most of these nociceptors are simply the free nerve ending that Von Frey first described as the pain sensors (Norrsell et al., 1999). Anatomically, nociceptive afferents form extensive free nerve endings in the epidermis of the hairy and the glabrous skin (Zylka et al., 2005) and terminate within lamina I and outer lamina II (II_0) of the spinal cord. Two classes of nociceptors exist: Aδ and C nociceptors. The first class is represented by medium-diameter myelinated (Aδ) afferents that mediate acute pain. The second class includes small-diameter unmyelinated C-fibers that convey slow pain. Most of the C-fiber nociceptors (>70%) respond to all forms of stimuli – thermal, mechanical and chemical – and are therefore called polymodal (Woolf and Ma, 2007; Basbaum et al., 2009). C-fiber nociceptors are heterogeneous, with subsets that respond preferentially to heat or chemical, rather than mechanical stimulation. For example, nociceptors that express the heat-gated ion channel TRPV1 are required for noxious thermoception and chemoception of capsaicin (Caterina et al., 1997). On the other hand, noxious cold is detected by nociceptors that express the ion channel TRPM8 (Knowlton et al., 2013). Finally, nociceptors that express the Mas-related G protein-coupled receptor D, Mrgprd, (they constitute > 90% of all nonpeptidergic $IB4^+$ fibers) innervate the epidermis and respond to "blunt" mechanical stimuli, such as a von Frey hair (Cavanaugh et al., 2009). In this paper, Cavanaugh et al. explored the behavioral consequences of selectively ablating two non-overlapping populations of nociceptors: one required for the response to mechanical, but not to thermal stimuli ($Mrgprd^+$ cells), the other, conversely, required for thermal, but not for mechanical sensitivity ($TRPV1^+$ cells) (**Fig.1.6)**. They also showed that combined elimination of these two populations yields an additive phenotype with no further behavioral deficits.

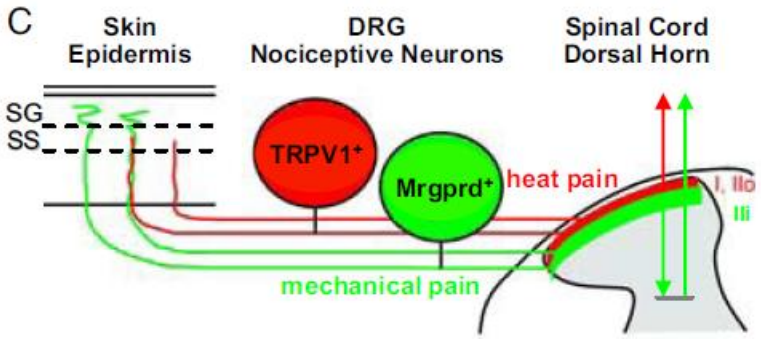

Figure 1.6 Schematic illustrating modality-specific contributions of $Mrgprd^+$ and $TRPV1^+$ fibers to behavior and their different termination zones in the epidermis and spinal cord (adapted from Cavanaugh et al., 2009).

Nociceptors can also be classified in two groups, according to the expression of specific markers (Luo et al., 2007):

- nonpeptidergic; this population comprises approximately 60% of total DRG neurons, expresses the tyrosine kinase receptor Ret, the signaling receptor for the Glial-Derived Neurotrophic Factor (GDNF) family of ligands (GFLs) (Dong et al., 2001); these neurons bind the IB4 lectin from *Griffonia simplicifolia*;
- peptidergic; this population expresses TrkA and respond to the calcitonin gene-related peptide (CGRP).

These two populations show different patterns of peripheral and central axonal projections. For instance, the peripheral axons of peptidergic neurons innervate the stratum spinosum (SS) of glabrous skin, while the central axons terminate in laminae I and II_0 of the dorsal horn of the spinal cord. Peripheral projection of Ret^+ neurons innervate the superficial stratum granulosum (SG) of the epidermis, while the central axons terminate in inner lamina II (II_i) of the spinal cord.

1.2.6 Signal transduction in nociception

All sensory systems have the role of converting environmental stimuli into electro-chemical signals. In the case of vision or olfaction, primary sensory neurons detect one type of stimulus (light or chemical odorants). Nociception, to this regard, is unique because individual primary sensory neurons have the ability to detect a wide range of stimulus modalities. A variety of noxious stimuli depolarize the bare nerve endings of afferent axons and generate action potentials that are propagated centrally. How is this achieved? The membrane of the nociceptor contains different types of receptors that transduce thermal, mechanical, or chemical stimuli into a change of membrane potential.

1.2.7 TRP Ion Channels and thermosensation

Transient receptor potential (TRP) channels make up the most abundant family of ion channels expressed in sensory neurons of mammals (Damann et al., 2008) (**Fig.1.7**).

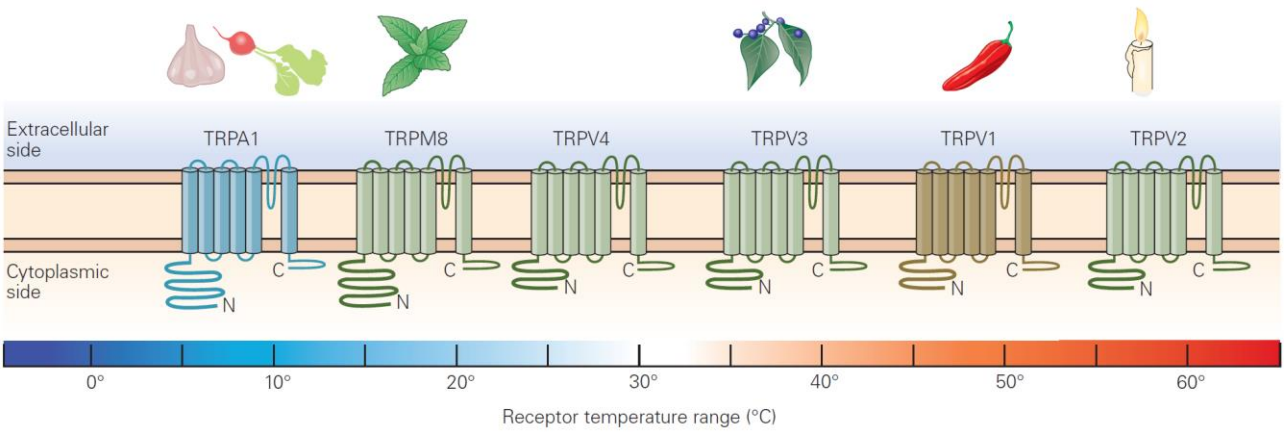

Figure 1.7 Classification of different TRP channels expressed by dorsal root ganglion neurons, their temperature response profiles, and some of their agonists (from Kandel, Principles of Neural Science, V edition, McG-H, 2013).

The prototype of this receptor-channel family, TRPV1, also known as VR1, was isolated in 1997 (Caterina et al., 1997). The TRPV1 transcript and protein were found to be maximally expressed in sensory neurons (Caterina et al., 1997) with predominant expression in small-diameter cell bodies, most of which give rise to unmyelinated C-fibers. TRPV1 immunoreactivity was also detected peripherally, in the sciatic nerve, and on the central terminals of afferents fibers projecting to the superficial layers of the spinal cord and the trigeminal nucleus caudalis.

This receptor is activated by elevated temperature and mediates the pain-producing actions of capsaicin, the active ingredient of hot peppers (Caterina and Julius, 2001). Interestingly, exposure of nociceptors to capsaicin not only causes their excitation, but also induces release of inflammatory mediators, such as substance P (SP) and CGRP. Another important aspect of the actions of capsaicin is that prolonged exposure of nociceptors to this chemical renders them insensitive to it, a process known as desensitization. VR1 is a non-selective plasma-membrane cation channel possessing a very steep temperature dependence and a thermal activation threshold of ~ 43°C. Thus, a correlation between heat and capsaicin sensitivity (i.e., chemoception) exists, arising from the existence of a common transducer. Additional studies demonstrated that TRPV1 could be activated at room temperature when proton concentration was increased (pH<6), indicating that protons directly gate TRPV1 (Tominaga et al., 2003). Although capsaicin is an exogenous ligand for TRPV1, it is possible that there endogenous, pain-producing, chemical regulators for this channel are also present. Indeed, different endogenous ligands have been identified, including anandamide,

lipoxygenase products and *N*-arachidonoyl dopamine. These lipid compounds have been proposed to modulate TRPV1 activity *in vivo* (Rosenbaum and Simon, 2007). Another endogenous ligand capable of activating TRPV1 is oxytocin. In a recent paper, it has been reported that oxytocin-induced suppression of nociceptor might be achieved directly through potentiation of the pain receptor TRPV1, causing analgesia upon desensitization of the channel (Nersesyan et al., 2017). Among inflammatory mediators, bradykinin and NGF, via bradykinin receptor and TrkA respectively, cause sensitization of TRPV1 and consequent hypersensitivity (Chuang et al., 2001). In particular, NGF, acting on TrkA, activates a signaling in which PI3 kinase plays an important early role, with Src kinase as the downstream element that binds to and phosphorylates TRPV1. These events induce insertion of further TRPV1 channel units into the surface membrane and explain the rapid sensitizing actions of NGF (Zhang et al., 2005). TRPV1 appears to be the principal molecule by which inflammatory mediators enhance sensitivity to heat, as demonstrated by absence of heat hyperalgesia in TRPV1 knockout mice (Caterina et al., 2000; Davis et al., 2000).

A protein with 49% identity to TRPV1 was isolated and called vanilloid-receptor-like protein 1 (VRL-1), and later renamed TRPV2 (Caterina and Julius, 2001). The TRPV2 channel is expressed predominantly in Aδ fiber terminals and is activated by very high temperature, with a threshold of ~ 52°C. Thus, temperatures activating TRPV2 are more harmful to the body than those activating TRPV1. Therefore, expression of TRPV2 in myelinated sensory fibers seems reasonable, because Aδ fibers transmit nociceptive information much faster than C-fibers, which express TRPV1.

TRPV3 and TRPV4 have been found to be activated by warm temperatures, ~ 34-38°C for TRPV3 and ~ 27-35°C for TRPV4, and to be expressed in multiple tissues, among others, sensory and hypothalamic neurons and keratinocytes (Guler et al., 2002; Peier et al., 2002; Smith et al., 2002; Xu et al., 2002). TRPV3 is also activated by the plant-derived compound camphor. TRPV3 knockout mice show impairment in thermotaxis behavior (Moqrich et al., 2005). The authors also observed behavioral deficits to acute thermal stimulation at temperatures > 50°C in TRPV3$^{-/-}$ mice, which indicates that TRPV3 and TRPV1 have overlapping functions in noxious thermoception.

In addition, defects in the expression of TRPV4 affect the detection of noxious mechanical stimuli and cause mechanical hypersensitivity to pain (Suzuki et al., 2003; Alessandri-Haber et al., 2004).

The cooling sensation of menthol, a chemical found in mint, is transduced by a nonselective cation channel, called TRPM8 (McKemy et al., 2002; Peier et al., 2002). TRPM8 is also activated by a temperature of ~25-28°C and by other cooling compounds, such as menthone, eucalyptol and icilin (Bandell et al., 2004). TRPM8 is expressed in a subset of DRG neurons that can be classified as small-diameter C-fiber (McKemy et al., 2002; Peier et al., 2002) and is not coexpressed with TRPV1.

TRPA1, is considered to be distantly related to TRP's, and is activated by cold with a lower threshold than TRPM8, namely 17°C; for this reason, it is involved in cold nociception. Unlike TRPM8, TRPA1 is specifically expressed in a subset of sensory neurons that express the markers CGRP and substance P (Story et al., 2003). Furthermore, TRPA1 is also coexpressed with TRPV1, raising the possibility that TRPA1 and TRPV1 mediate the function of a specific class of polymodal nociceptors. This coexpression might also explain the paradoxical hot sensation experience when one is exposed to a very cold stimulus.

1.2.8 Acid-Sensing Ion Channels

Acid-Sensing Ion Channels (ASICs) form a large family of proton-gated ion channels consisting of 7 isoforms, most of which are expressed in mechanosensory and nociceptive neurons (Lingueglia, 2007; Moshourab et al., 2013). The expression of ASIC proteins in sensory neurons is controlled also by neurotrophin signaling. Pro inflammatory mediators, including NGF, are involved in upregulating ASICs mRNA and NGF increases the density of -mediated currents in cultured sensory neurons (Mamet et al., 2002). The ASIC3 channel is specifically expressed in nociceptors and is well represented in fibers that innervate skeletal and cardiac muscle. ASIC3 channels are thought to be responsible for muscle or cardiac pain that results from changes in pH associated with ischemia. By contrast, genetic studies indicate that the products of the *MDEG* (*BNC1*) gene (ASIC2a and 2b) do not contribute to acid sensitivity in most non-cardiac nociceptors (Price et al., 2000).

Histological experiments have shown expression of ASIC2 and 3 in lanceolate endings and nerves innervating Meissner's corpuscles and Merkel cells. Gene knockout experiments in rodents show defects in mechanical sensitivities and firing properties of RA-fibers in the skin, while the behavioral effects have been very modest (Price et al., 2001; Mogil et al., 2005), thereby questioning the direct effects of ASICs in mechanotransduction of noxious stimuli.

1.2.9 Na^+ channels

The graded potentials arising from receptors in the distal branches of nociceptive fibers must be transformed into action potentials, in order to be conveyed to synapses in the dorsal horn of the spinal cord. Voltage-gated sodium channels are critical in this process, and one specific subtype of sodium channel (SCN9A, also called $Na_v1.7$) appears to be important for the transmission of nociceptive information. Altered activity of $Na_v1.7$ is responsible for a variety of human pain disorders. One class of mutations inactivates the channel and results in a complete inability to sense pain (Cox et al., 2006; Goldberg et al., 2007). $Na_v1.7$ deletion in mouse leads to increased transcription of *Penk* mRNA, along with higher levels of enkephalins in sensory neurons. The analgesia associated with loss of $Na_v1.7$ in both humans and mice is reversed by the opioid antagonist naloxone (Minett et al., 2015). A second class of mutations in the SCN9A gene changes the inactivation kinetics of this channel: individuals with these mutations exhibit an inherited condition called paroxysmal extreme pain disorder, characterized by rectal, ocular and submandibular pain (Drenth and Waxman, 2007).

The $Na_v1.8$ gene is expressed by most nociceptors (Renganathan et al., 2001), and is the main effector through which activation of TrkA influences the electrophysiological properties of rapidly conducting nociceptors (Fang et al., 2005). $Na_v1.8$ has been associated with the transmission of thermal information, in particular in the perception of cold pain. The $Na_v1.8$-null mice show minimal responses to noxious cold and mechanical stimulation at low temperatures (Zimmermann et al., 2007).

1.2.10 Piezo2

Piezo2 is expressed in around 20% of all DRG cells, most of which are $NF200^+$ mechanosensors, with some nociceptors included (Coste et al., 2010). Piezo2 has been established as the most prominent mechanically gated ion channel in mice (Ranade et al., 2014). Moreover, mice with conditional knockout of Piezo2 in proprioceptive neurons, obtained with expression of Cre recombinase under the control of the Parvalbumin or HoxB8 promoters, show profound defects in body movements and abnormal limb positions (Woo et al., 2015). In a recent paper, a class of nociceptors, “silent nociceptors”, characterized by the expression of the nicotinic acetylcholine receptor subunit alpha-3 (CHRNA3) was studied. They are insensitive to mechanical stimuli in basal conditions, but become sensitized when exposed to NGF, which exerts a

proinflammatory action. This process is specifically mediated by Piezo2 (Prato et al., 2017). Prato et al. hypothesized that Piezo2 is normally inhibited by a yet unknown protein, whereas sensitization is triggered by another unknown protein that is upregulated by NGF.

1.3 Nociceptive pathways

1.3.1 The first synapse in nociception

Incoming stimuli from the skin and viscera terminate in specific laminae of the dorsal horn of the spinal cord. When the axons of DRG neurons reach the dorsal horn, they branch into ascending and descending collaterals, forming the dorsolateral tract of Lissauer. At this level, axons typically run up and down for one or two spinal cord segments, before they penetrate the gray matter of the dorsal horn. Within the dorsal horn, the axons emit branches that contact neurons located in laminae I, II and V (**Fig.1.8**).

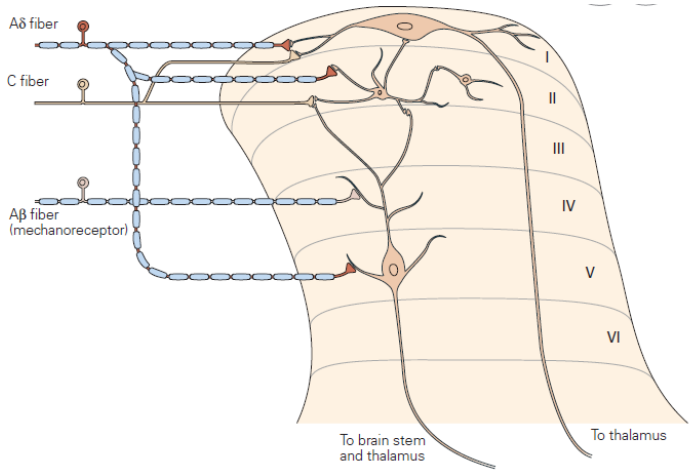

Figure 1.8 Neurons in lamina I of the dorsal horn receive direct input from Aδ fibers and both direct and indirect inputs from unmyelinated fibers, via interneurons in lamina II. Lamina V neurons receive input from myelinated fibers (Aβ) of mechanoreceptors, as well as inputs from nociceptive afferent fibers (adapted from Kandel, Principles of Neural Science V edition, McG-H, 2013).

The dorsal horn, in general, can be divided into six laminae as described by Rexed using Nissl staining of spinal cord section (Light and Perl, 1979). Laminae consist of combination of neurons can be distinguished by projections, morphology and different gene expression. Lamina I receives input from Aδ and C- afferents about pain and heat/cold sensing. Because they respond selectively to noxious stimulation, they have been called *nociception-specific neurons* and project to higher brain centers. Another class of neurons of lamina I respond to both innocuous and noxious mechanical stimuli and are termed *wide-dynamic-range neurons*.

Lamina II, or substantia gelatinosa, can be divided into two regions: lamina II_0 and II_i, which receive inputs from neurons carrying information about pain and touch, respectively. Lamina III and IV contain both interneurons and supraspinal projection neurons. Many of these neurons receive inputs from Aβ fibers that respond to innocuous cutaneous stimuli, such as deflection of hairs. Lamina V contains neurons that respond to a wide variety of noxious stimuli (inputs from Aβ and Aδ fibers) and send signals to the brain stem and thalamus. Neurons in lamina V also receive input from nociceptors in visceral tissues and are involved in the phenomenon called "referred pain", a condition in which pain from injury to visceral tissues is perceived as originating from a region on the body surface. Neurons in lamina VI receive inputs from large-diameter fibers of muscle and joints. These neurons are activated by innocuous joint movement and for this reason do not contribute to pain information.

Nearly 30-40 % of interneurons in the dorsal horn are inhibitory and use GABA and/or glycine as neurotransmitters, whereas the remaining interneurons are excitatory and use glutamate. In response to tissue injury or after intense stimulation of peripheral terminals, sensory neurons activate neurons in the dorsal horn releasing neuropeptides, such as Substance P, CGRP, somatostatin and galanin, in order to transmit the nociceptive information.

1.3.2 Distinct, Parallel Pathways for Pain

The classic pain pathway consists of a three-neuron chain that transmits pain information from the periphery to the cerebral cortex. As already mentioned, the first-order neuron has its cell body in the dorsal root ganglion and two axons, one extending distally to the tissue, while the other extending to the dorsal horn of the spinal cord, with a "T-pseudounipolar" morphology. At this level, this axon synapses with the second-order neuron which, in turn, crosses the spinal cord through the anterior white commissure and ascends to reach the brain. Second-order fibers in the anterolateral system (the neural pathway that conveys pain and temperature information) project to a number of different structures in the brainstem and forebrain. These central destinations are likely to mediate different aspects of the sensory and behavioral response to a painful stimulus. The pain pathway is now understood to be a dual system at each level and the sensation of pain that reaches the brain is composed of sensory-discriminative and affective-motivational components (**Fig.1.9**). The sensory-discriminative aspects of pain include quality, location and intensity processing

(Andersson et al., 1997) while the affective-emotional component of pain comprises the unpleasant character of pain perception (Craig, 2003b). The cognitive component is also involved in attention, anticipation and memory of past experiences and this component can interact with components from other senses giving rise to modulation of pain (Valet et al., 2004).

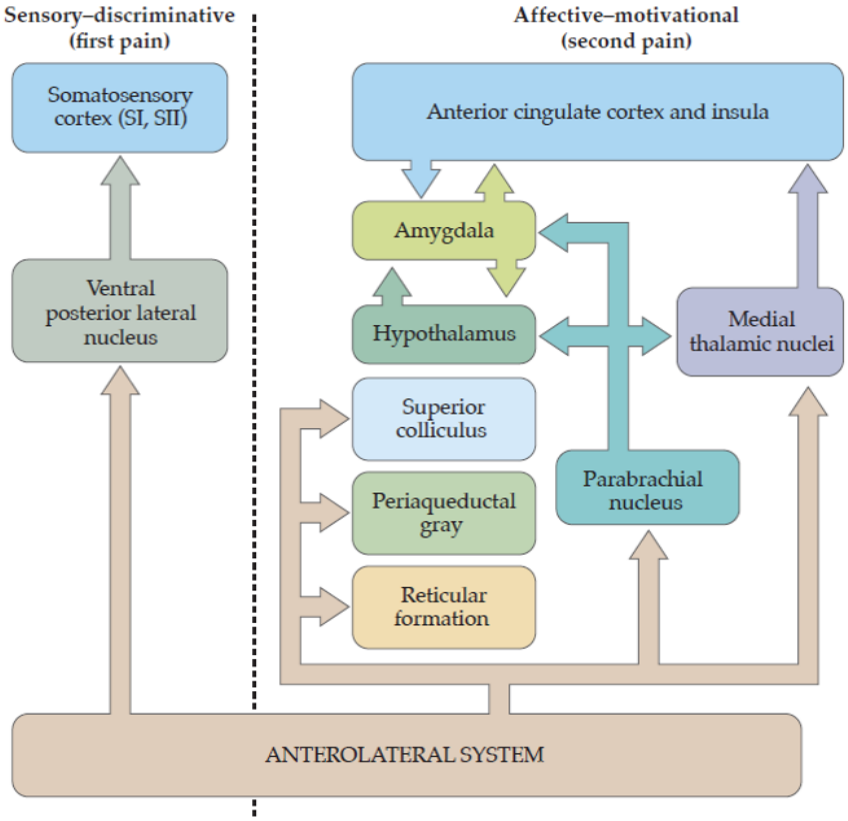

Figure 1.9 Different brain region involved in parallel aspects of pain experience. (adapted from Purves, Neuroscience, VI edition, Sinauer Associates, Sunderland, 2017).

1.3.3 Ascending pathways and processing of nociceptive information

The central processing of pain information is mediated by five major ascending pathways: the spinothalamic, spinoreticular, spinomesencephalic, cervicothalamic and spinohypothalamic tracts.

- The *spinothalamic tract* is the most prominent ascending pathway in the spinal cord. It includes the axons of nociception-specific and wide-dynamic-range neurons in lamina I and V of the dorsal horn. These axons cross the midline of the spinal cord and ascend within the anterolateral white matter before reaching the thalamic nuclei. This tract has an important role in the transmission of nociceptive information; electrical stimulation of the tract is sufficient to induce painful sensations, whereas lesions of this tract can result in a marked reduction of pain sensation. By virtue of an

anatomical connection between the sensory thalamus and the lateral amygdala (LA) (Nader et al., 2000), the spino-thalamic pathway has been studied as a potential circuit for transmission of the unconditioned stimulus (US) during Pavlovian fear conditioning (Shi and Davis, 1999).

- The *spinomesencephalic* (or *spinoparabrachial*) *tract* contains the axons of projection neurons in laminae I and V. This tract projects, within the anterolateral quadrant of the spinal cord, to the mesencephalic reticular formation and periaqueductal gray matter (PAG). Information transmitted along this tract is important because it contributes to the affective aspects of pain. Axons of this tract also project to the parabrachial nucleus (PBN) that, in turn, projects to the amygdala. Anterograde tracing studies show that most spinal lamina I projection neurons send their axons to the external lateral subdivision of the PBN (PBel) (Al-Khater and Todd, 2009), and field potential recordings *in vivo* show that noxious stimuli in the periphery induce activity in PBel (Bester et al., 2000) and central nucleus of amygdala (CeAl) (Neugebauer and Li, 2002). Consistently, neuronal tracing studies reveal that PBel neurons directly innervate CeAl neurons (Lu et al., 2015), and electrical stimulation of axonal fibers from the PBel induce depolarization of neurons in the CeAl (Jhamandas et al., 1996). In a recent paper, Sung Han and colleagues pursued the idea that the parabrachio-amygdaloid pathway is responsible for relaying the US pain signal to the CeAl during fear conditioning. Indeed, their findings reveal that CGRP neurons in the PBel convey the US signal to the CeAl, and that CGRPR neurons are the functional US-recipient neurons in the CeAl, thus beingcritical for establishing a threat memory (Sung et al., 2018).
- The *spinoreticular tract* is composed of the axons of projection neurons in laminae VII and VIII. This tract ascends within the anterolateral quadrant of the spinal cord, with no decussation, and terminates in the reticular formation and thalamus.
- The *cervicothalamic tract* contains the axons of neurons of the lateral cervical nucleus, which receives input from neurons in laminae III and IV of the dorsal horn. Many axons of this tract cross the midline and ascend within the medial lemniscus of the brain stem, terminating in midbrain nuclei and in the ventroposterior lateral and posteromedial nuclei of the thalamus. Other neurons in laminae III and IV send their axons directly into the dorsal columns, terminating in the cuneate and gracile nuclei of the medulla.

- The *spinohypothalamic tract* is composed of the axons of neurons from in laminae I, V and VII of the dorsal horn. This tract projects to the hypothalamic nuclei that serve as autonomic control centers involved in the neuroendocrine and cardiovascular responses that accompany pain.

Spinal projections to the brainstem are important for integrating nociceptive activity with homeostatic and autonomic processes, in addition to providing a means to indirectly convey nociceptive information to forebrain regions after brainstem processing. The capacity of projections to the brainstem to influence both spinal and forebrain activity suggests that these pathways play a direct role in affecting the pain experience.

1.3.4 Focus on the main brain areas involved in pain processing

The thalamus is one of the supra-spinal structures that receives projections from multiple ascending pathways. This structure is not only a relay centre, but is involved in processing nociceptive information before transmitting the information to various parts of the cortex (Craig, 2003a). The thalamus consists of several groups of nuclei and each group has important functions in the sensory discriminative and affective motivational components of pain. Spinal neurons of lamina I project extensively to the posterior group and to the ventrobasal complex that, in turn, project to the primary somatosensory cortex. This pathway constitutes the lateral pain system, that plays an important role in the discrimination of stimuli (Andersson et al., 1997). The affective-motivational aspect of pain is mediated by the medial pain pathway, which includes the intralaminar thalamic nuclei (Royce et al., 1989) and the posterior part of ventromedial thalamic nuclei that project to the somatosensory cortex and limbic structures (Shyu et al., 2004). For example, the amygdalostriatal area (AStr) is the main target of CGRP-projections from the posterior thalamus: this pathway plays an important role for the effects of CGRP, including induction of fear-like behaviors and antinociceptive effects (D'Hanis et al., 2007).

Given the complexity of the pain sensation, many cortical areas are involved in nociceptive processing, contributing to a large brain network together with the thalamus. For this reason, Melzack described a pain "*neuromatrix*", now known as the "*pain matrix*" or "*pain signature*" (Melzack, 1999). Activation of *signature* pain matrix has been related to perceived pain intensity, within and between individuals, and is now considered a candidate biomarker for drug discovery (Huang et al., 2013; Wager et al., 2013). Because different brain regions play a more or less active role in influencing pain perception, what comprises the

pain matrix is not unequivocally defined. However, there is a consensus in including at the core of the matrix: primary and secondary somatosensory cortices, insular cortex (IC), anterior cingulate cortex (ACC) and prefrontal cortex, amygdala, thalamus and periaqueductal gray (PAG) (Tracey and Mantyh, 2007). These areas and structures transmit and decode nociceptive information, amplify or reduce the pain sensation, and mediate the expression of defensive behavior.

The amygdala appears as a key component of the pain matrix (Simons et al., 2014). The amygdala provides an emotional value – either positive or negative – to sensory information, leading to adaptive behavioral and affective responses and contributing to emotional memory. This role has been extensively studied using the fear conditioning paradigm (LeDoux, 2000, 2014). The amygdala is, indeed, known to be a critical brain region that integrates the sensory (i.e., the conditioning stimulus, CS) and pain (i.e., the unconditioning stimulus, US) signals to create a memory that will produce a threat response when the subject will be re-exposed to the CS alone (Gross and Canteras, 2012). The amygdala is a heterogeneous structure of the limbic system, composed of a dozen of nuclei clustered in four groups: superficial, basolateral, central and medial (Sah et al., 2003). The lateral-basolateral nuclei (LA-BLA) form the input region for sensory (e.g. nociceptive) information from thalamus and cortical areas such as ACC, insula and other medial prefrontal cortical areas (Price, 2000). The BLA contains neurons that respond preferably to noxious stimuli and their projections reach the medial prefrontal cortex (mPFC), providing emotion- and value-based information to guide executive functions, such as decision-making and behavior control (McGaugh, 2004; Laviolette and Grace, 2006). The result of information processing in the LA-BLA network is transmitted to the central nucleus of the amygdala (CeA). The latter is also termed the “nociceptive amygdala” and it is considered as the output nucleus of the amygdaloid complex, projecting to pain modulatory systems through forebrain and brainstem connections (Price, 2000; Neugebauer et al., 2004). The CeA is also connected to rostral forebrain structures, such as the lateral part of the bed nucleus of the stria terminalis (BSTL) and the dorsal part of the substantia innominata. The CeA is strongly implicated in fear. Indeed, peptidergic CeA projection neurons are innervated by CGRP containing terminals from the parabrachial area and stimulate freezing behavior, whereas their silencing reduces conditioned fear responses (Campos et al., 2018). Neuronal activity changes in the amygdala are not simply a reflection of continued input from spinal cord

and other regions, but can also result from an imbalance between excitatory and inhibitory synaptic mechanisms internal to amygdala circuits.

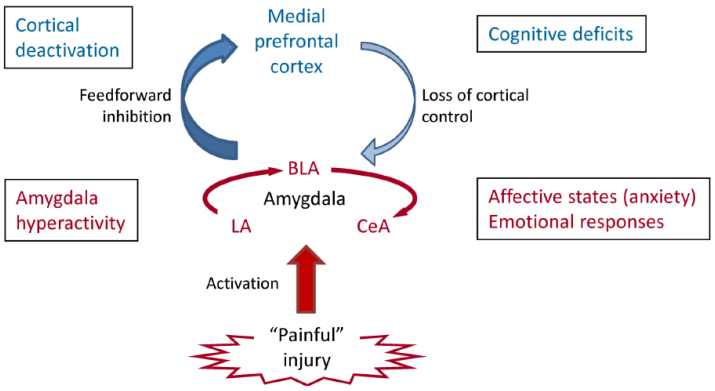

Figure 1.10 Role of amygdala in pain. Pain-producing events generate hyperactivity in the lateral, basolateral and central nuclei (LA, BLA, CeA) of the amygdala network .This can account for the emotional-affective aspects of pain. Output from BLA deactivates the medial prefrontal cortex through feedforward inhibition;its alterations can play a role in cognitive deficits such as impaired decision making. Decreased medial prefrontal cortical output to the amygdala allows the uncontrolled persistence of amygdala hyperactivity, hence contributing to the persistence of pain **(**adapted from Neugebauer et al., 2004).

The insular cortex (IC) comprehends three areas conserved across different species (i.e., mouse, man and non-human Primates): the granular, dysgranular and agranular subdivisions, according to their cytoarchitecture. The granular IC has a classical six-layered structure; in the dysgranular IC, layer 4 becomes thinner and, finally, the agranular IC is tri-laminar, completely lacking layer 4. The IC is strongly connected with an extensive network of cortical and subcortical regions, by which it mediates interoception. Indeed, the IC receives from the thalamus sensory inputs regarding information about the outer environment (somatosensory, olfactory, gustatory and visual information) and the inside of the body (interoceptive information). In this regard, the insula exerts an important control on autonomic functions, for instance, regulation of the heartbeat, blood pressure, or gastric motility. It performs these actions through direct projections to the hypothalamic area, the parabrachial nucleus and the nucleus of the solitary tract (Craig, 2002). In addition, the insula presents reciprocal connections with the limbic system and, using the Pavlovian fear-conditioning paradigm, fear-induced activation of the insular cortex across different species, from mouse to human was demonstrated (Kusumoto-Yoshida et al., 2015). Lesions or pharmacological inhibition of different insula regions show a significant role for insula in the consolidation of learned fear;

patients with large lesions in this area show deficits in the emotional dimension of pain (Berthier et al., 1988). In particular, patients with insular lesion can recognize pain but cannot attribute negative valence to adverse experiences as a result of lack an appropriate emotional response (Gogolla, 2017), which may indicate a role for the insula in mediating empathy. Electrical stimulation of several sites within the posterior insula has been shown to evoke unpleasant pain, often with distinct sensory qualities (Ostrowsky et al., 2002). These observations suggest that this area can be involved in creating both sensory and affective components of pain.

Different studies indicate that the ACC is a critical brain region involved in pain processing (Shackman et al., 2011) and its role is more complex than IC. ACC neurons appear to integrate multiple sensory inputs and their neuronal activity is associated with escape responses, attention and response selection in monkeys (Isomura and Takada, 2004). In particular, ACC activity increases during escape from a noxious thermal stimulus but not non-noxious chemical, mechanical and thermal stimuli (Koyama et al., 2001; Iwata et al., 2005). More in detail, neurons of the rostral anterior cingulate motor area appear to be involved in the selection of appropriate motor responses, as well as in the planning of movements (Isomura and Takada, 2004). Some neurons in ACC respond during cues that signal impending pain, participating in the anticipatory response to pain, whereas others respond to anticipation of a reward. This is consistent with neuroimaging studies showing that the rostral ACC is activated during anticipation of pain (Koyama et al., 2001). Besides, the ACC coordinates input from the insula and medial thalamic nuclei with prefrontal cortex and limbic structures, in order to provide an appropriate motor response, or action planning. Furthermore, activity in the ACC, but not in the somatosensory cortex, is closely related to the affective features of pain, such as subjective feelings of unpleasantness (Rainville et al., 1997; Tang et al., 2005). Studies in mouse models, using fear conditioning, show a role of ACC in memory recall, rather than memory formation (Frankland et al., 2004), providing evidence that the ACC is preferentially involved in the recall of remote fear memories.

1.3.5 Modulation of pain

The ability of higher centers of the brain to modulate the transmission of nociceptive information had been yet demonstrated in the 1900s by Sherrington, who showed that nociceptive reflexes were enhanced

following spinal cord transection (Sherrington, 1906). Over the last decades, increasing evidence shows that a variety of brain regions are involved in the descending modulation of pain and, in particular, that PAG plays an important role. Electrical stimulation of PAG, the area of the midbrain that surrounds the third ventricle and the cerebral aqueduct, causes a profound analgesia (Cui et al., 1999). Some neurons of PAG project directly to the dorsal horn of the spinal cord; others project to the rostroventral medulla (RVM), including serotoninergic neurons in the nucleus raphe magnus. The axons of these serotoninergic neurons project through the dorsal region of the lateral funiculus to the spinal cord, where they form inhibitory connections with neurons in laminae I, II and V of the dorsal horn. The noradrenergic system is the second major monoaminergic descending system, originated in the locus coeruleus and other nuclei of the medulla and pons. Both these pathways inhibit the activity of nociceptive neurons through direct connections as well as through interneurons in the superficial layers of the dorsal horn.

In addition to the noradrenergic and serotoninergic systems, the cholinergic system also has an impact on nociception and pain modulation. In the CNS, Acetylcholine (ACh) acts as a neurotransmitter and neuromodulator upon release from cholinergic projections and interneurons in both brain and spinal cord. In particular, cholinergic neurons in the striatum appear to modulate pain perception, via the interconnectivity between cholinergic and dopaminergic signaling. For instance, a decrease in dopamine signaling, particularly via D2 receptors, has been found to be related to a decrease in pain tolerance in chronic states such as back pain and Parkinson's disease (Hagelberg et al., 2004; Martikainen et al., 2015). In this process, the cholinergic system acts as a modulator of dopamine release: a decrease in cholinergic input determines a 90% reduction in dopamine release (Naser and Kuner, 2018).

The descending modulatory circuit is an “opioid-sensitive” circuit. Indeed, opioids, either endogenous or exogenous, are critical for the modulation of pain behavior and antinociception. Opioid peptides and their receptors are expressed in the nociceptive neural circuitry. To date, four different opioid receptors (Mu (μ), Delta (δ), Kappa (κ), opioid receptor like-1 (ORL1) have been characterized at cellular, molecular and pharmacological levels (Dhawan et al., 1996). In particular, μ-opioid receptors (MORs) are critically involved in the induction of endogenous and exogenous analgesia, reward and stress responsiveness (Vaccarino et al., 1999), as well as in the regulation of emotion (Zubieta et al., 2003). Mice lacking the μ-receptor gene show an increased sensitivity to painful stimuli (Sora et al., 1997).

On the other hand, three classes – the enkephalins, β-endorphins and dynorphins – of endogenous opioids have been well characterized. The PAG is rich in the expression of μ-opiate receptors and in neurons expressing encephalin and β-endorphin (Margolis et al., 2005), which is consistent with its important antinociceptive effects in response to exogenous opioids. Pharmacological (Amanzio and Benedetti, 1999) and neuroimaging (Benedetti et al., 2005) studies have also demonstrated the role of the opioid system in placebo analgesia. For example, morphine-induced analgesia can be blocked by injection of the opiate antagonist naloxone into the PAG or the nucleus raphe magnus.

Besides the PAG, also the hypothalamic paraventricular nucleus (PVN) regulates pain processes. PVN stimulation induces the synthesis and secretion of leucine-enkephalins and β-endorphins in the PAG and modulates nociceptive responses in dorsal horn wide dynamic range (WDR) neurons, thus favoring analgesia (Condes-Lara et al., 2008). Moreover, the PVN contributes to the modulation of pain by producing oxytocin (OT), a known neuropeptide that exerts an analgesic action at central and peripheral levels. More in detail, parvocellular OT (parvOT) neurons in the PVN modulate nociception in a two ways: i) directly, by release of OT from axons in the deep layers of the spinal cord to inhibit nociceptive transmission from Aδ- and C- primary afferents to WDR neurons; ii) indirectly, by stimulating OT release from magnocellular neurons into circuilation to reach the bodily periphery. The functional role of parvOT neurons was also tested in two rat models of peripheral painful sensitization, showing that activation of parvOT neurons can decrease mechanical and thermal sensitivities in inflammatory, but not in nerve injury-induced neuropathic pain (Eliava et al., 2016) (**Fig. 1.11**).

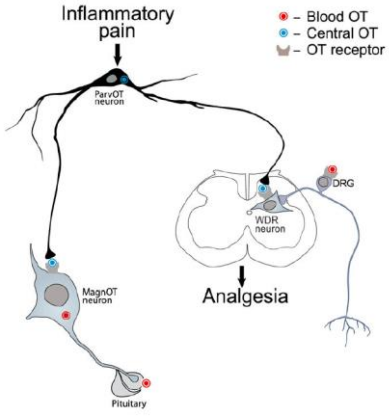

Figure 1.11 The role of ParvOT neurons to promote analgesia. (Adapted from Eliava et al., 2016).

1.4 Neuropathic pain and sensitization

Thus far, I have considered the mechanisms that convey noxious signals in the normal physiological state, but the normal process of sensory signaling can be altered to cause abnormal pain. Generally, the different types of abnormal pain are grouped together under the term *neuropathic*, to indicate that they are caused by a pathological state of the nervous system. In contrast, the word *nociceptive*, referring to the perception of a noxious event, is used to qualify normal pain, a sensation that everyone normally feels after an injury. How do we distinguish neuropathic from nociceptive pain? The International Association for the Study of Pain initially defined neuropathic pain as "pain initiated or caused by a primary lesion or dysfunction of the nervous system", and more recently changed it to "pain caused by a lesion or disease of the somatosensory nervous system" (Treede et al., 2008). The second definition focuses on the somatosensory nervous system, a component of the nervous system that deals with sensory information from the bodily exterior and interior. A neuropathic pain condition can occur spontaneously and can lead to a dramatic fall in pain threshold, while the duration and strength of the response to noxious stimuli are amplified. Another possible effect of disease is the onset of comorbidities such as depression, sleep diseases and anxiety with an important impairment of life quality. This persistent pain has no protective properties and can manifest as enhanced responses to a properly noxious stimulus (hyperalgesia) or pain perception to innocuous stimuli (allodynia). Hyperalgesia and allodynia cannot coexist and it is accepted that they are driven by distinct mechanisms in different sensory neurons (Lolignier et al., 2015).

Hyperalgesia can be defined as a lowered threshold for pain, an increased sensitivity to pain in response to supra-threshold stimuli and can also occur spontaneously (Treede et al., 1992). Hyperalgesia can be classified as primary (occurring at the site of injury) or secondary (occurring in the areas surrounding the injury) (Treede, 1995). Primary hyperalgesia occurs as a result of sensitization of nociceptive afferents, while secondary hyperalgesia can be caused by changes in the processing of sensory information in the central nervous system, and not by peripheral sensitization (Treede, 1995). The latter term was first used in the study of pain mechanisms to describe the enhanced responses of nociceptors in peripheral tissues to repeated stimulation or to inflammatory mediators. These studies showed that nociceptors lowered their response threshold and increased their excitability when subjected to repeated stimulation, to an inflammatory process or to an injury. This "sensitization of peripheral nociceptors" is also responsible for

the increased sensitivity to pain that occurs in the peripheral nervous system and organs after an injury or in presence of an inflammatory event. More recently, the term "sensitization" has also been used to describe the process of increased excitability of neurons in the spinal cord and the brain after a repetitive or persistent input from nociceptors. This phenomenon was named "central sensitization", as opposed to peripheral sensitization (Campbell and Meyer, 2006).The study of central sensitization opened new avenues for the identification of potential molecular mechanisms of chronic pain.

1.4.1 Mechanisms for Primary Hyperalgesia

Primary hyperalgesia develops as a result of peripheral sensitization that comes from the interaction of nociceptors with the "inflammatory soup" of substances released when a tissue is damaged. These substances are released by activated nociceptors or non-neuronal cells. Nociceptors release peptides and neurotransmitters such as substance P, CGRP, ATP. Non-neuronal cells, that include mast cells, platelets, endothelial cells, macrophages, fibroblasts, are responsible for releasing arachidonic acid and other lipid metabolites, bradykinin, histamine, serotonin, prostaglandins and different cytokines. These inflammatory agents interact directly with the receptors on the nerve terminals of Aδ- and/or C-fiber nociceptors, altering their thermos-mechanical thresholds and activation properties (Woolf and Ma, 2007; Basbaum et al., 2009). Hyperalgesia caused by sensitization to thermal stimuli has been studied in detail. For instance, the responses of TRPV1 to heat can be potentiated by interaction of the channel with extracellular protons or lipid metabolites. In addition, pro-nociceptive mediators such as NGF and bradykinin increase the membrane expression and the activity of TRPV1 through the actions of their specific cell-surface receptors (TrkA and bradykinin receptors, respectively) and corresponding intracellular pathways (Zhang et al., 2005). In addition, studies on mice lacking TRPV1 show absence of heat hyperalgesia after carrageenan-induced inflammation (Caterina et al., 2000; Davis et al., 2000). Similarly, TRPA1-deficient mice show deficits in bradykinin- or mustard oil-evoked hypersensitivity (Bautista et al., 2006). Finally, selective deletion of $Na_v1.8$ by diphtheria toxin cellular ablation led to a loss of cold and mechanical hyperalgesia after inflammation (Abrahamsen et al., 2008).

1.4.2 Secondary Hyperalgesia and Central Mechanisms of Mechanical Allodynia

Secondary hyperalgesia occurs in undamaged tissue surrounding the site of injury and it is a result of sensitization in the central nervous system. It is characterized by hyperalgesia to mechanical, but not heat, stimuli. Two types of mechanical hyperalgesia are observed: pain to light-stroking stimuli (allodynia) and enhanced pain to punctiform stimuli. Mechanical allodynia is defined as *pain due to a stimulus that normally does not cause pain* (Treede et al., 2008). Over the past years, knowledge on the mechanisms behind light touch feeling pain has progressed, due the discovery of the role of myelinated low-threshold mechanoreceptors in mediating plasticity of pain-transmitting neurons within the spinal cord (Dhandapani et al., 2018). Studies on human subjects with nerve injury or using capsaicin patches to mimic hyperalgesia showed that selective blockade of A-fiber nerve conduction eliminated brush-evoked allodynia, while blocking Aδ- and C-fiber nociceptors had no effect (LaMotte et al., 1992; Torebjork et al., 1992; Kilo et al., 1994). The lack of nociceptor sensitization to mechanical stimuli (LaMotte et al., 1992) confirmed the role of A-fibers in mediating allodynia. This result led to the hypothesis that allodynia is caused by central sensitization. For this reason, various mechanisms have been proposed for development and maintenance of allodynia, such as alteration in gene expression patterns, sprouting of myelinated fibers from lamina III/IV to lamina I of the spinal cord, and a disinhibition of inhibitory interneurons in the dorsal horn (Bridges et al., 2001; Lolignier et al., 2015). The latter process can explain mechanical allodynia in the spinal cord, and is based on the "gate control" theory, which postulates that touch stimuli normally inhibit acute pain by direct activation of inhibitory interneurons. A failure in this inhibition appears to contribute to mechanical allodynia. Different studies on the spinal cord have provided evidence that an injury actually causes disinhibition of spinal circuits, thus giving mechanosensitive neurons access to lamina I pain-projecting interneurons through a polysynaptic circuit composed of Somatostatin $(SOM)^+$ and SOM^+/Protein Kinase Cγ $(PKC\gamma)^+$ excitatory interneurons (Duan et al., 2014). A recent paper reported that a population of excitatory interneurons, expressing vesicular Glutamate Transporter isoform 3 (vGluT3), receives touch inputs. Activation of $vGluT3^+$ interneurons leads to mechanical allodynia, whereas their ablation reduces it, suggesting the presence of dedicated micro-circuits in the dorsal horn (Peirs et al., 2015). In addition to (inter)neurons, one of the candidates directly involved in mechanical allodynia is microglia. ATP released during injury induces the activation of microglia through upregulation of the P2X4 purinergic

receptor, which leads to increased the synthesis of Brain-Derived Neurotrophic Factor (BDNF). Microglia-derived BDNF, in turn, acts on its receptor TrkB to indirectly reduce GABAergic inhibition via the downregulation of the potassium-chloride exporter KCC2 (Coull et al., 2005). More in detail, decreased KCC2 activity decreases the inward gradient of Cl^-, thus dampening the effect of GABA receptor activation on neuronal excitability (Beggs and Salter, 2013).

Recruitment and proliferation of microglial cells are mediated by the over-expression of macrophage colony stimulating factor (CSF1) by injured sensory neurons (Guan et al., 2016). It is worth noting that, the known scavenger function of microglia is also involved in neuropathic pain; indeed, impairment of microglial phagocytosis in the dorsal horn in TMEM16F (Ca^{2+}-dependent phospholipid scramblase) knockout mice ablates injury-induced allodynia (Batti et al., 2016), suggesting a multi-faceted role of microglia cells in neuropathic pain.

Furthermore, a recent work from the Heppenstall group has identified a population of $TrkB^+$ sensory neurons that is necessary and sufficient for producing allodynia from light touch under neuropathic pain states. Their findings are also base on a novel, based upon a phototoxic derivative of BDNF, to directly target neurons responsible for mechanical allodynia (Dhandapani et al., 2018). In addition, Liu Y and colleagues have published this year a study on the role of a subset of corticospinal neurons (CSNs), originating in the primary and secondary somatosensory cortex, in the touch and tactile neuropathic pain sensitivity. They show that reduction in somatosensory CNS activity or transection of the corticospinal tract in mice impairs behavioral responses in light touch tests without altering responses to noxious stimuli. Manipulation of this neuron population attenuates tactile allodynia in a model of peripheral neuropathic pain. These results reveal direct cortical modulation of tactile sensation in normal conditions and allodynia in neuropathic pain states; the Authors also hypothesize that normalizing CSN excitability could be a new strategy for treating neuropathic pain, either by pharmacological or electromagnetic manipulation (i.e., transcranial direct current or magnetic stimulation; tDCS and TMS, respectively) (Liu et al., 2018).

1.5 The discovery of NGF and the "Neurotrophic Hypothesis"

The era of growth factor research began with the discovery of Nerve Growth Factor (NGF). In the early 1950s, Rita Levi-Montalcini, analyzing the effects of transplanting mouse sarcoma tissue into a chick

embryos, found that the tumor tissue induced hyperinnervation of internal organs. She hypothesized that this hyperinnervation was due to the release of diffusible molecule that was able to stimulate the growth and differentiation of the developing nerve cells. Then, in collaboration with the biochemist Stanley Cohen, Rita Levi-Montalcini performed a series of experiments in order to isolate the unknown molecule, which could be purified from mouse salivary glands, of whom they demonstrated the proteic nature (Levi-Montalcini, 1987). Levi-Montalcini and Cohen also produced large quantities of antibodies against NGF, which they exploited to demonstrate, for the first time, the functional significance of NGF for in *vivo* development of sympathetic and sensory ganglia (Levi-Montalcini and Angeletti, 1966; Hamburger, 1993; Cowan, 2001).

After NGF discovery, it became clear that it belonged to a family of structurally related proteins, named "neurotrophins", that comprises Brain-Derived Neurotrophic Factor (BDNF) (Barde et al., 1982), Neurotrophin-3 (NT-3) (Hohn et al., 1990; Jones and Reichardt, 1990; Rosenthal et al., 1990), and Neurotrophin-4/5 (NT-4-5) (Berkemeier et al., 1991).

Like most growth factors, neurotrophins are initially sintethized as a precursor or proneurotrophin (30-35 kDa) consisting of an N-terminal prodomain and a C-terminal mature domain. After translation, proneurotrophins form noncovalent dimers through interactions of the mature domain, which forms a cysteine knot-like structure (Bradshaw et al., 1993). Dimeric proneurotrophins can be cleaved intrarcellularly by furin or pro-proteases in the Golgi or in secretory vesicles to produce mature neurotrophins, which are about 12 kDa in size, form stable non-covalent dimers, and are normally expressed at very low levels during development. Indeed, during development, neurons compete with each other for a limited supply of a neurotrophins provided by target tissues; successful competitors survive, unsuccessful ones die. The discovery of NGF was instrumental to the formulation of the "Neurotrophic Factor Hypothesis". It is well established that the overall levels of neurotrophin(s) determine the balance between cell survival and apoptosis during development.

In addition to the known effects on neuronal cell survival, neurotrophins can also regulate axonal and dendritic growth and guidance, synaptic structure and connections, neurotransmitter release, long-term potentiation (LTP) and synaptic plasticity in general (McAllister et al., 1999). For instance, seminal contributions on the role of neurotrophins in regulating cortical development and plasticity, have come

from Lamberto Maffei and colleagues. Using the paradigm of monocular deprivation during the critical period in rats, they discovered that NGF administered via the lateral ventricles (intracerebroventricular i.c.v.) attenuated the expected ocular dominance (OD) shift (Maffei et al., 1992; Domenici et al., 1993). Moreover, i.c.v infusion of anti-NGF antibodies to visually normal rat pups altered visual system development at the functional and anatomical levels (Berardi et al., 1993). Exogenous manipulation of cortical levels of neurotrophins has important consequences on plasticity. BDNF and NGF infusion are able to prevent the delay in visual system development caused by dark rearing (Fagiolini et al., 1997). Finally, it is important to consider that the action of neurotrophins necessitates a certain amount of electrical activity to be present, because completely blocking afferent activity with intraocular injections of TTX abolishes the OD shift-preventing effect of NGF infusion (Caleo et al., 1999). These studies suggest that visual experience acts through neurotrophins to modify synaptic connections in developing cortex.

1.5.1 NGF Expression: the Levels of Neurotrophin Matter

The *Ngf* gene is located on chromosomes 3qF2.2, in *Mus musculus*, and 1p13.2 in *Homo sapiens*. The mammalian *Ngf* gene contains several 5'exons, encoding the 5'untranslated region (UTR), and one 3' exon encoding the NGF protein (Metsis, 2001). NGF is expressed in both neuronal and non-neuronal cells of the peripheral and central nervous system (Sofroniew et al., 2001). NGF is highly expressed in the target tissues of TrkA expressing neurons, which include dorsal root ganglia (DRG), cranial sensory neurons that mediate pain and temperature and sympathetic neurons. NGF is also localized in the striatum, and high mRNA levels are detected from postnatal day (P) 2 through P30. The increase in NGF protein is coincident with cholinergic neurochemical differentiation. Indeed, NGF acts, through TrkA, on developing caudate-putamen cholinergic neurons (CPCNs), which play an important role in the control of movement (Holtzman et al., 1993).

NGF is also present in the cerebral cortex, where mRNA expression peaks between P10 and P30 (Large et al., 1986). In particular, the cellular localization of NGF in the cortex shows the highest levels in deep layer (L) V and moderate levels in L-II/III, upper L-V and L-VI, whereas low expression is detected in L-IV (Pitts and Miller, 2000). In addition to the cortex, NGF is produced also in the hippocampus (Mufson et al., 1994). NGF acts on a number of forebrain and brainstem neurons, but most of the attention has been focused

on basal forebrain cholinergic neurons (BFCNs), because NGF is required for the correct differentiation of BFCNs. These projection neurons send their axons to innervate the hippocampus and neocortex and have a role in learning, attention and memory. When expression of the NGF gene was disrupted, BFCNs were smaller and showed decreased immunoreactivity for choline acetyltransferase (ChAT). Furthermore, heterozygous mutant mice displayed significant deficits in memory acquisition and retention in the Morris water maze (MWM) test (Crowley et al., 1994; Chen et al., 1997). Consistently, interfering with NGF signaling in the adult brain, using antibodies that selectively neutralize mature NGF or TrkA, causes deficits of the cholinergic system and a progressive neurodegeneration, in addition to synaptic and behavioral deficits (Capsoni et al., 2000; Ruberti et al., 2000). Changes in brain NGF homeostasis, have also been associated to Alzheimer's disease, whose pathogenesis is thought to arise also from an imbalance between pro-NGF and mature NGF levels (Cattaneo and Calissano, 2012).

Regarding non-neuronal cells, NGF is also able to influence microglia motility through the activation of TrkA (De Simone et al., 2007). NGF controls microglial homeostatic activities, protecting neurons from Aβ-induced loss of dendritic spines (Rizzi et al., 2018). Macrophages, the peripheral counterparts of microglia, are a target of both mature and pro-NGF. Indeed, NGF increases their membrane ruffling, calcium spiking, phagocytosis and growth factor secretion. In contrast, proNGF induces podosome formation, increases migration and suppresses calcium spikes (Williams et al., 2015). NGF is also produced by astrocytes, in which, by activating $p75^{NTR}$, it reduces the proliferation induced by other mitogens, such as EGF, thus demonstrating the cell-type specificity of neurotrophin functions in the brain (Cragnolini et al., 2009). Immature Schwann cells produce NGF during development, but in adults, NGF expression is undetectable in mature myelinated Schwann cells. However, after nerve injury, NGF expression is induced in reactive and dedifferentiated Schwann cells (Heumann et al., 1987; Lindholm et al., 1987).

Finally, it is important to remember that neurotrophins are also synthesized and released in an activity-dependent manner and that neural activity has profound effects on the neurotrophins levels (Blochl and Thoenen, 1995; Wang et al., 1998). For example, limbic seizures induce NGF expression within one hour from their onset in the dentate gyrus of the hippocampus, with expression in the neocortex and olfactory forebrain appearing some hours later (Gall and Isackson, 1989). In general, NGF and BDNF mRNAs are highly regulated by electrical stimulation and epileptic activity (Gall and Lauterborn, 1992).

1.5.2 NGF, receptors and downstream pathways

Neurotrophins bind two kinds of receptors: tyrosine receptor kinases, known as Trks (for Tropomyosin-Related Kinase), and a member of the tumor necrosis factor receptor superfamily, known as $p75^{NTR}$ (Chao, 2003). Three Trk receptors have been identified: TrkA, TrkB and TrkC, each one with its own preference for specific neurotrophins. TrkA is highly selective for NGF and, to a lesser extent, NT-3; TrkB binds BDNFand NT-4/5; TrkC binds NT-3. In contrast, $p75^{NTR}$ can bind all neurotrophins, and also acts as a co-receptor for Trks (Hempstead, 2002). In this regard, expression of $p75^{NTR}$ can increase the affinity of TrkA for NGF. (Hempstead et al., 1991). When NGF binds TrkA, receptor dimerization leads to trans-autophosphorylation, the activation of intracellular signaling cascades and finally the receptor can be targeted for degradation by ubiquitination. In particular, Nedd4-2, an E3 ubiquitin ligase, is able to bind TrkA through a PPXY motif, leading to the ubiquitination and downregulation of TrkA (Arevalo et al., 2006). The mechanism of TrkA signaling involves phosphorylation of specific tyrosine residues upon NGF binding. The Y490 and Y785 residues of the TrkA intracellular domain serve as the main docking sites to initiate downstream signaling pathways such as the extracellular signal-regulated kinase (ERK) and phospholipase C-γ (PLC- γ) pathways, respectively. The Y670, Y674 and Y675 residues, located within the tyrosine kinase domain, can also recruit adaptor proteins after phosphorylation, including Grb2 and SH2B. Shc binds the activated TrkA and mediates two separate intracellular signaling pathways: i) neuronal survival requires Shc binding to the receptor, resulting in increased phosphatidylinositol 3-kinase (PI3K) and Akt (protein kinase B) activities; ii) phosphorylation of Shc leads to increased activity of Ras and ERK. These events, in turn, influence transcriptional events, such as the activation of the cyclic AMP-response element binding (CREB) transcription factor. CREB affects cell cycle, neurite outgrowth and synaptic plasticity (Lonze and Ginty, 2002). Additionally, activated Akt promotes neuronal survival by inhibiting a forkhead transcription factor, FKHRL1, which, in turn, regulates expression of pro-apoptotic genes. Finally, PLC- γ initiates, upon TrkA binding, an intracellular signaling cascade that results in the release of inositol phosphates and activation of protein kinase C (PKC) (Ming et al., 1999).

In addition to direct activation through NGF, TrkA receptor is also transactivated intracellularly by adenosine and pituitary adenylate cyclase-activating polypeptide (PACAP) signaling through G-protein-coupled receptors (GPCRs), a mechanism requiring Src family kinases (SFK) and intracellular Ca^{2+} (Lee

et al., 2002). Both adenosine and PACAP have a long latency (more than 1-2hours) to activate Trk tyrosine kinase activity; both ligands stimulate PI3K and Akt, leading to enhanced cell survival after NGF withdrawal. In summary, transactivation is a process that might explain why neuronal survival in the adult CNS is not abolished by the lack of neurotrophins.

$p75^{NTR}$, through a different set of adaptor proteins, predominantly signals to (i) activate NF-κB, (ii) increase JunN-terminal kinase (JNK), (iii) produce ceramide, (iv) modulate RhoA activity (Roux and Barker, 2002). One known function of $p75^{NTR}$ is to promote cell death, providing a molecular mechanism for ensuring rapid apoptosis when a neuron is unsuccessful in competing for adequate amounts of neurotrophins (Majdan and Miller, 1999). $p75^{NTR}$-induced apoptosis also occurs after seizure or inflammation (Bhakar et al., 1999; Roux et al., 1999); in addition, spinal cord injury causes p75-dependent oligodendrocyte death (Beattie et al., 2002).

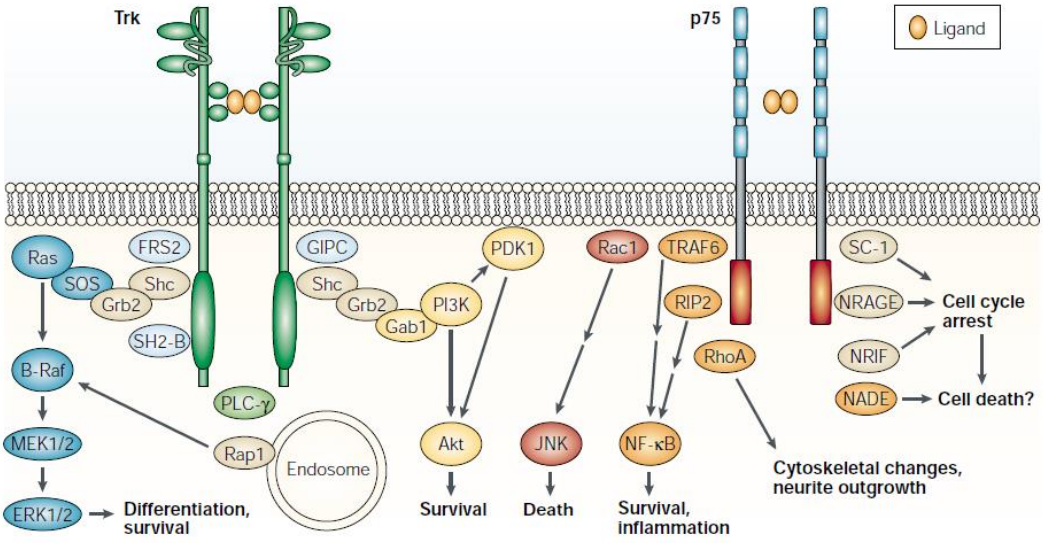

Figure 1.12 Signaling mediated by TrkA and $p75^{NTR}$ receptors (adapted from Chao, 2003).

Pro-NGF can be also released extracellularly (i.e., secreted), suggesting that this form may act as a ligand distinct from its mature counterpart (Lee et al., 2001). Indeed, compared to mature neurotrophins, that promote survival by binding Trks, pro-neurotrophins show higher affinity for p75 and, thus, biased towards inducing apoptosis. Interestingly, $p75^{NTR}$ can form heterodimers with a variety of other "auxiliary" receptors, most prominently Sortilin and neurite outgrowth inhibitor reticulon 4 (NOGO). Binding studies, using purified proNGF, demonstrate its interaction with a heteromeric receptor complex composed of

$p75^{NTR}$ and sortilin, wherein the prodomain interacts with sortilin and the mature domain interacts with $p75^{NTR}$, demonstrating the importance of sortilin in proNGF-induced neuronal death (Nykjaer et al., 2004). On the other hand, Nogo receptor closely associates with $p75^{NTR}$ through interactions between the respective extracellular domains. This association produces a repulsive effect on axonal growth: different proteins bind to the cytoplasmic domain of $p75^{NTR}$ and, among these, RhoA is the most relevant to inhibition of neurite outgrowth (Yamashita et al., 1999).

Many of the components of the pathways mediated by neurotrophins, such as ERK, Akt, PLC, PKC, JNK, Ras, are common effectors with pathways triggered by many other factors, such as cytokines and other growth factors. This complicates the problem of ascribing specific mechanisms to a particular response. Furthermore, the effects of neurotrophins are modulated by various factors, such as their levels and affinity to receptor (Chao, 1992). For this reason, it is not straightforward to dissect between changes in behavior or neuronal activity caused simply by reduction of neurotrophin levels or by more complex interactions with of the signaling pathways.

1.5.3 Signaling by retrograde transport of neurotrophin-Trk complexes

Secreted NGF binds TrkA, that is present on the distal axons of neurons (Campenot, 1977). Neurotrophin-mediated signals can, then, be propagated retrogradely along the axon to the cell body. This retrograde signaling is important not only for normal development of the nervous system, but also for helping neurons in responding to axonal insults and injury. The process starts when activated TrkA undergoes internalization following ligand engagement in distal axons, and it seems to be essential for retrograde survival signaling (Grimes et al., 1996). There are two models that explain how neurotrophin-Trk signaling is propagated to the cell body: i) the signaling endosome model and ii) the wave propagation model (Ginty and Segal, 2002). The signaling endosome model is based on retrogradely transported endosomes containing neurotrophin-Trk complexes associated with downstream adaptor and effector proteins. This model is supported by many studies showing endocytosis of neurotrophin-Trk complexes (Middlemas et al., 2003) and retrograde transport of Trk's and downstream signaling molecules. According to the wave propagation model, NGF binding to TrkA at distal axons generates a retrograde wave of Trk phosphorylation within the plasma membrane (Senger and Campenot, 1997). This model is supported by studies showing that treatment of

sympathetic axon terminals with covalently coupled NGF beads, which are supposed to prevent internalization of NGF-TrkA complexes, can continue to promote survival of the cell body (MacInnis and Campenot, 2002). Consistently, retrograde axonal transport of Trk's could be observed after stimulation of terminals with covalently coupled NGF beads (Heerssen et al., 2004). To date, the signaling endosome is the more accepted model. In addition, the ubiquitination process is considered a critical event for appropriate trafficking. In this regard, Nedd4-2 regulates the trafficking of TrkA and NGF functions in DRG neurons in response to NGF (Yu et al., 2011).

1.5.4 Molecular features of retrograde transport of NGF-TrkA

NGF-TrkA complexes are internalized via both clathrin-dependent and clathrin-independent endocytosis. Isolated clathrin-coated vesicles from NGF-treated cells were found to contain NGF, phosphorylated-TrkA, downstream signaling proteins and early endosome markers (Howe et al., 2001). On the other hand, one clathrin-independent mechanism for TrkA endocytosis is macropinocytosis, which involves the formation of multivesicular bodies composed of multiple NGF-TrkA-containing vesicles. This process is regulated by a GTPase, Pincher, whose inhibition causes neuronal death (Shao et al., 2002). Therefore, NGF binding to TrkA induces both types of endocytosis, but it remains unknown if the individual endocytic pathways have physiologically distinct functions. Internalized vesicles recruit various signaling molecules, thus forming signaling endosomes, which recruit all the three major effector pathways that have been described for TrkA, namely the PI3K-Akt, ERK and PLCγ (**Fig.1.13**). The activity of PI3K is necessary at an early stage of the endosome retrograde transport process. Pharmacological perturbation of PI3K in distal axons was shown to prevent the retrograde accumulation of NGF in cell bodies (Kuruvilla et al., 2000), although it remains unclear how PI3K regulates the retrograde transport. Signaling endosomes are localized along cytoskeletal structures and Trk receptors are capable of associating with cytoplasmic Dynein (Yano et al., 2001). Dynein exhibits a minus end-directed motor activity along microtubules, which can move signaling endosomes toward the cell body; indeed, Dynein inhibition abolishes retrograde survival signaling (Heerssen et al., 2004). Near the cell body, signaling endosomes activate transcription factors, such as CREB to promote neuronal survival program (Riccio et al., 1997); moreover, CREB-mediated transcriptional response is required for axonal growth over long periods of time (Cox et al., 2008). In

addition to CREB, other trophic factor-regulated transcriptional factors, such as serum response factor (SRF) and nuclear factor of activated T-cells (NFAT), have been implicated in promoting axonal outgrowth.

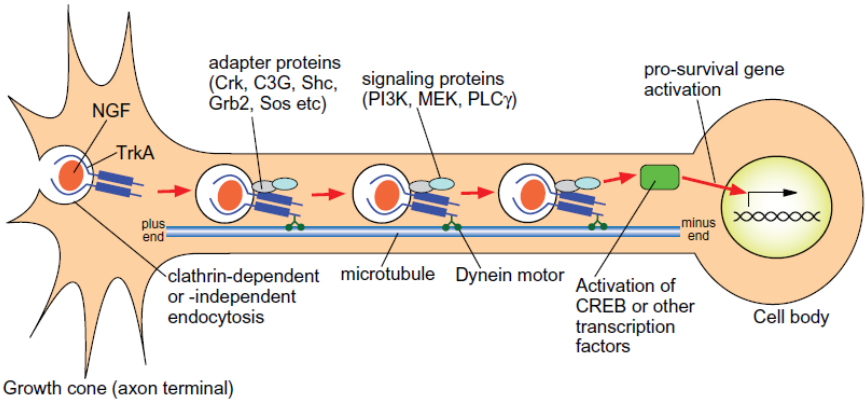

Figure 1.13 Retrograde signaling mediated by NGF-TrkA complexes. NGF binds TrkA and induces its endocytosis. The endocytosed vesicles recruit adapter and signaling proteins to form a "signaling endosome". TrkA interacts with cytoplasmic dynein motors, resulting in minus end-directed movement to the nucleus (adapted from Ito and Enomoto, 2016).

On the other hand, the mechanisms of TrkA anterograde axonal transport and its physiological relevance remain unknown. Tanaka and colleagues showed evidence that KIF1A, a microtubule plus end-directed motor protein, transports TrkA and is essential for NGF/TrkA/Ras/PI3K signaling to augment TRPV1 phosphorylation and cell surface presentation. Given the importance of TRPV1 in nociception, this suggests that anterograde axonal transport of TrkA by KIF1A is essential for sensory neuronal function (Tanaka et al., 2016).

Finally, the question of whether pro-neurotrophins move retrogradely or anterogradely along axons, also in comparison to their mature counterparts, has remained largely unexplored. To this regard, a recent paper by the Cattaneo group used a single-particle tracking approach to demonstrate that proNGF is retrogradely transported just like mature NGF, but with a lower flux and a different distribution in terms of number of pro-neurotrophin molecules per vesicle (De Nadai et al., 2016).

1.5.5 Retrograde apoptotic signaling mediated by p75^{NTR}

As well as for survival signaling, p75^{NTR}-mediated apoptosis requires a retrograde transport system to the nucleus, but the mechanisms involved are poorly understood.

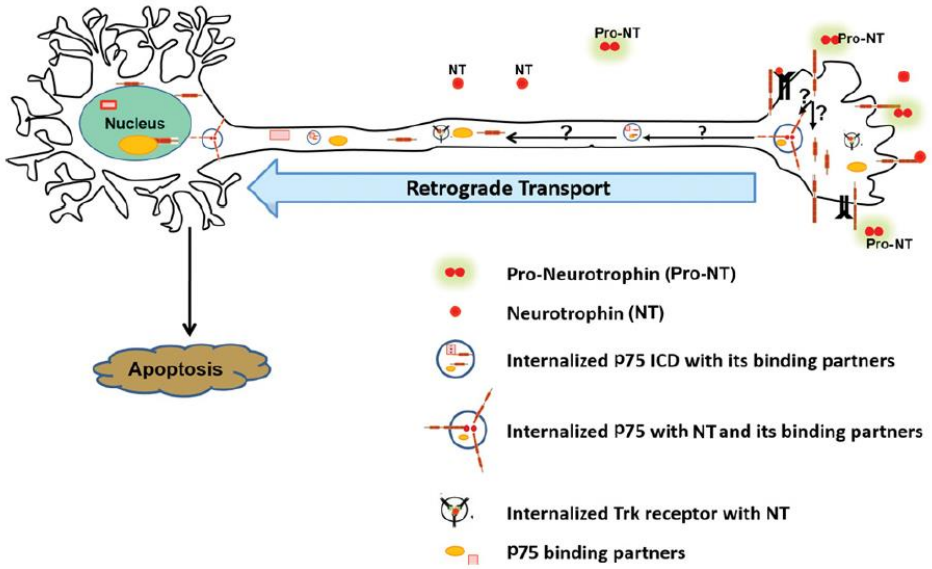

Figure 1.14 Retrograde apoptotic signaling by p75^{NTR}. Some questions are still open to debate: the mechanisms of internalization, the identity of the transport vesicles, where cleavage occurs, which fragments of p75^{NTR} are transported, and which components are present in the retrograde signaling complex (adapted Pathak and Carter, 2017).

Using an *in vitro* culture system, Teng et al. provided the first evidence for neuronal death through a p75^{NTR}-mediated retrograde signal (Yano et al., 2009). They cultured sympathetic neurons in compartmentalized cultures and added pro-NT3 exclusively to the distal axons, which resulted in neuronal death. Importantly, neurons from p75$^{NTR-/-}$ mice were resistant to the pro-apoptotic actions of pro-NT3. Thus, p75^{NTR}-dependent apoptosis may contribute to the already known degenerative retrograde signaling events triggered injury or trophic factor deprivation.

1.5.6 Multiple functions for retrograde neurotrophin signaling: What is their importance?

The actions of target-derived growth factors are clearly not limited to the promotion of cell survival. Increasing evidence suggests that proper lamina-specific axonal targeting of central projections of DRG neurons is regulated by a transcriptional activity that is initiated by retrograde signaling. For example, target-derived NGF activates TrkA that, expressed in small-diameter sensory neurons, produces a

retrograde signal that promotes maturation of both peptidergic and non-peptidergic nociceptors (Huang et al., 2015).

Retrograde transport is also required for the correct dendrite arborization. In particular, in sympathetic neurons, interruption of NGF-TrkA retrograde signaling by axotomy causes retraction of dendrites (Purves, 1975).

Regulation of neuronal specification and maturation is crucial for the functioning of the nervous system and requires retrograde transport. As mentioned above, NGF is essential to the acquisition of the nonpeptidergic phenotype through upregulation of *Ret*. In fact, NGF-dependent expression of *Ret* is required for expression of a large subset of nonpeptidergic-related genes (Luo et al., 2007). For instance, in the absence of *Runx1*, the central non-peptidergic projections of sensory neurons are abnormally shifted from lamina II to lamina I. NGF is also required for the expression of CGRP and the acquisition of peptidergic nociceptor specification (Patel et al., 2000).

Finally, retrograde signaling by neurotrophic factors is responsible for the development of correct synapse formation and maintenance. In postganglionic sympathetic neurons, NGF-TrkA complexes are required for the development of proper presynaptic and postsynaptic specializations; accordingly, application of NGF-blocking antibodies induces synaptic loss. Furthermore, the presence of TrkA signaling endosomes in dendrites is probably a prerequisite for postsynaptic density and synapse formation (Sharma et al., 2010).

1.5.6 NGF supports the development of peripheral neurons

In *vivo* gain and loss of function experiments using exogenous NGF or neutralizing NGF antibodies showed that NGF is an essential survival factor for sympathetic neurons and a subpopulation of sensory DRG neurons. Such studies reported that NGF, in addition to maintenance of sympathetic neurons, is involved in the regulation of the substance P (SP) content of embryonic and neonatal sensory neurons (Schwartz et al., 1982; Rich et al., 1984). Immunization of rats against NGF causes depletion of SP in DRG neurons both in animals exposed *in utero* (i.e., by immunization of pregnant rats) and in newborns, although the regenerative capacity of DRG neurons following axotomy in NGF-immunized animals was unimpaired (Johnson et al., 1989). Anti-NGF antibodies administered during early postnatal development in rats revealed that DRG neurons lose their dependency on NGF for survival shortly after birth; however, NGF

still has an influence on DRG phenotype for another 10 days. Chronic administration of NGF antisera at birth causes a change in the physiology of Aδ cutaneous afferents, leading to a switch of high-threshold mechanoreceptors, which respond to noxious mechanical stimulation of the skin, to mechanoreceptors that result sensitive to hair movement, innervating D-hairs (Ritter et al., 1991). Importantly, this phenotypic switch occurs in the absence of cell death of developing HTMRs despite loss of NGF and involve solely the redirection of fibers (Lewin et al., 1992).

The subsequent generation of mice carrying null mutations in the genes encoding each neurotrophin and their receptors demonstrated that all neurotrophins, as well as their receptors, play an important role in regulating the survival of peripheral neurons (**Fig. 1.15**).

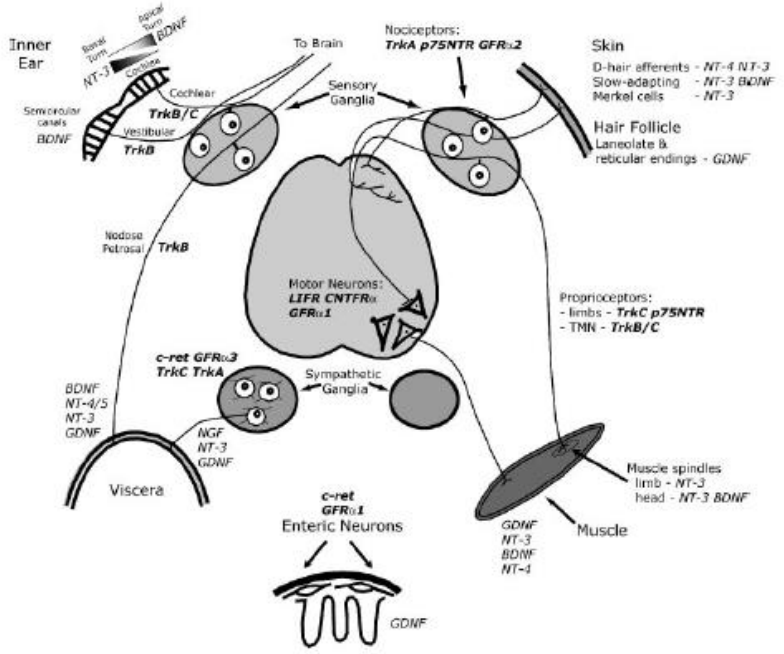

Figure 1.15 Pro-survival functions of neurotrophins in the peripheral nervous system. The picture shows different components in the peripheral nervous system, including sensory ganglia, sympathetic ganglia and enteric neurons. Only ligands or receptors causing a clear loss-of-function phenotype are indicated (Adapted from Huang and Reichardt, 2001).

Many sensory neurons express TrkA at some time during their development, and essentially all of these neurons are lost in null mice for TrkA or NGF (Crowley et al., 1994; Smeyne et al., 1994). Loss of a single allele of the NGF gene reduces the survival of TrkA-expressing DRG neurons (Crowley et al., 1994). Conversely, transgenic mice that overexpress NGF in the skin display increased survival of TrkA-expressing neurons, both in wild-type neurons (Albers et al., 1994) and in NGF-null mice (Harrison et al.,

2004). Regarding $p75^{NTR}$, its loss results in decreased pain sensitivity and reduced cutaneous innervation by nociceptors (Lee et al., 1992; Bergmann et al., 1997). Nociceptors from $p75^{NTR-/-}$ mice are less sensitive to NGF (Lee et al., 1992; Davies et al., 1993), which suggests that $p75^{NTR}$ likely augments NGF-TrkA signaling in nociceptors.

The availability of NGF in the skin regulates the number of C-fibers; indeed, decreasing NGF levels reduced the number of heat-responding C-fibers (Lewin and Mendell, 1994). It appears that limiting quantities of skin-derived NGF normally support the survival of TrkA-expressing DRG neurons during development. Interestingly, after target innervation has been completed, nociceptive neurons become dependent for their survival also on locally produced BDNF (Valdes-Sanchez et al., 2010).

Altogether, immunological and genetic studies of NGF deprivation during development and maturation demonstrate that NGF has three separate roles: i) survival and development of sensory and sympathetic neurons; ii) maintenance of the peptidergic phenotype of primary afferent neurons in the early postnatal period; iii) modulation of the expression of neurotransmitters, receptors and ion channels expressed by adult nociceptors. Regarding this last function, for example, the expression of nociceptor-specific ion channels, like TRPV1 and TRPM8, requires NGF signaling (Luo et al., 2007). In keeping with this, experiments using Calcium imaging showed that embryonic sensory neurons begin to respond to capsaicin at embryonic stages corresponding to their innervation of NGF-rich target tissues (Hjerling-Leffler et al., 2007).

1.5.7 NGF and pain

NGF plays a key role in pain transduction mechanisms in the adult nervous system (Julius and Basbaum, 2001). Cutaneous administration of NGF to humans (Dyck et al., 1997) and mice (Andreev et al., 1995) leads to a rapid sensitization of cutaneous nociceptors. These rapid effects are mediated in the rat by NGF binding to TrkA expressed on mast cells, causing degranulation and release of a different algogenic mediators, such as histamine, prostaglandin E2, serotonin, hydrogen ions and bradykinin, as well as additional NGF. NGF, indeed, has an important role in inflammatory pain. It is expressed and/or released by several immune cell types, including eosinophils, lymphocytes, macrophages and mast cells following injury. Moreover, NGF is up-regulated in experimental models of inflammation, such as formalin injection and complete Freund's adjuvant administration (Woolf et al., 1994), as well as in models of autoimmune

arthritis (Shelton et al., 2005). The NGF-induced release of inflammatory mediators contributes to sensitization of polymodal nociceptors to thermal and chemical stimuli *in vitro* and *in vivo* (Bennett et al., 1998; Shu and Mendell, 1999). Application of NGF to primary sensory neurons results in activation of TrkA and rapid sensitization of those neurons to a variety of stimuli, including noxious heat (Zhang et al., 2005), mechanical stimuli (Di Castro et al., 2006), or chemical stimuli (Winter et al., 1988). For example, heat hyperalgesia induced by NGF was found to be dependent on the presence of the TRPV1; in fact, this type of hyperalgesia does not occur in $TRPV1^{-/-}$ mice (Chuang et al., 2001). The role of TRPV1 in this context has been recently confirmed using the naked mole rat, in which reduced TrkA function was shown to decrease TRPV1 sensitization and subsequent NGF-induced hyperalgesia (Omerbasic et al., 2016). NGF is also involved in mechanical hyperalgesia; a pulse of NGF is sufficient to set in train a series of events that sustain mechanical hyperalgesia, often for days (Lewin et al., 1993).

Following immediate hypersensitivity by NGF release, early transcriptional changes occur in the sensory signalling pathway (as already described above). A delayed phase of the inflammatory response to NGF involves an indirect effect on synaptic transmission between nociceptors and second-order cells in laminae I and II of the spinal cord. Early pharmacological experiments indicated, for example, that long-lasting NGF-induced heat hyperalgesia is sustained by a central sensitization that requires NMDA receptors (Lewin and Mendell, 1994). One mechanism that contributes to the development of central sensitization in the dorsal horn is the NGF-dependent upregulation of BDNF in peptidergic nociceptors (Michael et al., 1997). BDNF is transported retrogradely to peripheral terminals and also anterogradely from the DRG neuronal cell bodies to terminals in the dorsal horn (Tonra et al., 1998). Expression of BDNF takes place in small-and medium-sized DRG neurons and its release requires strong pre-synaptic stimulation (Lever et al., 2001). Binding of BDNF to TrkB expressed by second-order cells can activate intracellular pathways that lead to upregulation of SP and CGRP synthesis. Collectively, different papers suggest that BDNF-dependent activation of TrkB signaling is required for the development of the central sensitization process that underlies the development of persistent heat and mechanical hypersensitivity in the setting of tissue inflammation or injury (Wang et al., 2009).

Local administration of NGF to normal peripheral nerves can also induce nerve sprouting of peptidergic ($TrkA^{+}$) nociceptors, leading to a remarkable reorganization of sensory and sympathetic nerve fibers. For

example, different studies have demonstrated significant sprouting of $CGRP^+$ nerve fibers following bone fracture in rat and in the arthritic joints of human and animals (Wu et al., 2002; Ashraf et al., 2011). These reports suggest that, following injury or disease of the skeleton, sprouting of $TrkA^+$ fibers, possibly as a result of massive release of NGF by inflammatory and immune cells (Skaper, 2001).

These findings suggest that interfering with nociception-activated NGF-TrkA signaling represents a promising target for pain relief therapies.

Although the general consensus is that the inflammatory component of pain is mediated by TrkA expressed on mast cells (Horigome et al., 1993), a growing body of evidence suggests that $p75^{NTR}$ signaling provides a significant contribution to pain transmission and sensitization (Nicol and Vasko, 2007). Indeed, NGF is able to increase the excitability of nociceptive sensory neurons through selective activation of $p75^{NTR}$ (Zhang and Nicol, 2004) and the subsequent sphingomyelin signaling is involved in peripheral sensitization (Khodorova et al., 2013). In addition, NGF increases the expression of bradykinin receptor in DRG cultures via $p75^{NTR}$; this up-regulation does not occur in neurons from mice $p75^{NTR-/-}$, showing that TrkA alone is not sufficient to trigger this response (Petersen et al., 1998). The expression of $p75^{NTR}$ colocalizes with TrkA, not only in DRGs, but also in spinal nerves (Obata et al., 2006), where it increases the ability of TrkA to bind and respond to NGF (Hempstead et al., 1991).

Finally, regarding the role of Sortilin, an elegant work, using Sortilin/$p75^{NTR}$ double knockout mice, showed a decrease of both mechanical and thermal sensitivity compared to single knockout mice. These alterations were due to a reduction in peripheral neuron numbers and to a degeneration of unmyelinated C fibers (Vaegter et al., 2011). In the same manuscript, it is also shown that lack of Sortilin reduces TrkA transport (Vaegter et al., 2011), thus suggesting the possibility that modulation of the receptor could dampen NGF-mediated sensitization.

1.5.8 NGF as a therapeutic target for clinical pain states

Persistent pain represents a major health and social problem, with a prevalence of 1 affected person in 5 people. It is associated with multiple comorbidities, such as depression, and has an important negative impact on quality of life. The area of chronic and inflammatory pain is, actually, a heterogeneous group of condition triggered by various pathologies, implying different origins and mechanisms of action. Treatment

depends on the type and severity of pain status. For example, mild inflammatory pain is conventionally treated with nonsteroidal anti-inflammatory drugs (NSAIDs), whereas more severe pain, including cancer pain, is treated with opioids (Nersesyan and Slavin, 2007). Current treatments for chronic and inflammatory pain are limited by inadequate efficacy; novel analgesics are therefore needed. To this end, there has been growing interest in targeting NGF and its downstream signaling pathways to obtain analgesia. A number of strategies have been developed to investigate the role of endogenous NGF in chronic pain, with encouraging data from preclinical models. The most straightforward approach has been to develop anti-NGF antibodies or a TrkA-IgG "scavenger" to sequester NGF, thus blocking its biological activity. Alternatively, NGF binding and activation of TrkA can be prevented, for example with antibodies or a small-molecule inhibitors (Denk et al., 2017).

Thermal and mechanical pain-related hypersensitivity caused by paw inflammation – using, for instance, complete Freund's adjuvant – could be blocked using either antibodies to NGF (Lewin et al., 1994; Woolf et al., 1994) or a TrkA-IgG molecule to sequester NGF (McMahon et al., 1995). Anti-NGF treatment produced analgesia but had no effect on tissue swelling, thus appearing to impact not the inflammatory response per se, but rather the downstream nociceptor sensitization. Anti-NGF has also been shown to reduce pain-related hypersensitivity in different preclinical pain models of human chronic pain disorders including bone cancer (Sevcik et al., 2005), postsurgical pain (plantar incision) (Zahn et al., 2004), and complex regional pain syndrome (bone fracture) (Sabsovich et al., 2008).

Several mechanisms have been proposed to explain how anti-NGF can decrease pain-related hypersensitivity. One possibility is a reduction in the spontaneous activity of nociceptive afferents evoked by inflammation (Koltzenburg et al., 1999). Anti-NGF can also reduce the inflammation-induced expression of neuromodulators by primary afferents (Woolf et al., 1996). Finally, anti-NGF can also affect excessive axon outgrowth: for example, in models of inflammatory arthropathy, sprouting of small fibers is prevented by anti-NGF treatment (Ghilardi et al., 2012).

TrkA also represents an important target for pain therapy. Ugolini et al demonstrated that MNAC13, the only neutralizing anti-human TrkA monoclonal antibody currently available, (Cattaneo et al., 1999) induces analgesia in both inflammatory and neuropathic pain models, with a long-lasting effect in the latter case. This paper showed that anti-TrkA treatment was also able to potentiate the antinociceptive effect of

morphine and fentanyl in the formalin injection model (Ugolini et al., 2007). Finally, a recent paper showed that NGF-induced production of Prostaglandin D2 in joint mast cells is critical for mechanical hypersensitivity reported in osteoarthritis pain (OA) and the inhibition of TrkA in mast cells constitutes a potential target for OA (Sousa-Valente et al., 2018).

Clinical trials have used a variety of different approaches to inhibit NGF-TrkA signaling. Several companies have developed humanized monoclonal antibodies to bind NGF with high specificity and affinity, preventing interaction with its receptor. In addition to the humanized version of the anti-NGF monoclonal antibody αD-11 developed by the Cattaneo group (Covaceuszach et al., 2009), drug companies are pursuing this avenue with, e.g., tanezumab (Patel et al., 2018) (Pfizer and Eli Lilly), fasinumab (Regeneron and Teva) and fulranumab (Janssen and Amgen). However, it is important to consider that the aim of immunotherapy should be to normalize NGF levels and signaling, not a complete elimination, which would cause side effects as a result of neurotrophin deprivation in adult tissues.

In addition to anti-NGF and anti-TrkA treatments, nociception can be reduced also by interfering with $p75^{NTR}$ signaling. In a neuropathic pain model, intrathecal injection of antisense oligodeoxynucleotides specific for $p75^{NTR}$ reduces the expression of this receptor in DRGs and attenuates thermal hyperalgesia (Obata et al., 2004). Administration of a neutralizing antibody for $p75^{NTR}$ is able to block the hyperalgesia caused by complete Freund's adjuvant or by intraplantar injection on NGF, thus providing a therapeutic approach for the treatment of inflammatory pain (Watanabe et al., 2008).

However, it is important to note that, if one considers the possible interactions between TrkA and $p75^{NTR}$, it is difficult to selectively block the actions of one receptor without affecting the other one.

1.6 HSAN diseases: the other side of the coin of pain

Hereditary sensory and autonomic neuropathies (HSAN), first described in 1852, are a clinically and genetically heterogeneous group of inherited peripheral neuropathies, primarily affecting peripheral sensory and autonomic neurons (Dyck et al., 1983). Patients generally exhibit prominent distal sensory loss that leads to chronic ulcerations in feet and hands, sometimes resulting in severe complications, such as tissue infections or amputations of toes and fingers. In some patients autonomic dysfunction manifestations, such as anhidrosis, fever, blood pressure fluctuations and gastro-intestinal disturbances, are also observed.

Axonal nerve damage to sensory neurons is often found, sometimes accompanied by demyelination (Auer-Grumbach et al., 2003). HSANs can be transmitted either as an autosomal dominant (AD) or autosomal recessive (AR) trait. AD types present marked sensory involvement and minimal autonomic and variable motor involvement. On the other hand, AR types present either as congenital syndromes with striking sensory and autonomic abnormalities, or as autonomic disorders (Verpoorten et al., 2006).

Seven genes have been identified for different types of HSAN. Missense mutations in serine palmitoyltransferase ling chain subunit 1 (SPTLC1) are found in families and individuals with HSAN type I, an AD type starting in the second to fourth decade with sensory loss and foot ulcers (Bejaoui et al., 2001; Dawkins et al., 2001). Mutations in the late endosomal protein RAB7 cause Charcot-Marie-Tooth disease type 2B (Verhoeven et al., 2003). Mutations in the WNK1/HSN2 gene cause AR HSAN type II, an early-onset ulcero-mutilating sensory neuropathy (Lafreniere et al., 2004). HSAN type III, also known as Familial Dysautonomia or Riley-Day syndrome, is caused by mutations in the inhibitor of Kappa-light polypeptide gene enhancer in B cells, kinase complex associated protein (IKBKAP) (Slaugenhaupt et al., 2001). Several different mutations (mostly nonsense mutations, but also missense, small insertions and deletions, splicing variants) in the TrkA gene have been identified and are associated with HSAN IV (Indo et al., 1996). HSAN IV is a rare recessive congenital insensitivity to pain with anhidrosis, caused by a failure of nociceptive and sympathetic neuron development. Patients are prone to oral injuries as well as multiple accidental injuries such as falls, burns and bone and joint fractures (Amano et al., 1998). Further key features of HSAN IV are a deficit in temperature sensing (Axelrod, 2002) and mental retardation. Recently, it has been shown that the lack of TrkA signaling also increases the susceptibility to infections, in particular to *Staphylococcus aureus*, through monocyte/macrophage-specific NGF/TrkA pathway (Hepburn et al., 2014). Finally, HSAN V is caused by mutations in the nerve growth factor beta gene (*ngfb*) (Einarsdottir et al., 2004) and will be described in the following paragraph.

In addition to these HSAN subtypes, other clinical associations have also been described, such as HSAN with gastroesophageal reflux and cough (Kok et al., 2003), and HSAN with spastic paraplegia (Bouhouche et al., 2006b). This last HSAN variant has been found to be associated with mutations in the gene encoding for a cytosolic chaperonin-containing *t*-complex peptide-1 (CCT5) (Bouhouche et al., 2006a).

1.6.1 HSAN V: a complex pathology caused by a point mutation

HSAN V has been described for the first time by Low, who identified a 6-year-old Lithuanian girl affected by insensitivity to pain with a reduction in the number of small-myelinated fibers in the sural nerve (Low et al., 1978). Later, Einarsdottir and Minde described this disease in three patients belonging to a large multi-generational family located in the Norrbottnian region of Sweden (Einarsdottir et al., 2004); for this reason, HSAN V is also known as Norrbottnian congenital insensitivity to pain. The transmission of the mutation was favored by mating between blood relatives.

HSAN V is associated with a mutation in a conserved region of the NGF gene located on chromosome 1p11.2-p13.2 and consists of the substitution of C to T at nucleotide 661. This turns a basic arginine (CGG) into a non-polar tryptophan (TGG) at the position corresponding to residue 211 in the proNGF, and position 100 in mature NGF (Einarsdottir et al., 2004).

The most evident clinical features of HSAN V patients are fractures located in the lower legs and feet, that appear during childhood in homozygous subjects (Einarsdottir et al., 2004; Minde et al., 2004; Minde, 2006; Capsoni, 2014). In contrast, in heterozygous subjects, fractures appear during adulthood and are less frequent than in homozygotes (Minde et al., 2009). This correlates with that fact that, in homozyotes, pain sensations are decreased mainly at the forearms and legs, whereas the pain sensation is normal at the level of the trunk (Einarsdottir et al., 2004). These symptoms are not present in heterozygous carriers (Minde et al., 2009). In both heterozygous and homozygous patients, cold and heat thresholds are increased, visceral pain is normal and, finally, sensitivity to soft touch, joint position and vibration sensation are normal (Einarsdottir et al., 2004; Minde et al., 2004; Minde et al., 2009). Motor conduction velocity and amplitude were measured in peripheral nerves of both heterozygous and homozygous patients and found to be normal (Einarsdottir et al., 2004; Minde et al., 2009). Sural nerve biopsies were also examined, and all patients showed a small reduction of Aδ fibers and a severe reduction of C fibers. This reduction was less severe in heterozygous patients, thus explaining the milder phenotype (Minde et al., 2009). Using in vivo corneal confocal microscopy (CCM) to quantify C-fiber loss in the cornea, Perini and colleagues showed that homozygotes present a significant afferent reduction compared to heterozygotes and control subjects. Importantly, peripheral C-fiber loss correlated negatively with subjective pain evaluation, as revealed by the results of Situational Pain Questionnaire (SPQ) (Perini et al., 2016).

1.6.2 Processing, secretion and biochemical features of R100W protein

Larsson et al. examined the functional consequences of the R100W (NGF^{R100W}) mutation on NGF processing and secretion (Larsson et al., 2009). They found that NGF^{R100W} fails to induce differentiation of PC12 cells, suggesting that the mutation causes a loss of function. They also found that PC12 and COS-7 cells transfected with human NGF^{R100W} secreted a very low amount of mature NGF in the culture medium compared to wild type NGF. On the contrary, transfected cells showed an increased intracellular accumulation of pro-NGF^{R100W}, with no signs of ER stress (Larson et al., 2009). The Authors argued that this accumulation of pro-NGF^{R100W} was not due to protease resistance, but to a different intracellular localization that would prevent the processing and secretion of mature NGF. Indeed, human pro-NGF^{R100W} was mainly found in the cytoplasm of PC12 cells, and only a small amount was found in secretory components, available for proteolytic processing and secretion (Larsson et al., 2009). Additional information about the possible alterations in processing and secretion comes by a paper by (Covaceuszach et al., 2010). They expressed human proNGF precursor proteins in *Escherichia coli* in order to purify the mature protein and they found that the yield of human NGF^{R100W} was very low. They concluded that the substitution of the positively charged arginine with tryptophan is likely to increase the hydrophobicity of the protein, thus inducing the formation of aggregates (Covaceuszach et al., 2010).

NGF^{R100W} binding to receptors was investigated by analysis of the crystallographic structures of the complexes formed with the extracellular domains of TrkA and $p75^{NTR}$. The major effect of the R100W mutation was predicted to impinge on the interaction with $p75^{NTR}$ and not so much on the interaction with TrkA. In particular, the R100 residue of NGF is involved in an electrostatic interaction with residue D75 of $p75^{NTR}$. Notably, residue D75 is conserved in $p75^{NTR}$ from most species, with the exception of *Danio rerio*. Similarly, residue R100 is conserved in the primary sequences of NGF and other neurotrophins from all species, with the only exception of *Danio rerio*. Moreover, residue R100 is not part of the contact zone between NGF and TrkA (Covaceuszach et al., 2010). Indeed, it has been verified that human NGF^{R100W} is characterized by a binding affinity for TrkA similar to wild-type NGF, whereas the R100W mutation induced a significant reduction of the binding of mature human NGF^{R100W}, but not human $proNGF^{R100W}$, to $p75^{NTR}$ (Covaceuszach et al., 2010).

Regarding the activation of signal transduction, NGF^{R100W} is able to bind TrkA, but the ensuing phosphorylation at Tyr490 was diminished, correlating with a strong reduction in the activation of both PLC-γ1 and ERK1/2 (Capsoni et al., 2011). In a recent paper, it has been reported that NGF^{R100W} does not elicit acute thermal or mechanical hyperalgesia *in vivo*, but the receptor binding and signaling capabilities necessary to induce hyperalgesia priming are retained (Sung et al., 2018). Sung et al. confirmed that NGF^{R100W} activates TrkA-mediated signaling pathways, but fails to stimulate downstream effectors of $p75^{NTR}$. The same paper also showed that NGF^{R100W} is retrogradely transported, inducing differentiation and supporting the survival of sensory neurons but was not able to potentiate their H^+-evoked responses (Sung et al., 2018). A new study identifies a further mutation (R121W) responsible for HSAN V and localized in the last residue of the furin cleavage motif RSKR in proNGF. This mutation does not affect the localization of NGF but interferes with the full cleavage of proNGF, abolishing the formation of mature NGF with only the proB form of proNGF being secreted. The R121W NGF shows reduced capability to induce neurite outgrowth in pc12 cells, whereas, the secreted proB form does not induce apoptosis. The authors hypothesize that the HSAN V phenotype is caused by reduced availability of mature NGF, rather than the effects of apoptosis on developing nociceptors (Shaikh et al., 2018).

2. AIM of the THESIS

NGF is an essential survival factor for sympathetic neurons and a subpopulation of sensory dorsal root ganglia neurons (see above, Introduction). Many studies reported that NGF plays a key role in pain transduction mechanisms in the adult nervous system. NGF is a key mediator of pain transmission at the peripheral level, a role that has been reinforced by the discovery that NGF mutations cause congenital forms of insensitivity to pain (Hereditary Sensory and Autonomic Neuropathy type V, or HSAN V). However, the precise role of NGF in constructing the "pain" perception in the brain has received scarce attention. In addition, whether and how the pain experience can influence learning of fear responses is still debated. Finally, the impact of the HSAN V R100W point mutation on these phenomena is unknown.

- Considering that a valid model for HSAN V disease does not exist, the first aim of this project was the generation and characterization of a knock-in mouse model carrying the human R100W mutation;
- A second goal was to analyzing the pain sensitizing properties of the human NGF^{R100W} protein, in comparison to those of the wild type counterpart, by studying pain-related pathways in DRG cultures;
- Finally, this thesis also focuses on investigating the mechanisms underlying the central processing of peripheral nociceptive inputs to construct the "pain" perception, an essential sensory experience, instrumental to the acquisition of memories endowed with affective and emotional meaning. In particular, the experiments focus on the interplay between nociception and construction of the pain perception in heterozygous knock-in mice ($NGF^{R100W/m}$) and HSAN V heterozygous human carriers.

3. MATERIALS and METHODS

3.1 Generation of knock in human $NGF^{h/m}$ and $NGF^{R100W/m}$ mice

pCMV6-XL5-human NGF^{WT} plasmid was obtained from OriGene Company (MD, USA; #SC123827) and pCMV6-XL5-hNGF^{R100W} was generated using site-specific mutagenesis PCR.

The targeting constructs were generated using classical cloning technologies. Briefly, a BAC vector (clone RP24-160F12) containing the entire regions of interest flaking the NGF sequence, was used to generate intermediate plasmids by cloning in pBluescript SK(-) the 5' homology arm (from 89489 to 94076, restriction site MfeI) and 3' homology arm (from 94803 to 99710, restriction site HindIII). The human NGF coding sequence (OriGene #SC123827) and the human NGF^{R100W}, obtained by PCR, were cloned in pBluescript SK^-.Then, the coding regions (WT and R100W), flanked by the homology arms, were cloned in pKO2.1 targeting vector carrying the DTA negative selection cassette (kindly provided by Dr. L. Ronfani). Neo cassette was cloned blunt in AgeI site downstream of hNGF. The final targeting vectors were linearized prior to electroporation using the NotI restriction site. The targeting vectors were transfected into R1p.15 cells (background SV129) and positive clones were selected using Neomycin resistance.

3.2 Southern Blot analysis

Genomic DNA was extracted by means of phenol:chloroform:isoamyl alcohol from about 350 cell clones electroporated with either WT or R100W targeting vectors. DNAs were incubated first with EcoRI (for 5' screening), then positive clones were confirmed with XbaI digestion (for 3' screening). Digestions were run in a 0.8% agarose gel O/N at 50 V. After a mild depurination and denaturation, gels were blotted on nitrocellulose and filters incubated with an external 5' or 3' probe (Fig. 1). The 5' probe labels a 10.7 kb EcoRI band in the WT allele (Fig. 1A) and a 5.2 kb EcoRI band in recombinant alleles (Fig. 1B). The 3' probe labels an 8 kb XbaI band in the WT allele (Fig. 1A) and a 12.7 kb XbaI band in recombinant alleles (Fig. 1B).

Positive clones were injected into the blastocysts of C57BL/6 mice and chimeric animals were obtained. Mice were genotyped by PCR. The following PCR primers were used:

fw_human: 5'-TTTAGCACCCAGCCTCCCCGTGAAG-3'

fw_mouse: 5'-CAGAAGGAGACTCTGTCCCTG-3'

rev_human-mouse: 5'-CACCTCCTTGCCCTTGATGTCTG-3'

Band sizes are: wild-type 400 bp, mutant 200 bp (Fig. 1C).

3.3 Ethics statement on mouse experiments

All animal procedures were approved by the Italian Ministry of Health and were fully compliant with Italian (Ministry of Health guidelines, Legislative Decree n°26/2014) and European Union (Directive n°2010/63/UE) laws on animal research. The experiments were carried out in strict accordance with the approved guidelines. In addition, the principles of the Basel Declaration, including the "3R" concept, have been considered throughout the whole project.

3.4 Behavioral analyses

Experiments were performed on $NGF^{m/m}$, $NGF^{R100W/m}$, $NGF^{h/m}$, $mNGF^{+/+}$, $mNGF^{+/-}$ mice. Mice were kept under a 12 h / 12 h light/dark cycle, with food and water *ad libitum*.

3.5 NGF treatment

Mouse wild type NGF protein was administered daily at the dose of 1 µg/kg to pregnant dams by subcutaneous injection; treatment was protracted until 10 days after delivery. From postnatal day (P) 10 to P60, pups received a daily subcutaneous injection (1 µg/ kg) and intranasal administration (480 ng/kg) of NGF. A 21-day washout period was allowed before subsequent experiments.

3.6 Object recognition test

The apparatus consisted of a PVC arena (60 × 60 × 30 cm) with white floor and black walls. The test was performed in 3 days. On day 1, mice were subjected to a habituation phase in which they received two 5-min sessions in the empty arena, separated by a 30-min interval. On day 2, mice were exposed to two identical objects for 7 min to evaluate the total time of exploration. On day 3, mice were placed back in the arena and exposed to a familiar object and another novel object (memory phase). The time spent exploring each object was recorded.

3.7 Morris water maze (MWM)

The test was performed in a water tank (120 cm diameter) filled with white opaque water. The platform, placed in the center of SW quadrant, was submerged 1 cm below the water surface. 6-months-old mice were trained with 2 trials per day, with a 40 min interval, for 9 consecutive days. Mice were allowed up to 2 min to locate the platform and the latency to reach it was recorded. If the mouse failed, the experimenter guided it onto the platform. Data were acquired and analyzed using an automated tracking system (Noldus Ethovision XT, NE).

3.8 Y-maze test

A PVC maze consisting of three identical arms (40 × 13 × 10 cm) that converged at an equal angle was employed. Each mouse was placed in the center of the maze and allowed to explore freely the arms during an 8-min session. An entry was scored when the mouse was at least halfway through an arm of the maze. An alternation was scored when all the three arms were entered on consecutive events. The percentage of spontaneous alternations (% SAP) was calculated according to the following formula: % SAP = number of alternations / total entries × 100.

3.9 Elevated plus maze

The elevated plus maze consisted of two closed arms and two open arms (each 30 × 5 cm) extending from a central platform at 90°. Mice were placed on the central platform and allowed to freely explore the maze; the times spent in the open arms, closed arms and center were measured.

3.10 Marble burying test

Mice were put O/N in a cage containing 6 glass marbles placed on a 5-cm deep layer of bedding. The next morning, mice were removed from the cage and the number of marbles buried with bedding at least to 2/3 of their diameter was counted.

3.11 Nest building test

Following the protocol reported in (Deacon, 2006), 1 h before the onset of the dark phase, mice were put in a testing cage containing the material (paper) for a nest. The following morning, the nest was examined and its appearance was classified according to the published scoring scale (1 to 5).

3.12 Hot plate test

Mice were placed on a surface heated from 42°C to 54°C with 3°C steps. Animals were sequentially tested, allowing a 10-min resting period between each temperature step. The temperature threshold required to observe paw licking and the time required to observe this reaction at each temperature step were recorded.

3.13 Cold sensitivity test

Mice were put in a plastic cage and habituated for 30 min. Acetone (50 µl; Sigma-Aldrich) was sprayed onto the plantar surface of the hind paw using a Gilson pipette and the responses were reported as a four-point score: 0 = no response, 1 = brisk withdrawal or flick of the paw, 2 = repeated flicking of paw, 3 = repeated flicking of the hind paw with licking. Acetone was applied six times, alternating between paws, with an interval of 5 min between each application. The frequency of response, expressed as a percentage (number of trial characterized by a response / total number of trials) was evaluated.

3.14 Capsaicin injection test

Mice were placed individually in a Plexiglas box for 15 min before drug injection to allow habituation. Capsaicin (Abcam, UK; #141000) was dissolved in dimethyl sulfoxide (DMSO) and injected in the ventral surface of the right hind paw using a Hamilton syringe at a concentration of 3 µg/µl in saline solution (total injection volume 10 µl; 0.1% DMSO final concentration). Control mice were injected with 10 µl of 0.1% DMSO in saline. Following the injection, mice were observed for 15 min and the amount of time spent licking and/or lifting the injected paw was measured.

3.15 Tape response assay

Mice were habituated to a plexiglass container for 5 min and then a 3-cm piece of adhesive tape was applied to the back. Mice were observed for 5 min to measure the latency to the first tape removal attempt and the total number of attempts.

3.16 Cotton swab assay

Mice were placed in an arena consisting of an elevated chamber with a grid floor and allowed to habituate for 1 h. A cotton swab was stroked through the floor along the plantar paw surface five times, alternating between paws with a 10-s interval. The number of withdrawals were counted and expressed as percentage of the total number of trials.

3.17 *In vivo* nociceptive assay

As reported in (Capsoni et al., 2011), CD1 male mice (Charles River, I) were subjected to a mechanical allodynia behavioral test after the injection of either WT or R100W NGF in the hind paw plantar surface at a 0.2 μg/μl concentration (corresponding to 4 μg in a total injection volume of 20 μl) in saline. Control mice were injected with 20 μl of saline. The von Frey test (Ugo Basile, I) was performed before treatment and 1, 3, 4 and 5 h post-injection.

3.18 Cued fear conditioning

A sample group of adult mice (two- and six-months old) was subjected to a preliminary trial to evaluate the foot-shock electric threshold; the resulting response was scored as: 0 = no response, 1 = flinch, 2 = jump/run, 3 = vocalization. The threshold was set as the minimal current intensity causing a “score 3” response. The test was performed in three days. On day 1, mice were habituated to the apparatus, i.e., were left free to explore the testing chamber for 3 min; on day 2, mice were subjected to the “association phase” characterized by 5 repetitions of a tone lasting 10 s that, at second 9, was associated to a 1-s electrical stimulus. On day 3, mice were put in a different chamber and in the “recall phase”, the 1-s tone alone was repeated 8 times and the amount of time spent in freezing was assessed. Freezing was defined as the complete absence of motion, including motion of the vibrissae, for a minimum of 0.5 s. On day 3, mice

were transcardially perfused with 4% PFA in PBS (pH 7.4) within 90 min from the end of the recall phase, and the brains were collected to perform c-Fos immunohistochemistry (see above for method). The number of c-Fos-immunoreactive cells was manually counted using ImageJ software and normalized on the area of interest.

3.19 Contextual fear conditioning

On day 1, mice were subjected to a habituation phase, i.e., they were left free to explore the chamber for 3 min; on day 2, mice were placed again in the testing chamber and received 5 electrical stimuli. On day 3, mice were put in the same context and the amount of time spent in freezing time was assessed (recall phase); after 1 h, mice were put in a different context (reversal phase) and the freezing time was measured.

3.20 Predator fear

The experiments were performed according to the protocol reported in (Silva et al., 2013). Briefly, on days 1 to 3, mice were free to explore the entire apparatus in a single 20-min daily session (habituation phase); on day 4, after 10 min of exploration, mice were confined to the stimulus compartment and exposed for 10 s to a rat (predator phase). The behavior in the first 3 min of days 1-3 and in the first 3 min after rat exposure were scored by quantifying the time spent in immobility or locomotion.

3.21 Immunohistochemistry

Mice were transcardially perfused with 4% PFA in PBS (pH 7.4), and brains were dissected and post-fixed O/N in the same solution, then cryoprotected in 30% sucrose in PBS for 36 h. The brains were sectioned with a sliding freezing microtome (Leica Microsystem, Germany) to obtain 45 µm-thick coronal sections that were washed 3 times in TBS with 0.3% Triton X-100, then treated with 3.5% H_20_2 in TBS to inactivate endogenous peroxidases. Free-floating sections were blocked for 30 min with 10% FBS, 0.3% Triton X-100 in TBS, followed by an O/N incubation at 4°C with either 1:500 goat anti-ChAT (Millipore #AB144P), 1:1000 rabbit anti-c-Fos (Millipore #ABE457), 1:1000 rabbit anti-oxytocin (Millipore #AB911), 1:1000 rabbit anti-CGRP (Millipore #AB5705). Biotinylated secondary antibodies (Vector Labs) were diluted in 10% FBS in PBS for 3 h at RT. Finally, sections were incubated in Vectastain ABC HRP Kit (Vector Labs,

CA, USA) in PBS for 1 h, followed by another incubation in TBS solution containing 3,3'-diaminobenzidine HCl (DAB, Sigma-Aldrich) and the enzyme Glucose Oxidase Type VII (Sigma-Aldrich); the reaction was stopped after 10 min. Stained sections were mounted on glass slides using DPX medium. Images were acquired with a Nikon Eclipse E600 optical microscope and the density of immunoreactive cells was calculated using ImageJ.

For β-endorphin immunofluorescence experiments, free-floating sections were blocked for 30 min at RT in 5% Normal Goat Serum, 0.2% Triton X-100 in PBS, followed by an O/N incubation at 4°C with 1:1000 rabbit anti- β-endorphin (Chemicon, #AB5028) in 1% Normal Goat Serum, 0.2% Triton X-100 in PBS . Sections were revealed by incubation with 1:200 anti-rabbit secondary antibody conjugated to Alexa Fluor-488 fluorophore (Thermo Fisher Scientific, MA, USA) diluted in 1% Normal Goat Serum, 0.2% Triton X-100 in PBS for 2h at RT. Images of β-endorphin immunoreactivity in arcuate nucleus were acquired using a Leica TCS SP confocal laser-scanning microscope (Leica, Germany).

For brain microglia staining, free-floating sections were blocked for 30 min at RT in 10% Normal Goat Serum, 0.3% Triton X-100 in PBS, followed by an O/N incubation at 4°C with 1:500 rabbit anti- IBA1 (Wako, NCNP24) in 5% Normal Goat Serum, 0.3% Triton X-100 in PBS . Sections were revealed by incubation with 1:100 anti-rabbit secondary antibody conjugated to Alexa Fluor-488 fluorophore (Thermo Fisher Scientific, MA, USA) diluted in 5% Normal Goat Serum in PBS for 3h at RT. Images for microglia analysis were acquired using a Leica TCS SP confocal laser-scanning microscope (Leica, Germany). Images elaboration and analysis were conducted using Bitplane's software Imaris (Zurich, Switzerland).

3.22 Electrophysiological recordings

Mice were sacrificed using CO_2 inhalation and the saphenous nerve was dissected and placed in an organ bath(Lewin et al., 2014). The chamber was perfused with a synthetic interstitial fluid (SIF) buffer containing (in mM): NaCl 123, KCl 3.5, $MgSO_4$ 0.7, NaH_2PO_4 1.7, $CaCl_2$ 2.0, Na-gluconate 9.5, glucose 5.5, sucrose 7.5, and HEPES 10, pH 7.4) at 3 ml/min at 32°C. The distal part of the nerve was placed in the organ bath, while the proximal part was placed in an adjacent chamber filled with mineral oil for recording. An electric probe was used to stimulate the nerve and a compound action potential was recorded and analyzed using LabChart4 (AD Instruments, AU) software. Each electrical stimulus elicited a response consisting of three

peaks, corresponding to the Aβ, Aδ and C fibers, respectively. To measure the conduction velocity of each fiber type, the time elapsed from the beginning of the stimulus to the appearance of the peak was divided by the distance between the electric probe and the recording electrode.

3.23 Skin and DRG immunofluorescence

DRGs from adult mice (two- and six-month old) were collected in an eppendorf tube containing cold PBS, then post-fixed in 4% PFA for 30 min at RT, embedded in 2% agarose and sectioned at 50 µm thickness using a vibratome. Sections were washed twice with PBS-Triton 0.3%, then subjected to a 30-min blocking step in 5% NGS and 0.3% Triton X-100 in PBS, followed by an O/N incubation at 4°C with primary antibodies diluted as shown below. AlexaFluor-conjugated secondary antibodies (Thermo Fisher Scientific, MA, USA) were diluted 1:1000 in 0.3% Triton X-100, 5% NGS in PBS for 2 h at RT. Sections were mounted using Prolong Gold medium (Invitrogen, CA, USA).

For immunofluorescence analysis, the hairy and glabrous skins were collected, allowed to dry and post-fixed in 4% PFA at 4°C O/N, then incubated in 30% sucrose in PBS and frozen in OCT medium (Leica, Germany). Sections (50-µm thick for hairy skin, 20-µm thick for glabrous skin) were obtained using a cryostat. Immunostaining was performed as described above.

The antibodies and dilutions used were: 1:500 mouse anti-NF200 (Sigma-Aldrich, Germany), 1:200 mouse anti-CGRP (Rockland, PA, USA), 1:100 isolectin GS-B4-biotin conjugate (Invitrogen), 1:200 rabbit anti-B2R (Alomone Labs, IL), 1:300 mouse anti-TRPV1 (Millipore, MA, USA), 1:200 rabbit anti-PGP 9.5 (Dako-Agilent, CA, USA), 1:300 rabbit anti- NGF M20 (Santa Cruz Biotech., TX, USA).

All images were acquired with a Leica SP5 confocal microscope and analyzed with Fiji (NIH, MD, USA).

3.24 RNA preparation for microarray analysis

DRG from wild type and $NGF^{R100W/m}$ mice (six months of age) were isolated and collected. The total RNA was extracted with Trizol reagent (Life Technologies, Rockville, MD, USA) according to the manufacturer's instructions, DNAse-treated and purified using Qiagen columns. RNA content was determined on a NanoDrop UV-VIS. Only samples with an absorbance ratio of 1.8< OD260/OD280 <2.0

were further processed. Each sample was then quality-checked for integrity using an Agilent BioAnalyzer 2100 (Agilent G2938C, RNA 6000 nano kit).

3.25 Whole genome expression profiling

Gene expression profiling was performed using the Agilent one-color microarray System. Two hundred ng of Poly A+RNA were retrotranscribed using oligo-dT primers linked to the T7- promoter and the resulting cDNA was used as a template for cyanine 3-CTP labelled cRNA preparation, using the Agilent Low Input Linear Amplification Kit. The labeled cRNA was purified with RNeasy mini spin columns (Qiagen). To monitor both the labelling reactions and the microarray performance, Agilent Spike-In Mix was added to the mRNA samples prior to labelling reactions according the RNA Spike-In protocol. Cyanine 3 labelled cRNA was hybridized to Agilent 8x60K whole mouse genome oligonucleotide microarrays (Grid ID 028005). Microarray hybridizations were carried out in SureHyb Hybridization Chambers (Agilent) containing 600 ng of Cyanine 3-labelled cRNA per hybridization. The hybridization reactions were performed at 65°C for 17 h using Gene Expression Hybridization Kit (Agilent). The hybridized microarrays were disassembled at RT in Gene Expression Wash Buffer 1 (Agilent). After disassembly, the microarrays were washed in Gene expression Buffer 1 for 1 min at RT, followed by washing with Gene Expression Wash Buffer 2 for 1 min at 37°C. Then, microarrays were treated with acetonitrile for 1 min at RT. Fluorescence signals of the hybridized Agilent Microarrays were detected using Microarray Scanner System (G2564B, Agilent). The Feature Extraction Software (ver 10.7.3.1, Agilent) was used to process the microarray image files.

3.26 Microarray data analysis

Data filtering, normalization, analysis and plotting were performed using R-Bionconductor (https://www.bioconductor.org/). In particular, differential expression was analyzed with the R package limma v3.5 (Ritchie et al., 2015). All the features with the flag gIsWellAboveBG=0 (too close to background) were filtered out and excluded from the following analysis. Filtered data were normalized by aligning samples to the 75th percentile. Differentially expressed genes were selected by a combination of fold-change and moderated t-test thresholds (R limma test with FDR < 0.05, |Log2 foldchange ratio| > 1.0).

Pathway analysis and network plotting of differential gene lists was performed using the online tool StringDB (https://string-db.org ; (Szklarczyk et al., 2015).

3.27 Electron microscopy

Fixed nerves were washed in phosphate buffer at RT (10×5 min), osmicated in 2% (w/v) OsO4 in H2O (2 h at 4°C), washed again (0.05 M maleate buffer, pH 5.15 – 10×5 min) than dehydrated in ethanol (70 % (v/v) – 15 min; 80 % (v/v) – 15 min; 90 % (v/v) – 15 min; 100 % – 4×15 min). Subsequently, nerves were infiltrated first with propylene-oxide (Propylene-oxide – 2×15 min) then with a mixture of 50 % (v/v) propylene-oxide and 50 % (v/v) resin catalyzed with 2% DMP30 overnight at RT. Embedding (100% resin catalyzed with 2% DMP30) was followed by 24 h heat treatment for proper polymerization of resin at 65°C. Myelinated axons were counted on semi-thin (1 µm thick) sections stained with toluidine blue and imaged with a Zeiss Axioplan light microscope. Myelinated fibres were counted individually using MetaMorph software (MetaImaging, USA). In cases of multiple nerve components (i.e. separate bundles of fibers, with individual connective sheets), fiber counts were performed for each component and the corresponding values summed up. Unmyelinated axons were counted with the aid of Transmission Electron Microscopy (TEM) at 20.000× magnification. Sectioning was performed using a Leica Ultracut ultra-microtome (Leica, Germany). Ultra-thin sections (90 nm thick) were collected on single-hole copper grids (Formvar Support Film Slots, 2×1 mm Cu grids; FF2010-CU). Images were obtained using a Jeol 1200EX II transmission electron microscope (Jeol, Italy) equipped with a charge-coupled device (CCD) Olympus Veleta Megaview (Olympus, Germany) camera covering 5% of the total cross-section area of the nerve. Based on the cross-sectional area, a total of 211 fields/ $NGF^{m/m}$ and 146 fields/ $NGF^{R100W/m}$ samples were obtained covering central as well as peripheral portions of each nerve systematically. Image files were saved as TIFF and transferred to MetaMorph, where axons were counted manually.

3.28 NGF immunoprecipitation and western blot

Cerebral cortices were isolated from adult mice and quickly frozen in dry ice. Samples were then homogenated and proteins were extracted with lysis buffer (Tris-HCl 100 mM, NaCl 400 mM, SDS 0.1%, Triton X-100 1%). The homogenates were sonicated, incubated in ice for 30 min and centrifuged at

15000×g for 30 min at 4°C. Protein concentration in the supernatant was quantified using the Bradford method (Bio-Rad, CA, USA). 4 mg of protein were immunoprecipitated with an excess of anti-NGF αD11 antibody in NET gel buffer (Tris-HCl pH 7.5 50 mM, NaCl 150 mM, 0.1% Nonidet P-40, EDTA pH 8 1 mM, 0,25% gelatin, 0.02% NaN). After IP, total lysates were loaded on 12% acrylamide gels and blotted using nitrocellulose membranes. Blots were blocked using a solution of 5% milk and 0.5% Tween-20 in TBS, for 1h at RT. The primary antibody solution contained 2% milk, 0,5% Tween-20 and anti-NGF M20 (1:500, Santa Cruz Biotech.), in TBS. Incubation lasted overnight at 4°C. Blots were then incubated with 1:500 HRP-conjugated goat anti-rabbit secondary antibody (Santa Cruz Biotech.), for 1h at RT. The signal was detected by enhanced chemiluminescence (ECL) and images were acquired using a ChemiDoc system (Bio-Rad); the optical density was quantified using ImageJ (NIH).

3.29 Oxytocin and NGF ELISA

To measure oxytocin levels in plasma, blood samples were drawn from the right ventricle of adult mice and centrifuged at 1000×g for 15 min. Oxytocin and NGF concentration was determined using a commercial kit, respectively (Fitzgerald, MA, USA; Millipore, USA).

3.30 Hek293 cells culture

Hek293 cells were maintained at 37°C, 5% CO_2, in DMEM/F-12 medium supplemented with 10% FBS, 1% L-Glutamine and 1% penicillin/streptomycin (Gibco-ThermoFisher). Hek293 cells were transfected with pCMV6-XL5-human NGF^{WT} and pCMV6-XL5-human NGF^{R100W} plasmids following the manufacturer's instructions for Lipofectamine 2000 (Invitrogen). 48h after transfection, the supernatants were immunoprecipitated and subjected to Western blotting as described above.

3.31 Human NGF^{R100W} purification

Human NGF^{R100W} cDNA was cloned into the prokaryotic expression vector pET19b downstream the sequence of the human BDNF prodomain, to produce a chimeric human proBDNF/NGF^{R100W} construct, and expressed in the *E. coli* strain Rosetta(DE3)PLysS. The corresponding chimeric protein was refolded from inclusion bodies and purified using an adaptation of the protocol used for proNGF in Paoletti F et

al., 2015.

The purified proBDNF-NGF^{R100W} was proteolitically processed with trypsin to produce mature NGF^{R100W}, as previously described in (Paoletti et al., 2015).

3.32 Dorsal root ganglia neurons primary cultures

Dorsal root ganglia (DRGs) neurons were prepared from neonatal (5 days, P5) Wistar rats (Charles River, I) from both sexes, as reported in (Bonnington and McNaughton, 2003; Taneda et al., 2010). Briefly, DRGs were collected, incubated for 1 hour at 37°C with 0.125% collagenase (Sigma-Aldrich), mechanically dissociated and plated onto coverslips or Petri dishes pretreated with 10 μg/mL poly-L-lysine (Sigma-Aldrich), at a density of 50000 cells/well of a 48 well tissue culture plate. DRG cultures were maintained in serum-free medium, consisting of Dulbecco's modified Eagle's medium (DMEM)/F12 (Invitrogen) supplemented with 87.5 ng/mL 5-fluoro-2′-deoxyuridine, 37.5 ng/mL uridine, 50 U/mL penicillin and 50 μg/mL streptomycin (all from Sigma) and 0.05% N2 supplement (Invitrogen) at 37 °C in 5% CO_2. The treatment with N2 supplement allows the presence of a physiological level of growth factors, thus preventing the occurrence of a neurotrophin withdrawal state. After 2–3 days in vitro, DRG cultures were stimulated for experimental procedures using either control human NGF^{WT} or human NGF^{R100W} (100 ng/ml) for 5 days, or maintained in basal medium conditions (CTRL). At the end of this incubation period, B2R and phospho-TRPV1 (pTRPV1) protein expression was measured by Western blot after 3 h bradykinin (1 μM) application (antibodies used: rabbit anti-B2R, 1:1000, Alomone Labs; rabbit anti-pTRPV1 and anti-TRPV1, both 1:1000, Millipore). Substance P (SP) was quantified in the culture medium using commercial enzyme immunoassay (EIA), according to the manufacturer's instructions (Cayman Chemical, MI, USA). To characterize neuronal viability, DRG cultures were fixed in 4% PFA for 10 min at RT, incubated O/N at 4°C with mouse anti-NeuN (1:200, Sigma-Aldrich), and rabbit anti-Neurofilament 200 (1:200, Sigma-Aldrich) followed by goat anti-mouse secondary antibody (1:400, Sigma-Aldrich), goat anti-rabbit rhodamine-conjugated secondary antibody (1:1000, Sigma-Aldrich) and Hoechst 33258 (0.25 μg/ml) for 1 h and 5 min, respectively, at RT. Fluorescence images were acquired using an Olympus BX51 microscope and a 60× oil immersion objective (N.A. 1.4). The number of NeuN-immunoreactive cells was normalized

on the total number of cells (i.e., Hoechst-stained). At least 40 microscopic fields per coverslip, in four coverslips from three independent experiments, were quantified for each experimental group.

3.33 Behavioral tasks on human subjects

Twelve individuals heterozygous for the R100W mutation (mean age = 36.2, SD = 15.4 years) were tested using a paradigm published in (Perini et al., 2013) and compared to age, gender and education matched controls (n = 12; 6 males; mean age = 35.8, SD = 15.8). All participants gave informed consent, in accordance with the Declaration of Helsinki and approval by the local ethics committee, and were compensated for their participation. Before scanning, individuals' discriminative and noxious thresholds for heat were collected. A series of predetermined stimulation temperatures were presented to the participants. Stimuli were delivered using a peltier thermode (Pathway model ATS, 30 mm, Medoc). Discriminative scores reflected individual thresholds for cool-warm discrimination, whereas noxious scores reflected threshold for pain (8 on a numeric rating scale, NRS, with anchors 0 = no pain; 10 = intense pain). Stimulation temperatures in the functional Magnetic Resonance Imaging (fMRI) experiment were based on the resulting individual thresholds.

The experimental paradigm was adapted from Perini et al.,. A series of 24 thermal stimulations (noxious and innocuous heat) was delivered on the dorsal part of the left hand in the MRI scanner. The stimuli were pseudorandomized within 2 different sequences during 2 separate runs, counterbalanced across subjects. The duration of each stimulation was 4 s. In all trials, the thermode had reached the target temperature when it was applied to the participant's hand. The interstimulus interval (ISI) varied from 10 s to 50 s. In one of the two runs, the participants were instructed to respond as quickly as possible to noxious, but not to innocuous, stimulation by pressing a button. In the other run, the participants responded only if the stimulation was nonpainful. For each participant the ratio of "hits" (correct responses to target stimulation), "misses" (missed responses to target stimulation), "false alarms" (wrong responses to non-target stimulation) and "correct rejection" (correct responses to non-target stimulation) on overall trial number were calculated and entered in a signal detection analysis. Resulting criterion scores were extracted and compared between groups. Criterion scores reflect the threshold of differentiation between signal and noise.

Due to scan discomfort one R100W participant discontinued during the second run. Three additional runs (one for a control and two for two R100W participants) were excluded because of inconsistent matrix dimension. Following scanning, participants underwent an additional behavioral paradigm which addressed voluntary motor behavior to painful and nonpainful stimulation. The paradigm tested the participants' motivational urge to escape ongoing stimulation. Thermal noxious heat and innocuous warm stimulation were applied to the dorsal part of the left hand for 4 s. As for the main experiment, stimulation temperatures were tailored to individual thresholds. Participants were asked to continuously rate their "urge to move" the stimulated hand away from the thermode, using a mouse positioned on the right hand. A scale going from "no urge" to "high urge" was displayed on a computer screen. For each participant the slope value of the continuous rating was calculated on the whole stimulation duration (0-4 s) and compared across conditions and between groups. In addition, the final urge score was extracted and compared across condition and between groups. This task allows the measurement of the motivational urge to produce escape movements to painful and non-painful stimulation.

3.34 fMRI acquisition and data analysis

Data were collected on a 1.5-T Philips Intera magnetic resonance imaging (MRI) scanner with a SENSE head coil. For functional imaging, a single-shot echo-planar imaging sequence was used to acquire the whole brain (T2*-weighted, gradient echo sequence, repetition time_3000, echo time_35 ms, flipangle_90°, field of view_200×244×128 mm). To minimize head movement, the participants' heads were stabilized with a vacuum hood filled with polystyrene balls (Vacuform Hood, Cambridge Research Systems, Cambridge, UK). Preprocessing and statistical analysis of MRI data were performed using BrainVoyager QX 2.1 (Brain Innovation, Maastricht, NE). Two dummy volumes were acquired before each scan in order to reduce possible effects of T1 saturation. Functional data were motion corrected and low-frequency drifts were removed with a temporal highpass filter (0.006 Hz). Spatial smoothing was applied with a 6-mm full width at half-maximum filter. Functional data were manually coregistered with 3-dimensional (3D) anatomical T1 scans (1 x 0.93 x 0.93 mm resolution resampled to 1 × 1 × 1 mm), on the basis of anatomical landmarks for each individual. The 3D anatomical scans were transformed into Talairach space. For each participant, general linear models were created for each of the 4 runs. One predictor (convolved with a

standard model of the hemodynamic response function, two gamma HRF) modeled each of the 8 conditions ("painful heat movement", "painful cold movement", "painful heat no-movement", "painful cold no-movement"; "nonpainful heat movement", "nonpainful cold movement", "nonpainful heat no-movement", "nonpainful cold no-movement"). To control for potential confounding factors related to movement we also included motion regressors in our analysis. Each predictor modeled the 1-s interval beginning with the onset of the cue during the last second of stimulation. Whole-brain random-effects contrasts were thresholded at $t = 3.2$ ($p < 0.001$), uncorrected for multiple comparisons. All maps have been thresholded at $p < 0.001$ uncorrected.

3.35 Data analysis and statistics

Statistical significance was assessed using SigmaStat 12 (Systat software, CA,USA) for mouse experiments, and FMRIB's Software Library (FMRIB, Oxford, UK, www.fmrib.ox.ac.uk/fsl) for fMRI data. Behavioral and beta values were analysed using IBM® SPSS® Statistics 25.0. Data are presented as mean ± SEM.

4. RESULTS

4.1 A new mouse model for HSAN V: characterization of homozygous mice

4.1.1 Generation of a new mouse model for HSAN V

Considering that a model to elucidate *in vivo* the mechanisms responsible for altered pain in HSAN V disease was missing, I have, first of all, generated two mouse knock-in lines carrying (i) the wild type human *ngfb* coding sequence ($NGF^{h/m}$ mice), at the locus of the mouse *ngfb* gene, to be used as a control line, and (ii) the HSAN V human NGF^{R100W} mutation in the human *ngfb* gene at the same locus (**Fig. 4.1**). Detailed steps performed for the cloning strategy are shown in **Appendix I**.

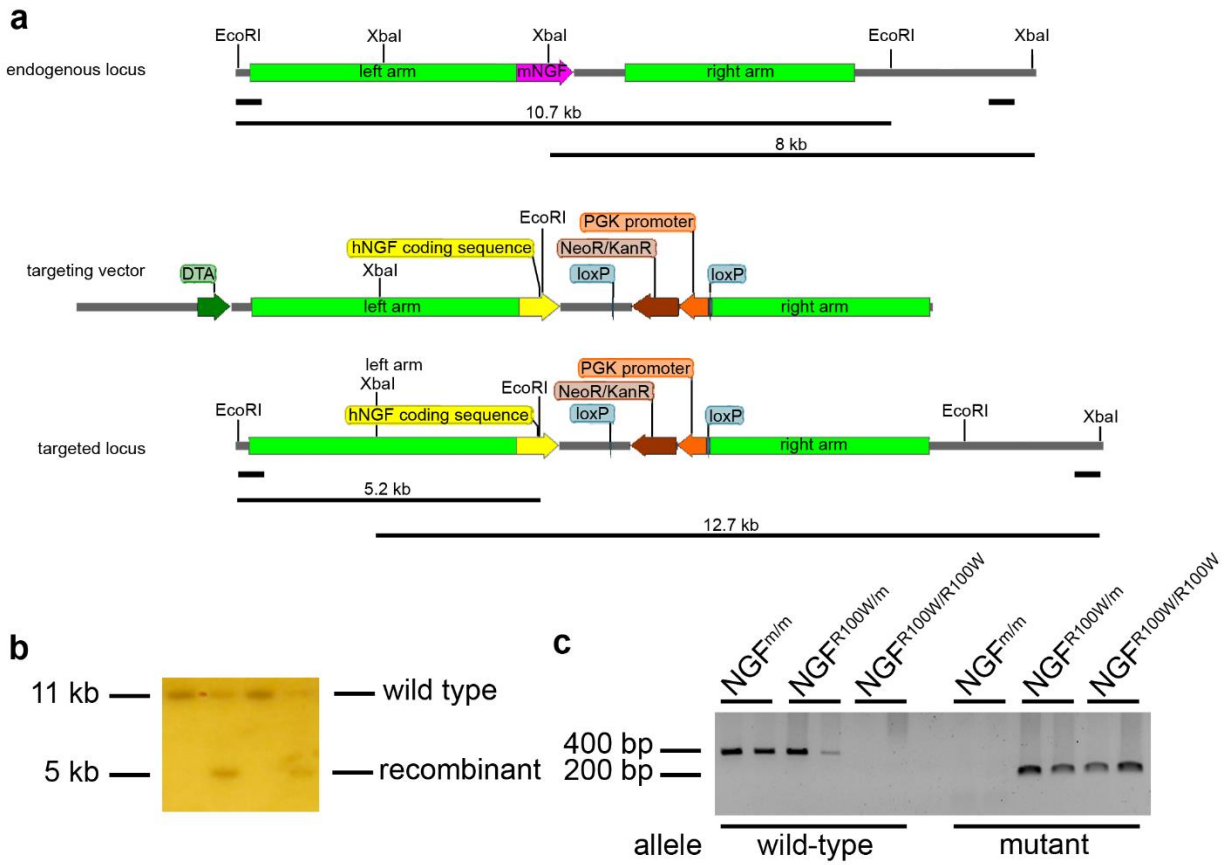

Figure 4.1 Molecular strategy for the generation of wild type and R100W knock-in mice. (A) *Top*, endogenous mouse NGF locus with 5' and 3' Southern blot probes and expected sizes of wild type bands; *middle*, targeting vector for site-specific recombination; *bottom*, targeted NGF locus with 5' and 3' Southern blot probes and expected sizes of recombinant Southern blot bands. Color codes are: pink, mouse NGF coding sequence; yellow, human NGF coding sequence; brown, NeoR positive selection cassette; orange, PGK promotor; blue, loxP sites; light green, left and right homology arms; dark green, Diphteria Toxin A (DTA) negative selection marker. **(B)** Representative image of ES cells Southern Blot. **(C)** PCR genotyping of $NGF^{R100W/m}$, $NGF^{m/m}$ and $NGF^{R100W/R100W}$ mice; wild type band: 400bp, mutant band: 200bp.

4.1.2 Homozygous NGF$^{R100W/R100W}$ mice display an early lethality that is rescued by NGF treatment

Compared to the only three known homozygous patients who reached the adult age despite their severe nociceptive defects (Einarsdottir 2004), homozygous NGF$^{R100W/R100W}$ mice die within the first month of life (**Fig. 4.2A**). I tested the hypothesis that this phenotype might be due to defects caused by the known inefficient secretion of the NGF^{R100W} protein ((Larsson et al., 2009); **Fig. 4.15A**, shown and discussed below), and therefore to a reduced bioavailability of NGF. Indeed, treatment of pregnant dams with subcutaneous NGF (1µg/kg) during gestation and until 10 days after delivery (thus allowing release of NGF in their milk), followed by intranasal NGF (480 ng/kg) to pups (to achieve access of NGF to the brain), reversed the early lethal phenotype of NGF$^{R100W/R100W}$ mice (**Fig. 4.2A**).

At birth, homozygous NGF$^{R100W/R100W}$ mice appear normal and their body weight is comparable to control mice, whereas at P15 the body weight of NGF$^{R100W/R100W}$ mice was significantly lower than wild type mice (**Fig. 4.2B**). After postnatal day 15 (P15), the body weight of NGF$^{R100W/R100W}$ mice could not be accurately sampled in a statistically significant way, because most of them died. NGF treatment was able to improve not only survival, but also to ameliorate the decreased body weight of NGF$^{R100W/R100W}$ mice; indeed, NGF-treated homozygous mice show a body weight that is totally overlapping to that of controls up to P15 (**Fig. 4.2C**). After this time point, the body weight of NGF-treated NGF$^{R100W/R100W}$ mice reached a plateau, whereas NGF$^{m/m}$ controls continued their postnatal growth (**Fig. 4.2C**).

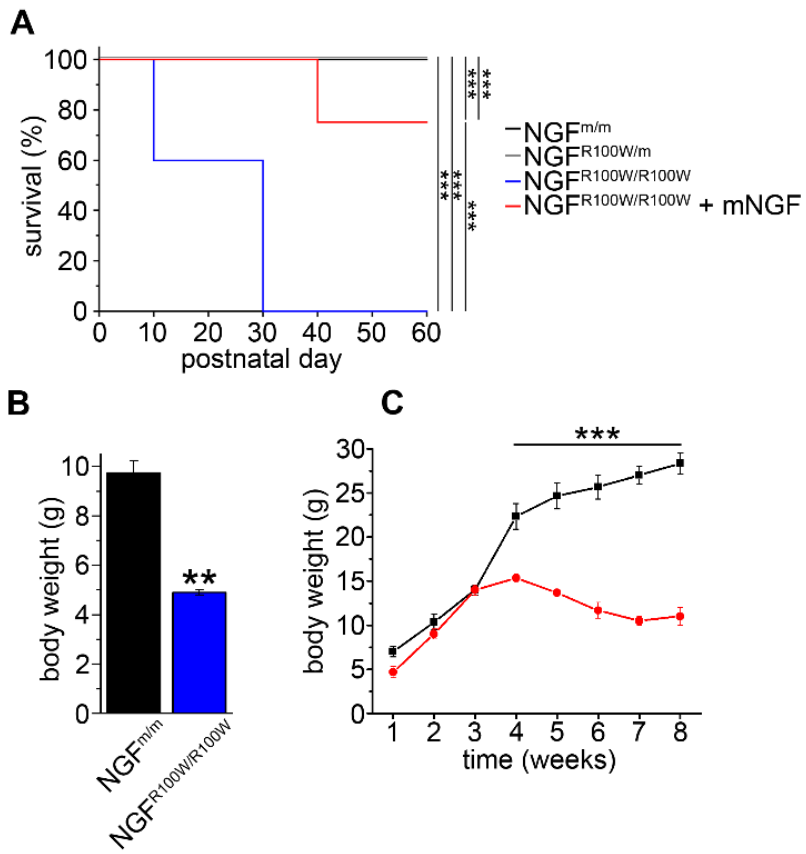

Figure 4.2 Rescue of early lethality of homozygous R100W mice by NGF^{WT} treatment. (**A**) Homozygous mice die within the first month of life. Daily treatment of pregnant dams with subcutaneous NGF until 10 days post-delivery, followed by subcutaneous and intranasal NGF to pups until two months of age, rescued lethality in NGF$^{R100W/R100W}$ mice. (**B**) At P15 the body weight of NGF$^{R100W/R100W}$ is lower than wild type mice. (**C**) NGF treatment improves the body weight of homozygous during early postnatal development.

4.1.3 Effects of NGF^{R100W} on cholinergic neurons of homozygous NGF$^{R100W/R100W}$ mice

NGF acts as an essential neurotrophic factor by regulating the function of forebrain cholinergic neurons via TrkA and p75^{NTR} receptors (Johnston et al., 1987). For this reason, I measured the number of Choline Acetyl-Transferase (ChAT)-immunoreactive neurons in the basal forebrain and striatum of NGF$^{R100W/R100W}$ mice. The density of ChAT^{+} neurons was unaffected in the medial septum (**Fig. 4.3A**) and nucleus basalis of Meynert (**Fig. 4.3B**), whereas, the density of ChAT^{+} neurons in the striatum of NGF$^{R100W/R100W}$ mice was increased (**Fig. 4.3C**). These results show that the bioavailability of mature NGF^{R100W} in the brain of NGF$^{R100W/R100W}$ mice is sufficient to achieve full neurotrophic support of target cholinergic neurons, despite its reduced secretion and suggest that NGF^{R100W} is able to preserve its neurotrophic functions on the

development and phenotypic maintenance of cholinergic neurons as well as of other target neuron (see below **Fig 4.6**).

The global bioavailability of NGF^{R100W} protein in the brain of homozogous $NGF^{R100W/R100W}$ mice could be ensured by the residual secreted mature NGF^{R100W} as well as by the cleavage of secreted $proNGF^{R100W}$ by extracellular proteases (Iulita and Cuello, 2014).

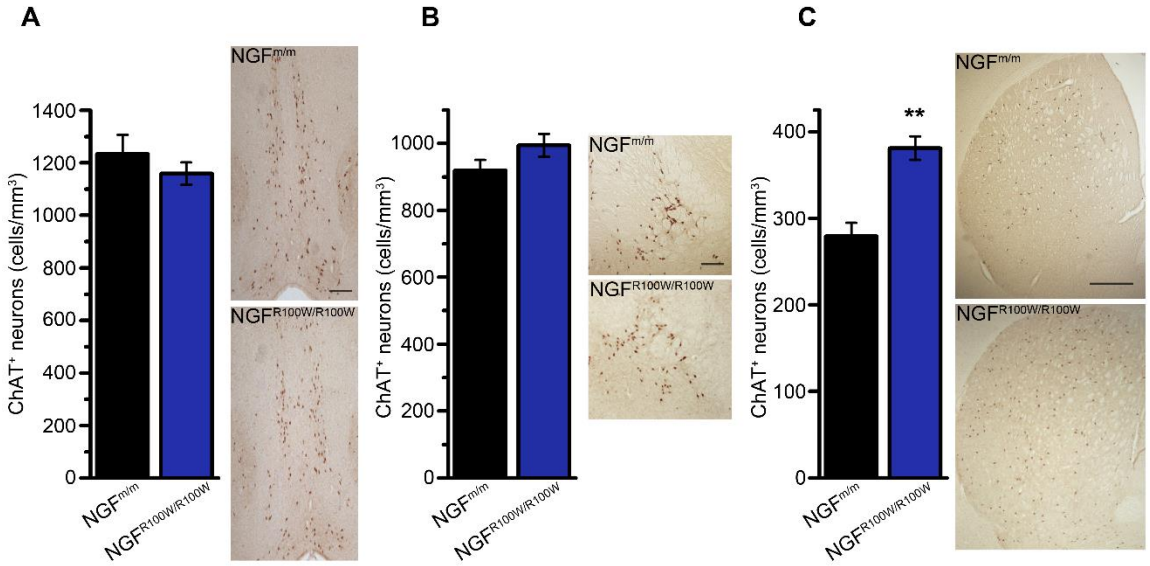

Figure 4.3 $ChAT^+$ neuron density specifically increased in the striatum of $NGF^{R100W/R100W}$ mice. Unaffected $ChAT^+$ neuron density in (**A**) basal forebrain and (**B**) nucleus basalis of Meynert of homozygous mice (scale bars, 200 µm). (**C**) Increased number of $ChAT^+$ neurons in striatum of $NGF^{R100W/R100W}$ mice compared to controls (scale bars, 500 µm).

4.2 Characterization of heterozygous HSAN V mice

4.2.1 Tactile-and pain-related behavioral characterization of heterozygous NGF$^{R100W/m}$ mice

In contrast to homozygote HSAN V patients, heterozygous human carriers do not present severe pain-related deficits, they lead a normal life and have been identified only through pedigree and genetic screening (Minde et al., 2009). Similarly to patients, NGF$^{R100W/m}$ mice develop normally and show no visible gross deficit. To shed light on the phenotypic consequences of R100W mutation, I performed an array of behavioral test to examine the ability of heterozygous NGF$^{R100W/m}$ mice to respond to noxious stimuli at two and six months of age, time points corresponding to youth and adulthood.

Injection of capsaicin into the hind paw causes acute thermal hypersensitivity and involves TRPV1 signaling (Tominaga and Caterina, 2004). I analyzed the behavioral response of NGF$^{R100W/m}$ mice for 15 minutes after capsaicin injection, and found that heterozygous HSAN V mice presented a significantly lower paw licking at both ages (**Fig. 4.4A**), indicating a reduced sensitivity to capsaicin-induced pain.

To look for possible alterations in thermoception, I used the hot plate and acetone drop tests to evaluate the response to hot and cold stimuli, respectively. Sensitivity to hot stimuli appeared to be normal at 2 months of age, whereas 6-month-old NGF$^{R100W/m}$ mice showed an increased latency to respond to high temperatures and an increased threshold for limb retraction at 55°C (**Fig. 4.4B**). Regarding cold sensitivity, both juvenile and adult heterozygous HSAN V mice showed a decreased response to evaporative cooling of the hind paw evoked by acetone (**Fig. 4.4C**).

I went on to examine tactile sensitivity to non-noxious mechanical stimuli in heterozygous NGF$^{R100W/m}$ mice, and noticed that the ability to detect and remove a small piece of tape stuck on their back was unaffected at 2 months of age, whereas the response latency was significantly increased at 6 months (**Fig. 4.4D**). To this regard, I also tested responses to dynamic mechanical stimulation of the skin by brushing the plantar surface of a hind paw using a cotton swab. I observed no alteration at 2 and 6 months (**Fig. 4.4E**), indicating that light touch sensation was normal.

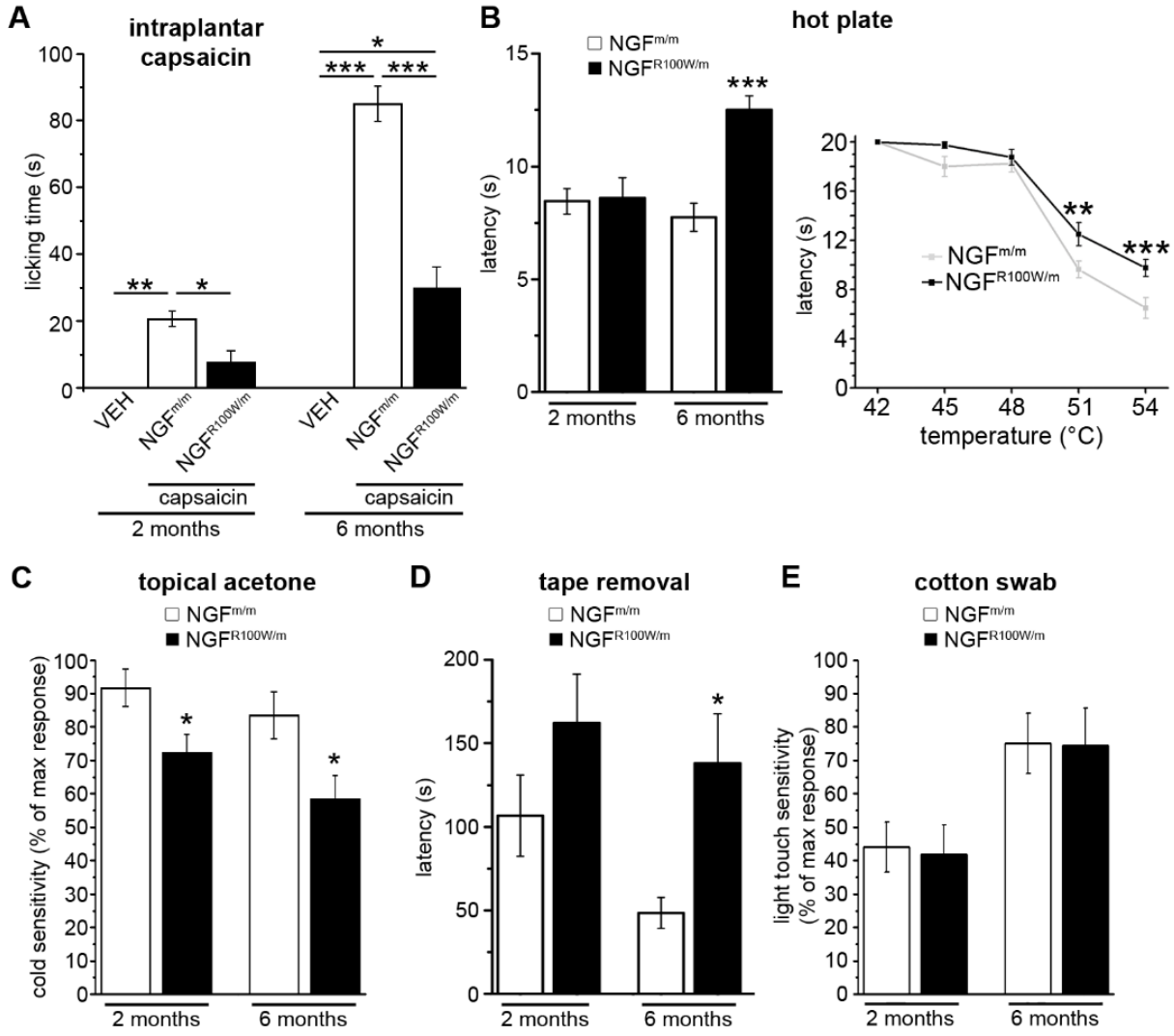

Figure 4.4 The R100W mutation induces an increased latency to respond to noxious stimuli but does not affect the light touch in glabrous skin. (A) Decreased hyperalgesic response to capsaicin in juveniles and adults. **(B)** Normal thermoception at 2 months of age, but increased latency to respond to high temperatures in $NGF^{R100W/m}$ mice at 6 months. **(C)** Impaired cold sensitivity in both juveniles and adults. **(D)** Decreased hairy skin sensitivity in adult HSAN V mice. **(E)** Normal light touch sensation.

4.2.2 The NGF R100W mutation does not affect peptidergic and non-peptidergic nociceptors in DRGs of $NGF^{R100W/m}$ mice

NGF plays an important role during the development of sensory neurons which, in fact, are completely lost in mice with nullizygosity for either TrkA or NGF (Crowley et al., 1994; Smeyne et al., 1994). Based on this, I analyzed dorsal root ganglia (DRGs) of $NGF^{R100W/m}$ mice to examine these neural structures, representing the first step in sensory transduction. I focused on the main NGF-sensitive neuronal

populations, evaluating the expression of (i) NF200, a marker for myelinated sensory neurons; (ii) Isolectin B4 (IB4), a marker for non-peptidergic nociceptors; (iii) Calcitonin Gene-Related Peptide (CGRP), a marker for peptidergic nociceptors. I found no change in the percentages of these DRGs neuronal populations, at neither of the ages tested (**Fig. 4.5**). In addition, I found no change in the total number of DRG neurons of $NGF^{R100W/m}$ mice (2 months, $NGF^{R100W/m}$ 1040.4±37.9, $NGF^{m/m}$ 1003.3±52.7 cells/mm^2, n=3 per group, Student's t-test, p=0.598, t=-0.571; 6 months, $NGF^{R100W/m}$ 1340.4±36.8, $NGF^{m/m}$ 1391.1±29.5 cells/mm^2, Student's t-test, p=0.324, t=1.044, $NGF^{R100W/m}$ n=6, $NGF^{m/m}$ n=5). These results show that the gross organization of the DRGs from $NGF^{R100W/m}$ mice is unchanged, providing an additional demonstration that the NGF^{R100W} protein has full neurotrophic potency, despite a possible reduced secretion. Indeed, human NGF^{R100W} has unchanged neurotrophic properties and supports survival of DRG neurons to a similar extent as wild type NGF (**Fig. 4.6**).

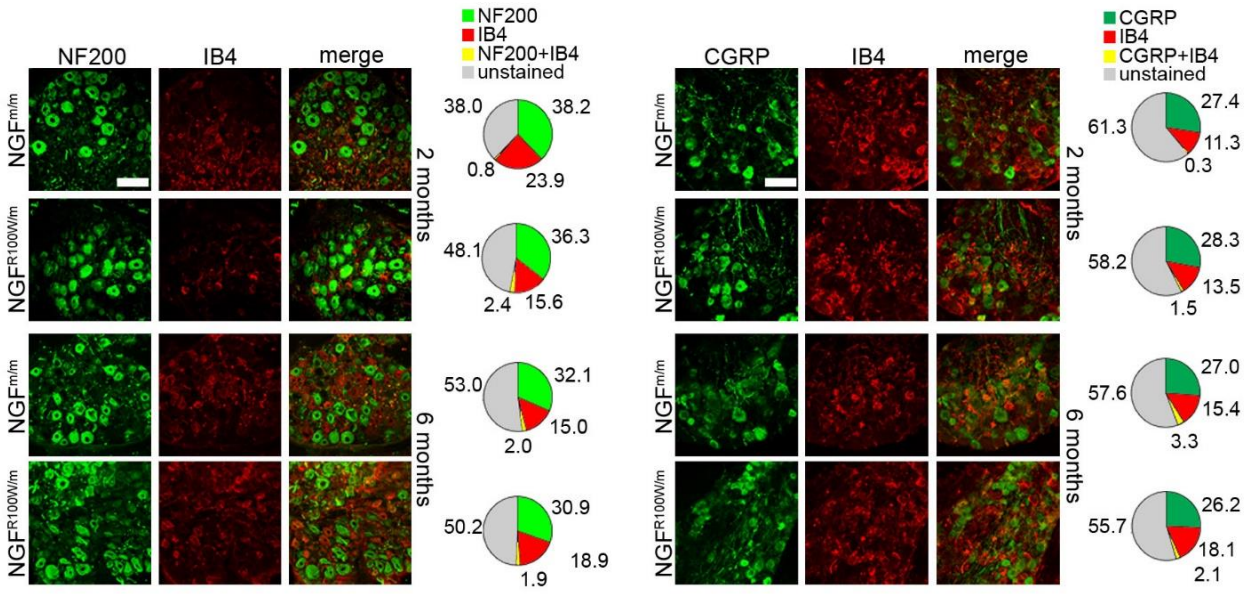

Figure 4.5 Normal development and differentiation of DRG neurons in $NGF^{R100W/m}$ mice. Normal expression of NF200, IB4 and CGRP in DRG neurons in both juveniles and adults (scale bars, 100 µm).

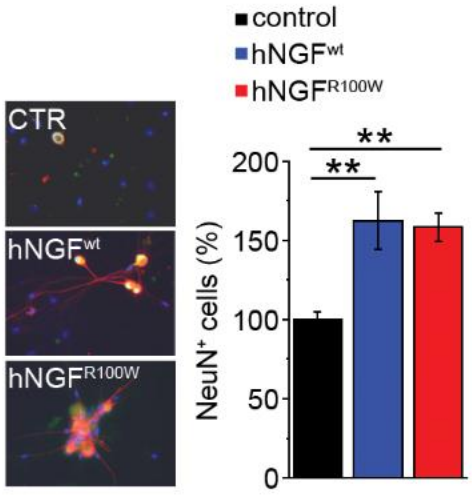

Figure 4.6 Neurotrophic effect of hNGF^{R100W} in DRG cultures. Comparable number of NeuN-immunoreactive cells after treatment with human NGF^{WT} and human NGF^{R100W}.

4.2.3 The NGF R100W mutation induces a limited number of specific transcriptomic changes in DRGs of NGF$^{R100W/m}$ mice

To obtain a broader vision of the features of DRGs from NGF$^{R100W/m}$ mice, and on the changes, with respect to DRGs from control mice, I performed (in collaboration with Dr. Ivan Arisi, EBRI, Rome, Italy) a transcriptomic analysis of adult DRGs (six months of age) to identify differentially expressed genes (DEGs) between NGF$^{R100W/m}$ and NGF$^{m/m}$ mice (**Fig. 4.7A**). I extracted RNA from DRGs and the gene expression profiling was performed using the one-color microarray system. The analysis revealed that only a limited number of genes were differentially expressed between the NGF$^{R100W/m}$ and control mice (150 DEGs in total). A pathway and network analysis of the DEGs revealed an effect of the R100W mutation on specific pathways implicated in immune response, phagocytosis and Rho GTPase activity (**Fig. 4.7B**), suggesting a minor change in neuron-specific genes and an intriguing involvement of glia. Among the regulated genes, TyroBP (TREM2) and Toll-Like Receptor 2 (TLR2) are noteworthy for their involvement in glial function (Liu et al., 2012; Shboul et al., 2018).

The specific consequences of how these mRNA expression changes contribute to the HSAN V phenotype is beyond the scope of this thesis, but the analysis of DRG neuronal populations and their expression profiles suggest that the NGF^{R100W} mutation has a limited global impact on the neuronal component of DRGs, and opens an intriguing window on an effect on their glial component.

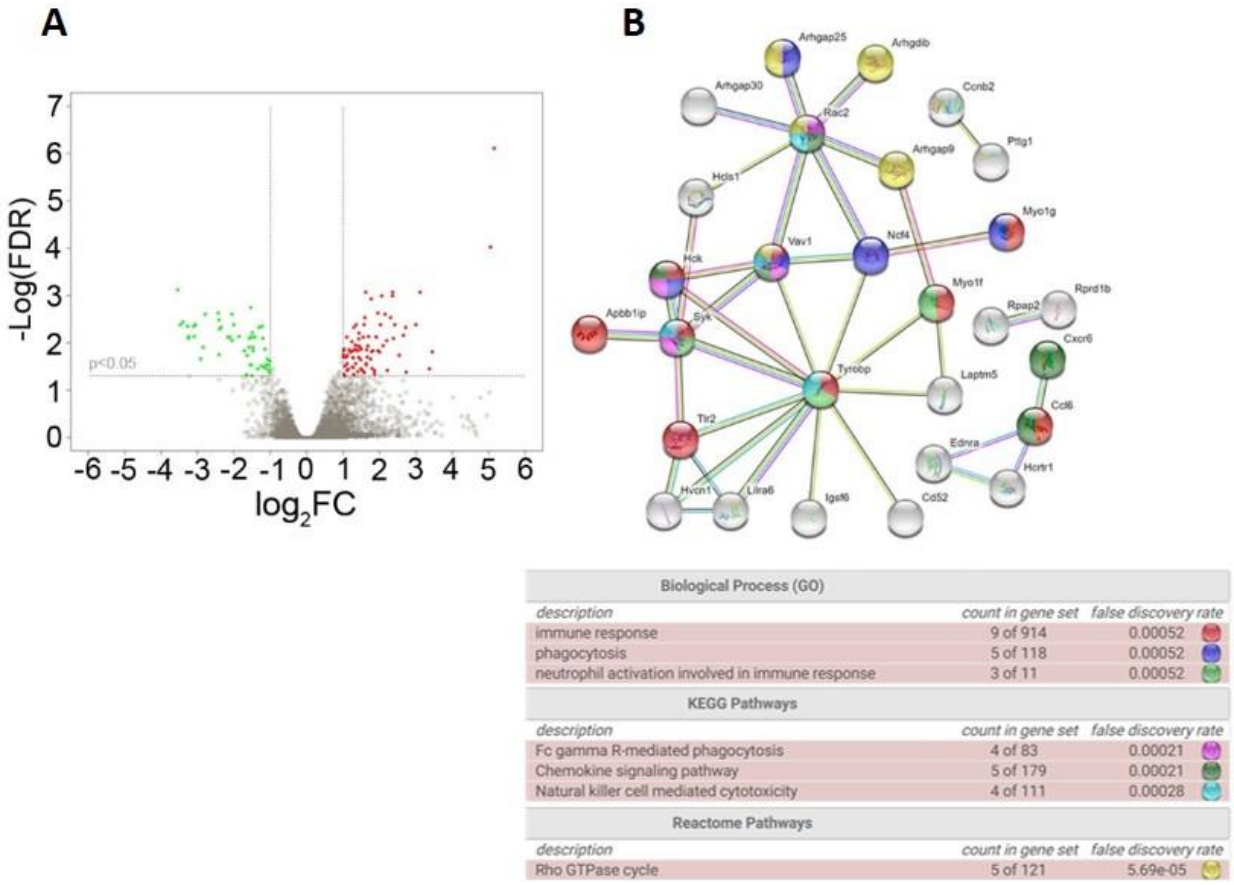

Biological Process (GO)		
description	*count in gene set*	*false discovery rate*
immune response	9 of 914	0.00052
phagocytosis	5 of 118	0.00052
neutrophil activation involved in immune response	3 of 11	0.00052
KEGG Pathways		
description	*count in gene set*	*false discovery rate*
Fc gamma R-mediated phagocytosis	4 of 83	0.00021
Chemokine signaling pathway	5 of 179	0.00021
Natural killer cell mediated cytotoxicity	4 of 111	0.00028
Reactome Pathways		
description	*count in gene set*	*false discovery rate*
Rho GTPase cycle	5 of 121	5.69e-05

Figure 4.7 Effect of R100W mutation on trascriptomic profile of DRG from HSAN V mice. (**A**) Volcano plot for Differentially Expressed Genes in DRGs. The X axis corresponds to the differential expression level (FoldChange) in $\log_2$ scale and the Y axis to −Log(False Discovery Rate) (FDR), as obtained from the uncorrected p-value by the Benjamini-Hochberg procedure. Red and Green regions show 2.0 fold up- and down- regulated genes respectively with FDR adjusted p-value ≤0.05. The horizontal dashed line has ordinate -Log(0.05), and the vertical dashed line has abscissa $\log_2(\pm 2.0)$. (**B**) Pathway analysis of Differentially Expressed Genes. The gene-gene network was obtained by the StringDB tool (https://string-db.org). Colors indicate genes belonging to the main over-represented pathways and functional categories: immune response and chemokines (red and green), phagocytosis (blue and purple), killer cells mediated cytotoxicity (light blue), Rho GTPase (yellow).

4.2.4 *In vivo* pain response and *in vitro* pain transduction pathways mediated by NGF^{R100W}

In order to understand whether the R100W mutation induces specific changes in DRG function, that might be directly ascribed to pain-related responses, I analyzed the ability of human NGF^{R100W} to sensitize DRGs, *in vivo* and *in vitro*. To this aim, I focused on molecular pain pathways mediated by NGF^{R100W}, and simulated an NGF priming of nociceptive responses. DRG cultured neurons were exposed for 5 days to wild type NGF and mutant NGF^{R100W}, followed by acute administration of the known inflammatory

neuropeptide bradykinin (BK). Bradykinin induced a significantly lower release of the Substance P neuropeptide in DRG cultures treated with NGF^{R100W} protein, with respect to sister cultures exposed to NGF^{WT} (**Fig. 4.8A**). This demonstrates that while NGF^{WT} primes DRG neurons to respond strongly to the bradykinin nociceptive stimulus, NGF^{R100W} is significantly less effective in sensitizing DRG neurons, despite its equal neurotrophic potency on these same neurons. From a mechanistic point of view, wild type NGF significantly increased bradykinin receptor 2 (B2R) protein expression, while NGF^{R100W} led to the opposite effect (**Fig. 4.8B**). BK has been reported to sensitize and activate TRPV1 in DRG neurons (Tang et al., 2004). Both NGF and BK increase the membrane expression and the activity of the TRPV1 receptors through the actions of their cell-surface receptors and associated intracellular pathways (Zhang et al., 2005). For this reason, I examined by Western Blot the phosphorylation status of TRPV1, following BK treatment of DRG cultures exposed to NGF^{R100W} or NGF^{WT}. BK induced a significant increase in the phosphorylation of TRPV1 in DRGs that had been pre-treated with wild type NGF, whereas NGF^{R100W} failed to do so (**Fig. 4.8C**).

Finally, I tested the ability of NGF^{R100W} to induce mechanical allodynia after acute injection in the hind paw of adult CD1 mice, and found that pain-related reactions induced by NGF^{R100W} were significantly lower than NGF^{WT} (**Fig. 4.8D**).

Altogether, these results demonstrate that NGF^{R100W} displays a reduced effectiveness in nociceptor sensitization and in eliciting nociceptive response, in comparison to wild type NGF.

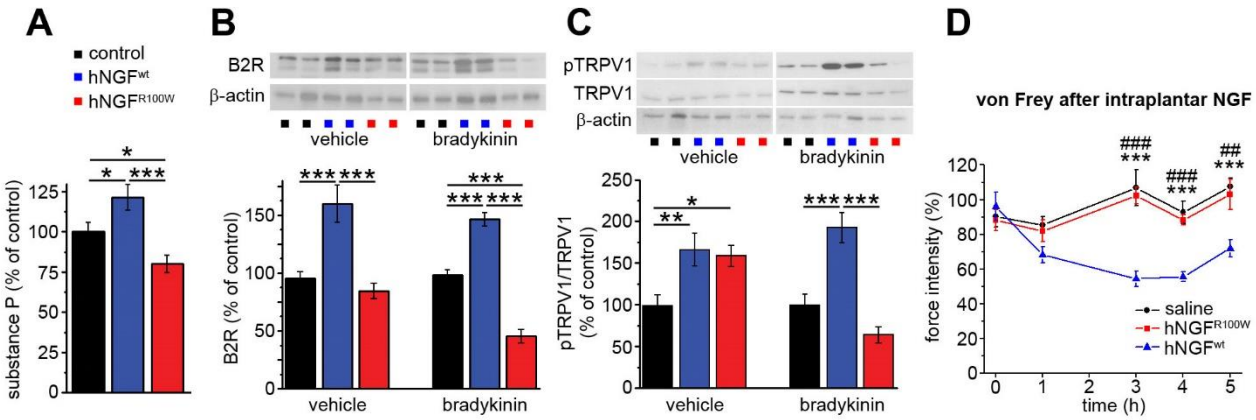

Figure 4.8 Biochemical features of NGF^{R100W}. (A) SP release in DRG cultures is reduced by human NGF^{R100W} compared to human NGF^{WT}. **(B)** Downregulation of BK-induced B2R expression in DRG cultures after pre-treatment of with human NGF^{R100W}. **(C)** Reduction in BK-induced phosphorylation of TRPV1 in DRG cultures pretreated with human NGF^{R100W}. **(D)** Intraplantar injection of human NGF^{R100W} causes reduced mechanical sensitization in comparison to human NGF^{WT}.

Finally, I also evaluated B2R and TRPV1 expression *in vivo* on DRGs dissected from 6-month-old $NGF^{R100W/m}$ mice. These DRGs display a significant reduction in the levels of both receptors (**Fig. 4.9**). Thus, a chronic exposure to NGF^{R100W} leads DRG neurons into a state less prone to be sensitized.

In conclusion, NGF^{R100W} displays a neurotrophic ability indistinguishable from that of wild type NGF, while showing a reduced ability to sensitize sensory neurons.

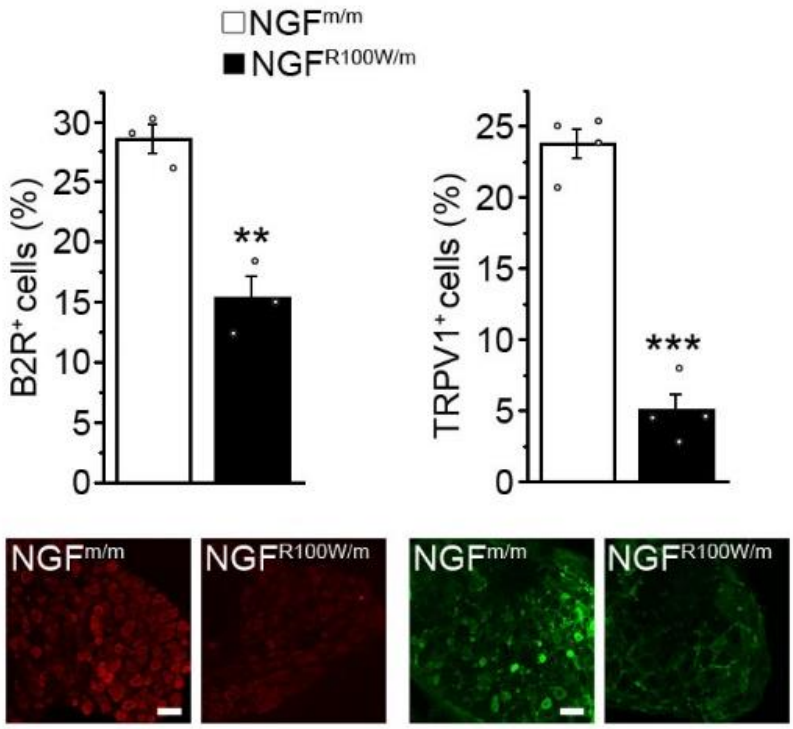

Figure 4.9 Reduced expression of B2R and TRPV1 in DRG neurons of adult HSAN V mice.

4.2.5 Exploring nociceptive information routes in $NGF^{R100W/wt}$ mice

The results described above, prompted me to walk backwards along the nociceptive input path.

To this aim, I measured the conduction velocity of the saphenous nerve, which was found to be normal in $NGF^{R100W/m}$ mice. This was observed in all the three main peaks of the stimulus-evoked electrophysiological response, corresponding to the Aβ-, Aδ- and C-fibers (**Fig. 4.10**).

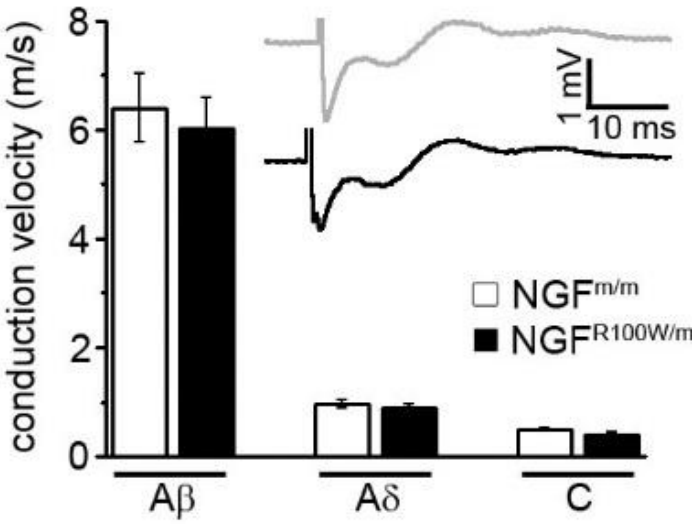

Figure 4.10 No alterations in the conduction velocity of Aβ-, Aδ- and C-fibers in adult mice.

To analyze in detail the sciatic nerve, in collaboration with Dr. Enrica Strettoi (Institute of Neuroscience, National Research Council, Pisa, Italy), we explored its ultrastructure using Transmission Electron Microscopy (TEM). The sciatic nerve diameter of $NGF^{R100W/m}$ mice was significantly smaller compared to controls (**Fig. 4.11A**). In addition, we found no differences in the number of myelinated fibers contained in the nerve (**Fig. 4.11B**), whereas a significant reduction in the number of non-myelinated axons in $NGF^{R100W/m}$ mice was observed (**Fig. 4.11C**), which can be responsible for the smaller nerve area. Regarding non-myelinated fibers, the picture shows an apparent reduced cytoskeletal density within each axon of these fibers, which however remains to be properly investigated and analyzed.

Notably, these neurophysiological (conduction velocity) and untrastructural data (TEM data) match analogous findings in HSAN V heterozygous carriers (Minde et al., 2009). Indeed, heterozygous HSAN V patients display a normal motor conduction velocity and amplitude in peripheral nerves, whereas, their sciatic nerve presents normal large-diameter myelinated fibers and very sparse unmyelinated C fibers (Einarsdottir et al., 2004; Minde et al., 2009).

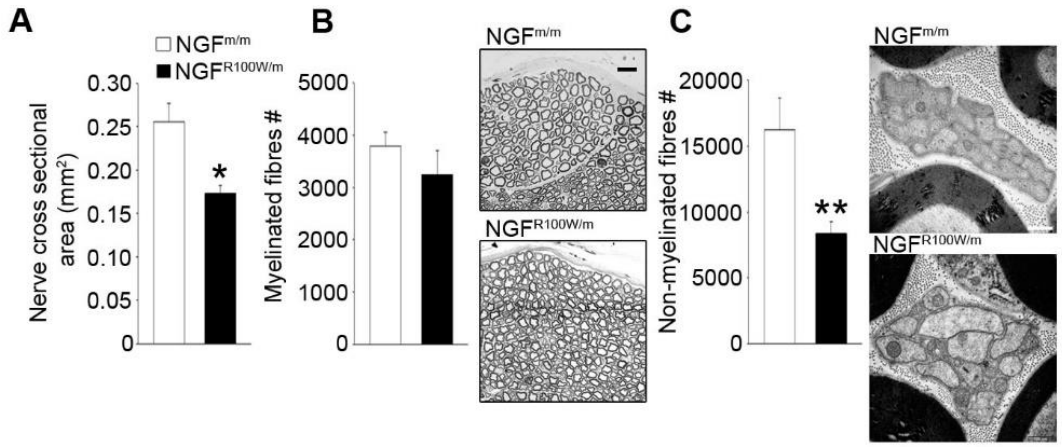

Figure 4.11. Ultrastructural analysis of sciatic nerve in HSAN V mouse model. (**A**) Significant reduction of sciatic nerve area. (**B**) No alterations in the number of myelinated fibers (scale bar, 20 μm). (**C**) Significant reduction of non-myelinated fibers in $NGF^{R100W/m}$ mice compared to controls (scale bar, 500 nm).

Then, I analyzed target tissues of sensory fibers, namely hairy and glabrous skin, using the neuronal marker PGP9.5. Hairy skin covers more than 90% of the body and has an important role in discriminative touch (Zimmerman et al., 2014). $NGF^{R100W/m}$ mice showed unaltered hairy skin innervation at 2 months of age, whereas a significant reduction was observed at 6 months (**Fig. 4.12A**). This loss of innervation in adult mice nicely correlates with the longer latency in tape removal test (**Fig. 4.4D** above). On the other hand, the number of reaches in the same test was unaffected (**Fig. 4.12B**), thus indicating a normal execution of the task from a motor point of view.

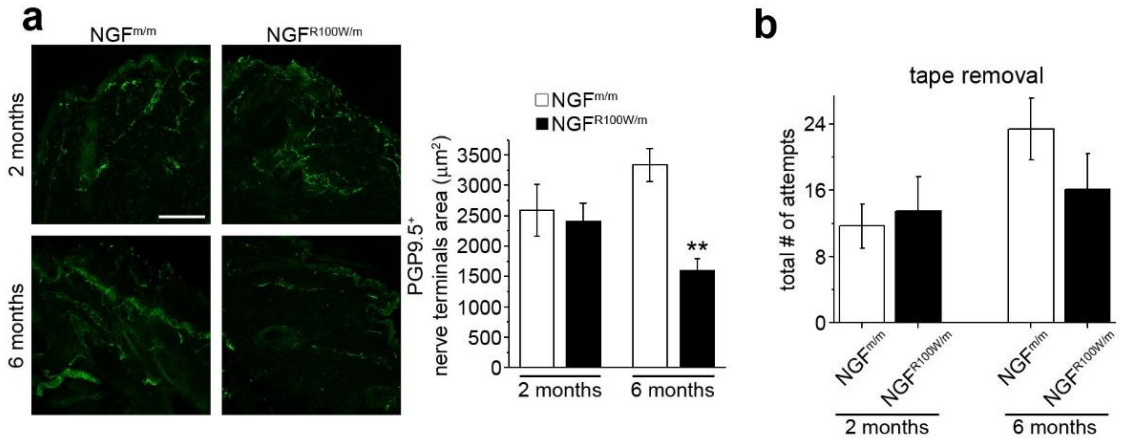

Figure 4.12 Hairy skin innervation and associated mechanoception-evoked responses in $NGF^{R100W/m}$ mice. (A) Representative images and quantification of PGP9.5 expression show normal innervation at 2 months and a significant reduction of immunoreactivity at 6 months of age (scale bars, 50 μm). **(B)** Latency of response in the tape removal test is increased at 6 months of age, whereas the total number of attempts is unimpaired in both juveniles and adults.

Regarding the glabrous skin, $NGF^{R100W/m}$ mice showed decreased innervation at 2 months of age and a complete loss of innervation at 6 months (**Fig. 4.13A**). Since target-derived NGF modulates innervation (Purves et al., 1988), I measured NGF levels in the glabrous skin via immunofluorescence and found a significant reduction of NGF in $NGF^{R100W/m}$ mice, compared to $NGF^{m/m}$ mice (**Fig. 4.13B**).

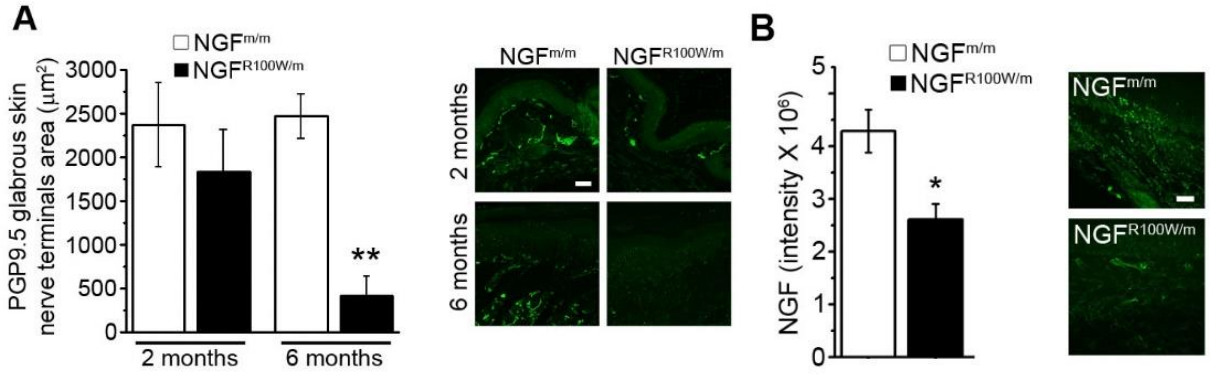

Figure 4.13 Glabrous skin innervation in $NGF^{R100W/m}$ mice. (A) Age-dependent reduction in glabrous skin innervation in HSAN V mice (scale bars, 50 µm). **(B)** Decreased NGF levels in the glabrous skin of adult HSAN V mice (scale bars, 50 µm).

Taking into account the reduction of NGF in the peripheral target sites of sensory fiber, I postulated that the observed pain-related behavioral deficits in $NGF^{R100W/m}$ might be due to the lower bioavailability of NGF due to the R100W mutation. In order to test this hypothesis I reasoned that exogenous administration of wild type NGF could be used to rescue the nociceptive deficit of $NGF^{R100W/wt}$ mice. To this aim, I examined the capsaicin response in heterozygous mice subjected to long-term treatment with mouse wild type NGF, starting from gestation and continuing after weaning (see Methods section). In accordance with my hypothesis, capsaicin sensitivity of $NGF^{R100W/m}$ mice was restored by a continuous NGF treatment (**Fig. 4.14**).

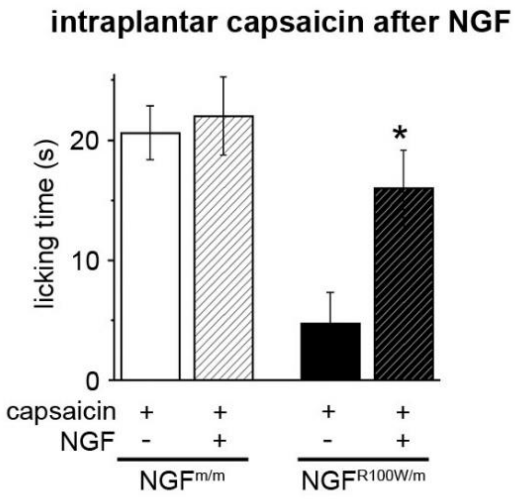

Figure 4.14 Rescue of the sensitivity to capsaicin after treatment with mouse wild type NGF from gestation until 2 months of age.

4.2.6 Absence of cognitive deficits in NGF$^{R100W/m}$ mice

Besides its importance for development and function of DRG neurons, NGF plays an essential role in a number of forebrain and brainstem structures, acting as a key mediator of brain development, in addition to being required for learning and memory process (Chao, 2003). Indeed, heterozygous murine NGF knock out (i.e., mNGF$^{+/-}$) mice, which lack one NGF allele (Crowley et al., 1994), are characterized by lower brain levels of NGF, and display significant deficits in memory acquisition and retention (Chen et al., 1997). NGF is a homodimer and in heterozygous NGF$^{R100W/m}$ mice the wild type and the mutant chains are co-expressed. The R100W mutation causes an impairment in the secretion of mature NGF (Larsson et al., 2009), but it is not known whether NGF^{R100W} interferes with the secretion of NGF^{WT} when the two are co-expressed, as it happens in heterozygous condition. To investigate this aspect, I first co-transfected plasmids encoding R100W or wild type NGF on HEK293 cells, followed by quantification of NGF in the culture medium. When expressed alone, NGF^{R100W} shows a marked decreased secretion in comparison to wild type NGF, extending also to human cells the result previously found for rat PC12 cells (Larsson et al., 2009). Interestingly, co-expression of both R100W and wild type NGF – which mimics the heterozygous NGF$^{R100W/m}$ cellular condition– also leads to decreased NGF abundance in the cell medium. This indicates that NGF^{R100W} interferes with the secretion of wild type NGF (**Fig. 4.15A**). In keeping with this hypothesis, the amount of NGF in plasma and in cortical extracts (measured by ELISA and immunoprecipitation,

respectively) from NGF$^{R100W/m}$ animals was significantly decreased (**Fig. 4.15B, C**). Thus, heterozygous NGF$^{R100W/m}$ mice are expected to have a reduction of secreted NGF similar to heterozygous mNGF$^{+/-}$mice.

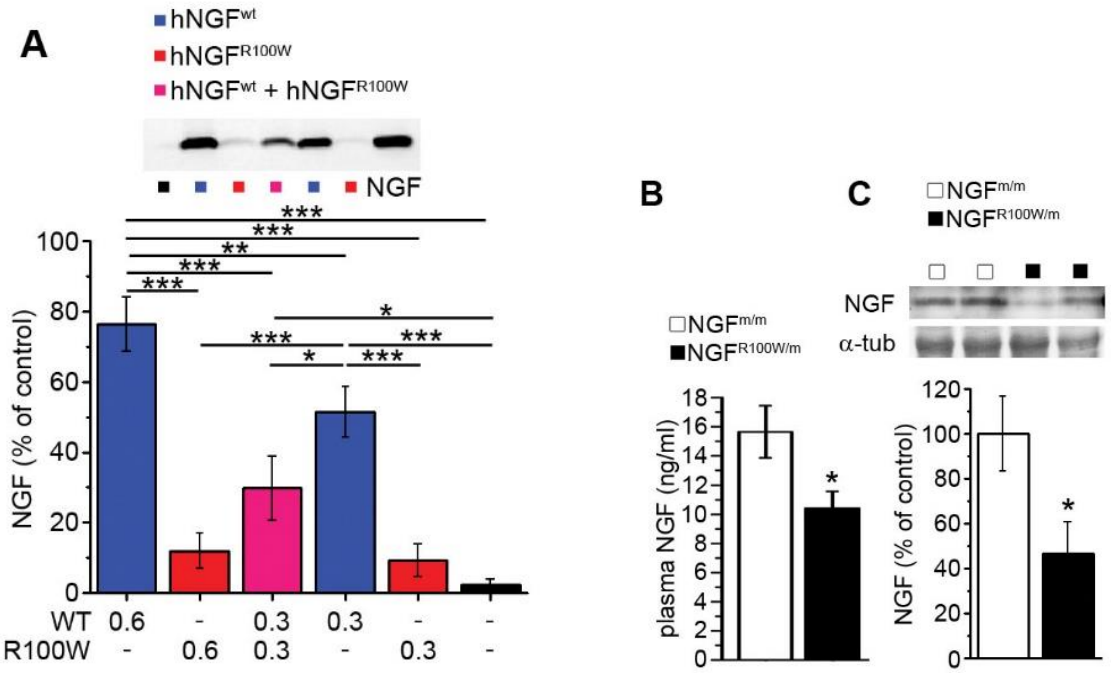

Figure 4.15 Effects of the R100W mutation on NGF bioavailability. (A) Impaired secretion of human NGF^{R100W} in HEK293 cells transfected with the corresponding plasmid, similarly to what reported in Larsson et al., 2009. Co-transfection of HEK293 cells with human NGF^{WT} and human NGF^{R100W}, to mimic heterozygous condition, shows a decrease in the secretion of human NGF^{WT}. **(B)** Decreased plasmatic levels of NGF in HSAN V mice. **(C)** Significant decrease in the amount of NGF in brain extracts from NGF$^{R100W/m}$ mice.

Based on these data, I next asked whether the altered secretion of NGF could affect learning and memory of NGF$^{R100W/m}$ mice, as it does in NGF$^{+/-}$ mice. To address this point, I performed the Morris Water maze and Novel object recognition tests and I analyzed heterozygous NGF$^{R100W/m}$ mice and murine NGF knock-out mice. Heterozygous HSAN V mice showed no learning and memory deficits (**Fig. 4.16A, C, D**); on the contrary, mNGF$^{+/-}$ mice show, in agreement with previous literature (Chen et al., 1997), a deficit in both tests (**Fig. 4.16B-D**).

Basal forebrain cholinergic neurons (BFCNs) are involved in attention and cognition, and NGF is required for their correct differentiation and survival (Johnston et al., 1987). I analyzed the number of ChAT-immunoreactive neurons in basal forebrain and striatum of NGF$^{R100W/m}$ and mNGF$^{+/-}$ mice. No alterations were observed in HSAN V mice, whereas, a significant reduction of ChAT-immunoreactive neurons was

present in the medial septum of the basal forebrain and striatum in mNGF$^{+/-}$ mice (**Fig. 4.16E, F**), in correlation with the corresponding cognitive behavioural phenotypes.

Thus, the R100W mutation, unlike the total deletion of the *ngf* gene, does not affect learning and memory processes, in keeping with the clinical phenotype of heterozygous R100W human carriers, who are reported to be cognitively normal (Einarsdottir et al., 2004).

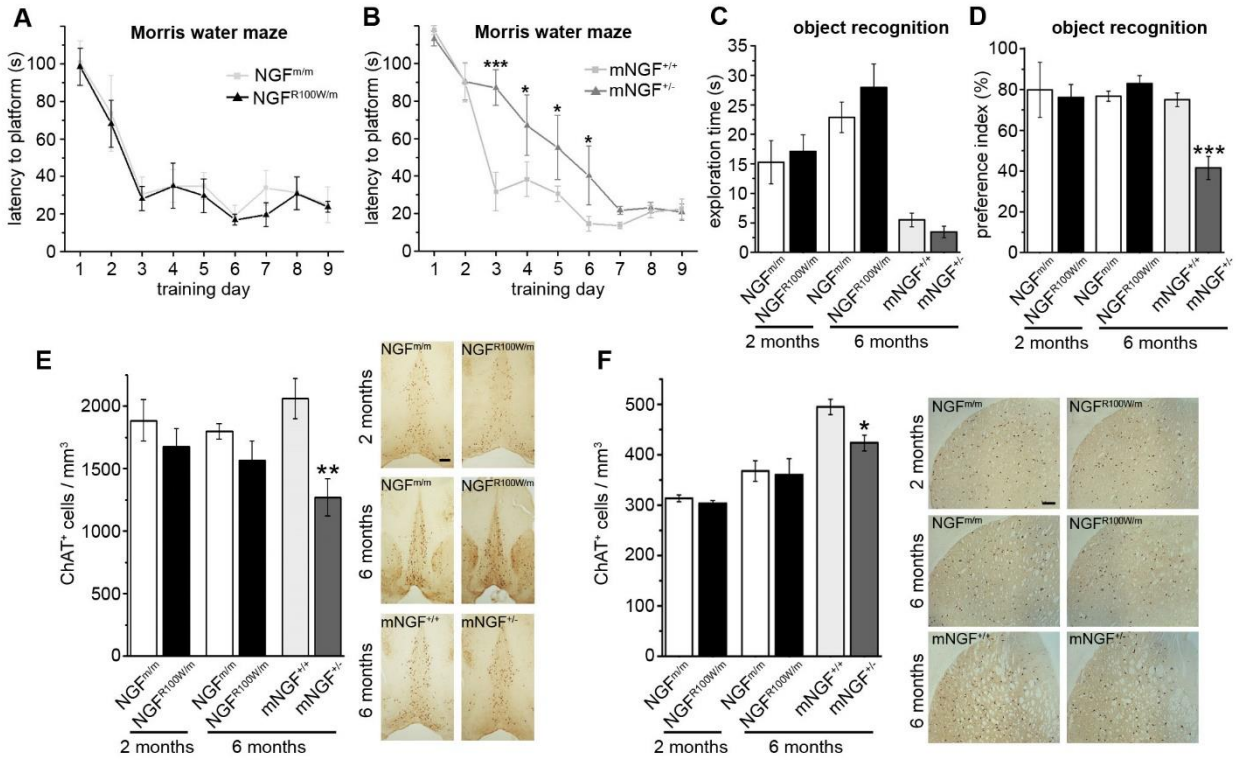

Figure 4.16 Cognitive performance of NGF^{R100W} and mNGF$^{+/-}$ mice. (A) Normal Morris water maze learning curve for HSAN V mice. **(B)** Delayed Morris water maze learning curve for mNGF$^{+/-}$ mice. **(C)** Unimpaired NOR sample phase for HSAN V and mNGF$^{+/-}$ mice. **(D)** Unimpaired NOR test phase for HSAN V and visual recognition memory deficit for mNGF$^{+/-}$ mice. (**E, F**) Normal septal and striatal ChAT$^+$ neuron density in juvenile and adult HSAN V mice, and decreased density in mNGF$^{+/-}$ mice (scale bars, 200 µm).

4.2.7 The R100W mutation impairs acquired, but not innate, fear

Having characterized the phenotype of HSAN V mice, I decided to exploit this model to investigate the central consequences of growing with an altered transmission and perception of pain and if this condition affects the development of central emotions. To address these questions, I used heterozygous NGF$^{R100W/m}$ mice that have a milder painlessness condition.

As a first test, I evaluated anxiety-like behaviors in HSAN V mice. To this aim, I performed the elevated plus maze, marble burying and nest building tests. In comparison to wild type controls, $NGF^{R100W/m}$ mice show an age-related reduction of anxiety in all tests (**Fig. 4.17A-C**). I reasoned that this might reflect $NGF^{R100W/m}$ mice being less anxious about unexpected potentially harmful events.

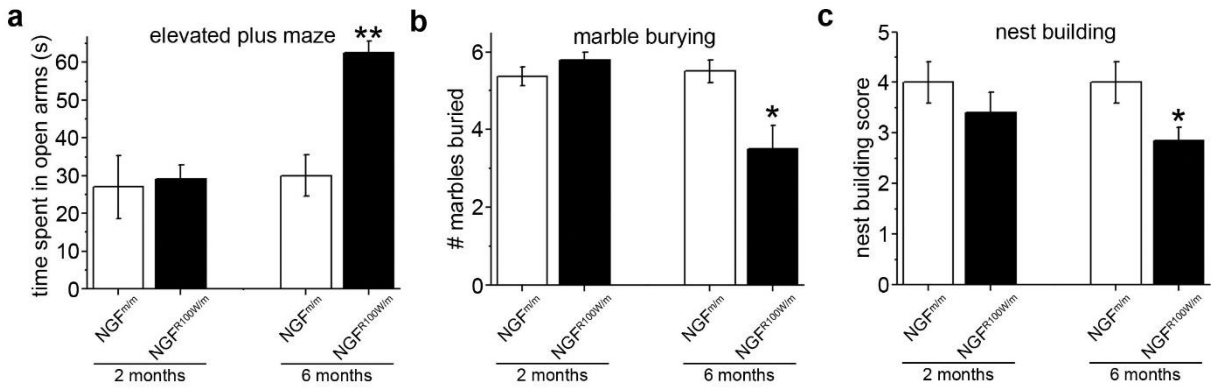

Figure 4.17 Age-related effect of the R100W mutation on anxiety behavior. (A) In the elevated plus maze, 6-month-old $NGF^{R100W/m}$ mice spent more time in the open arms than $NGF^{m/m}$. **(B)** The amount of marbles buried by $NGF^{R100W/m}$ and $NGF^{m/m}$ is similar at 2 months of age, but significantly reduced in $NGF^{R100W/m}$ at 6 months of age. **(C)** The nesting ability is normal in juvenile, but impaired in adult HSAN V mice.

Therefore, I investigated whether the R100W mutation affects the acquisition of pain-related memories. To answer this question, I used the fear conditioning test (LeDoux, 2014), a paradigm frequently used in rodents to evaluate the formation of new associative memories in response to noxious stimuli. I tested whether central processing of pain-related events and memory processes might be affected in these mice, by performing the fear conditioning test in HSAN V mice at 2 and 6 months of age. As a control, I used knock-in mice heterozygous for wild type human NGF gene ($NGF^{h/m}$). $NGF^{h/m}$ animals can be considered to be ideal controls for these experiments, as they reproduce the genotype of $NGF^{R100W/m}$, except for the R100W point mutation. Importantly, the phenotype of $NGF^{h/m}$ mice is indistinguishable from that of $NGF^{m/m}$ animals, as shown by the lack of significant differences, between $NGF^{h/m}$ and $NGF^{m/m}$ mice, in a number of behavioral tests, namely tape removal, cotton swab, hot plate, open field and object recognition tests (**Fig. 4.18)**.

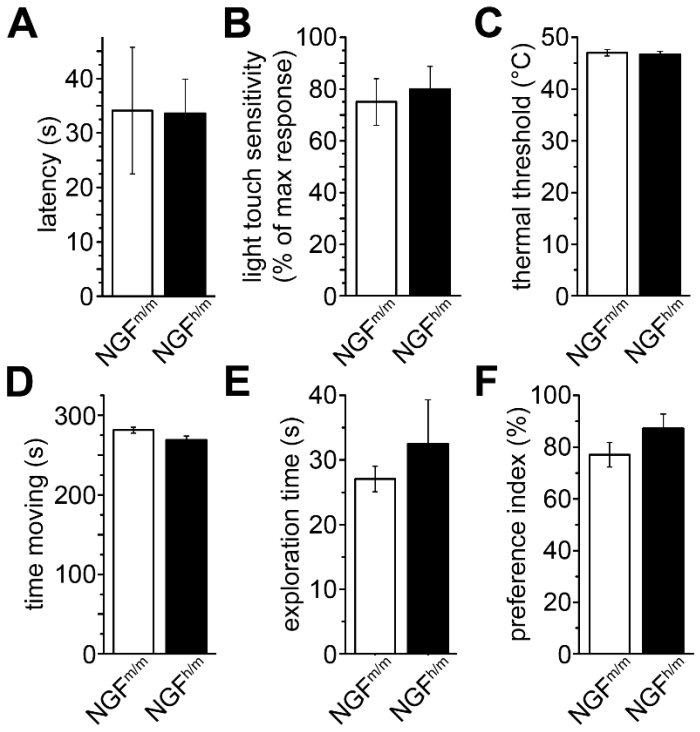

Figure 4.18 Comparison between the phenotypes of $NGF^{m/m}$ and $NGF^{h/m}$ mice.

In order to perform a meaningful comparison between $NGF^{h/m}$ and $NGF^{R100W/m}$ mice, the two groups should receive an unconditioned shock of the same subjective intensity. For this reason, prior to the fear conditioning test, an initial cohort of animals was used to assess the relationship between behavioural response and stimulus intensity. At both ages, $NGF^{R100W/m}$ mice required a higher current intensity than $NGF^{h/m}$ controls to reach a similar behavioural response (**Fig. 4.19A**). Therefore, the intensity of the foot shock stimulus was adjusted to elicit vocalization, resulting in an identical, maximal response in both groups. When tested in the cued fear conditioning, $NGF^{R100W/m}$ and $NGF^{h/m}$ were similarly able to associate the conditioned (i.e., acoustic tone) and unconditioned (i.e., foot shock) stimuli, as demonstrated by the progressive increase in freezing along repeated tone presentations and by the total freezing time (**Fig. 4.19B-C**). This result indicates that, by adjusting the stimulus intensity, the decreased pain sensitivity can be overcome in $NGF^{R100W/m}$ mice, to obtain a normal behavioral response. Surprisingly, in the recall phase of the test $NGF^{R100W/m}$ mice, unlike control $NGF^{h/m}$ mice, do not show a fear freezing response when presented with the auditory cue alone (**Fig. 4.19D**). To control that the reduced freezing response was not due to an auditory deficit, I also performed contextual fear conditioning; HSAN V mice failed to show a

freezing response also in the recall phase of this version of the test (**Fig. 4.19E**). Finally, to exclude that the low tendency to freeze of HSAN V mice might be due to a hyperactive behavior, I measured the exploratory behavior in the open field test and found no differences between $NGF^{R100W/m}$ and $NGF^{h/m}$ mice (**Fig. 4.19F**). These results suggest that $NGF^{R100W/m}$ mice are not able to form the association between the conditioning and the noxious unconditioned stimuli, thus failing to interpret the former as an event potentially leading to pain, despite a normal response to the shock *per se*.

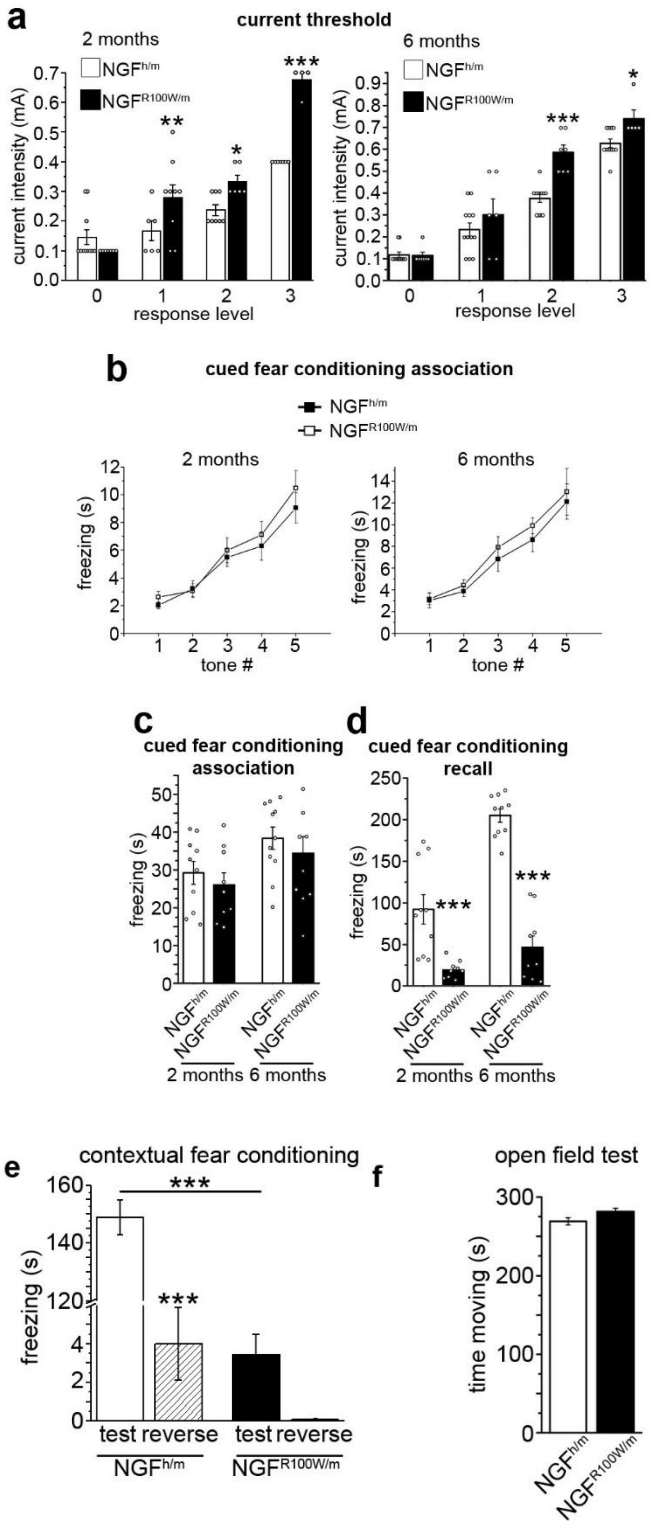

Figure 4.19 Impaired memory of acquired fear conditioning in NGF^{R100W} mice. (A) 2- and 6-month-old HSAN V mice show higher current intensity threshold for eliciting a maximal response than wild type controls. **(B,C)** No differences in the freezing responses during the association phase of cued fear conditioning. **(D)** Impaired cued fear memory in HSAN V mice. **(E)** Reduced freezing of adult HSAN V mice in the contextual fear conditioning. **(F)** Unchanged exploratory behavior of NGF$^{R100W/m}$ mice.

Painful stimuli have a number of different attributes, including peripherally encoded sensory-discriminative features (such as location, intensity and quality), as well as centrally encoded affective and emotional valence (such as unpleasantness). Taking into account that these attributes are processed in different brain areas, it was of interest to quantitatively evaluate neuronal activation in different relevant brain areas of $NGF^{R100W/m}$ versus $NGF^{h/m}$ mice, by c-fos immunohistochemistry activity mapping. I focused my attention either on areas directly involved in processing and generating fear-related perception (such as amygdala, hippocampus and anterior cingulate cortex), or on areas involved in mediating the behavioral output triggered by the above mentioned areas (such as motor cortex, caudate nucleus). The number of c-fos-immunoreactive neurons activated during the recall phase of cued fear conditioning in the amygdala, hippocampus and anterior cingulate cortex, as well as in the motor cortex and anterior caudate nucleus of $NGF^{R100W/m}$ mice was significantly lower than in $NGF^{h/m}$ mice. Importantly, the number of c-fos-immunoreactive neurons in primary somatosensory cortex was similar in $NGF^{h/m}$ and $NGF^{R100W/m}$ mice, indicating that the information on noxious stimuli is normally transmitted to the primary somatosensory cortex (**Fig. 4.20**). Thus, the defect in fear conditioning is not due to abnormal transmission of painful stimuli but resides in subsequent associative processing of painful stimulus.

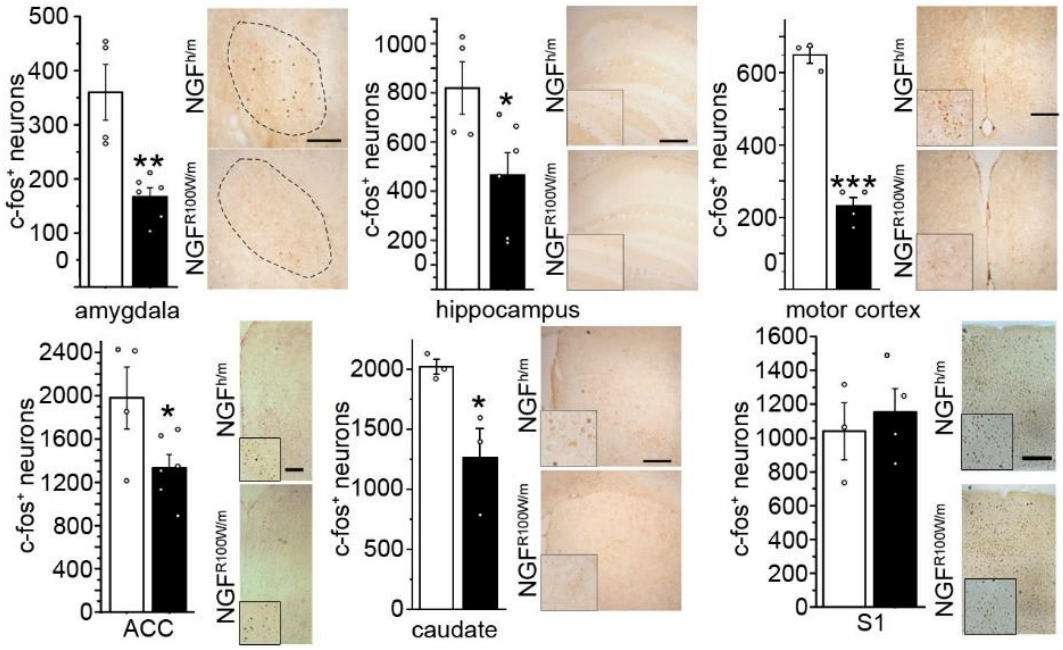

Figure 4.20 Decreased c-fos immunostaining after cued fear conditioning in amygdala, hippocampus, motor cortex, anterior cingulate cortex and caudate nucleus of HSAN V mice, along with significant difference in the primary somatosensory cortex (scale bars, 200 µm, except for ACC, 100 µm).

Calcitonin Gene-Related Peptide (CGRP) is an abundantly expressed neuropeptide in the parabrachial and posterior thalamic nuclei, which send projections to central amygdala, thus taking part in regulating fear-like behaviors (D'Hanis et al., 2007; Han et al., 2015). This evidence prompted me to analyze the expression of CGRP in HSAN V mice. I found a decrease in the density of CGRP-positive fibers terminals in the central amygdala (**Fig. 4.21**). This suggests that a reduced activity of CGRP afferents might mediate the observed reduced fear response in HSAN V mice, in agreement with a recent paper by Campos et al., reporting that the activation of CGRP afferents to the amygdala stimulates freezing, whereas conditioned fear responses are reduced by their inhibition (Campos et al., 2018).

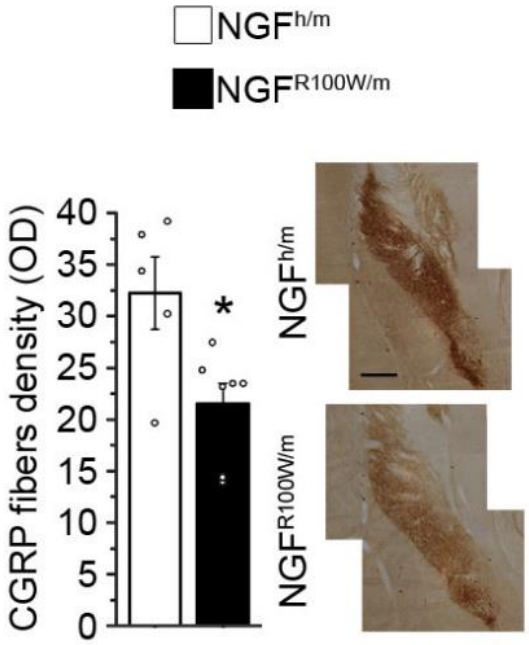

Figure 4.21 Decreased density of CGRP-positive fiber terminals in the central amygdala of $NGF^{R100W/m}$ mice.

Is the lack of fear response observed in $NGF^{R100W/m}$ mice specific to painful stimuli? To answer this question, I challenged $NGF^{R100W/m}$ mice with a paradigm of innate fear not related to pain, namely exposure of the mice to a predator. In this behavioral test, $NGF^{R100W/m}$ mice behaved identically to control $NGF^{h/m}$ mice, showing an identical fear response (**Fig. 4.22A**). In addition, after exposure to the predator, the c-fos activation pattern in the ventromedial hypothalamic nucleus (VMH), which is reported to mediate this specific fear response (Silva et al., 2013), is not significantly different in $NGF^{R100W/m}$ mice, compared to wild type controls (**Fig. 4.22B**).

These data show that NGF$^{R100W/m}$ mice do not have a general deficit in the fear response system but have a deficit specific for learned fear responses triggered by painful events, which may be caused by a specifically altered interpretation of pain-related afferent signals.

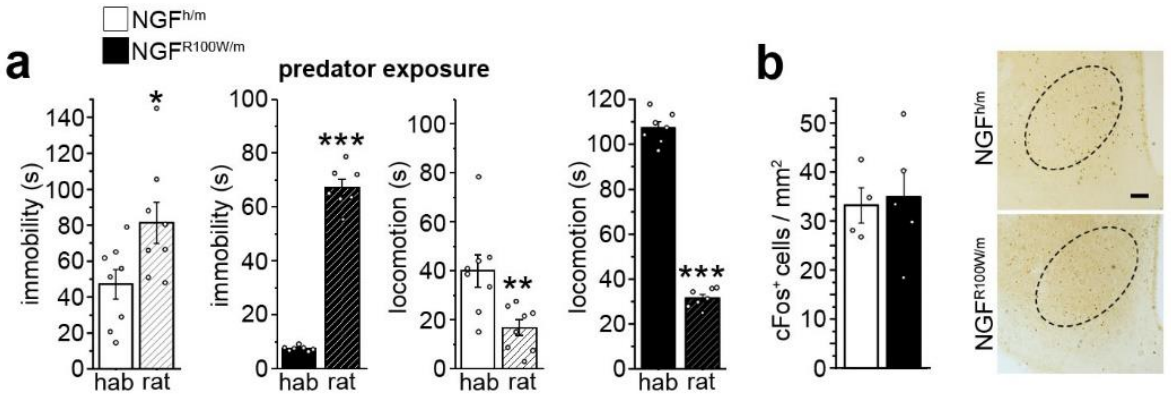

Figure 4.22. Pain insensitivity does not impair innate fear. (A) The R100W mutation does not affect innate fear, indeed predator exposure reduces locomotion and increases immobility in both NGF$^{R100W/m}$ and NGF$^{h/m}$ mice. **(B)** No significant differences in c-fos immunostaining in the hypothalamic VMH of adult HSAN V and control mice after predator exposure (scale bars, 200 µm).

4.2.8 Reduced levels of pain-related neuropeptides in NGF$^{R100W/m}$ mice

The peculiar findings described above might be ascribed, in principle, to a simple increase in the levels of endogenous analgesic peptides. This prompted me to investigated the levels of a number such peptides in the relevant brain areas. To this regard, I quantified the density of β-endorphin-immunoreactive cells in the arcuate nucleus of hypothalamus, finding a significant reduction in adult HSAN V mice, compared to NGF$^{h/m}$ control mice (**Fig. 4.23A**). Oxytocin is another key component of the endogenous analgesic system, with a direct involvement in fear responses (Knobloch et al., 2012). The number of oxytocin-immunoreactive neurons in the paraventricular hypothalamic nucleus (PVH) was greatly decreased in NGF$^{R100W/m}$ mice, before and after fear conditioning (**Fig. 4.23B**); HSAN V mice also present a reduction of plasma oxytocin levels (**Fig. 4.23C**). On the other hand, both plasma levels and hypothalamic immunoreactivity for oxytocin were unaffected in mNGF$^{+/-}$ mice (**Fig. 4.23D, E**), indicating that the reduction of oxytocin is specific to the mutation and does not result from reduced NGF levels. This result highlights differences in signaling between NGF and NGF^{R100W} in the brain. Furthermore, it is known that R100W mutation affects binding to p75^{NTR} and the corresponding signaling pathways (Covaceuszach et al.,

2010; Capsoni et al., 2011; Sung et al., 2018). Interestingly, the number of oxytocin-immunoreactive neurons was also reduced in the PVH nucleus of $p75^{NTR}$ knock out mouse ($p75^{NTR-/-}$) (**Fig. 4.23F**).

On the whole, these results show that various neuropeptides endowed with endogenous analgesic properties are down regulated in $NGF^{R100W/m}$ mice.

These findings are the opposite to the above mentioned possibility, suggesting that the phenotype of $NGF^{R100W/m}$ mice might be due to enhanced endogenous analgesia and might reflect, on the other hand, a homeostatic response to the mild reduction in nociception and in the afferent pain signals.

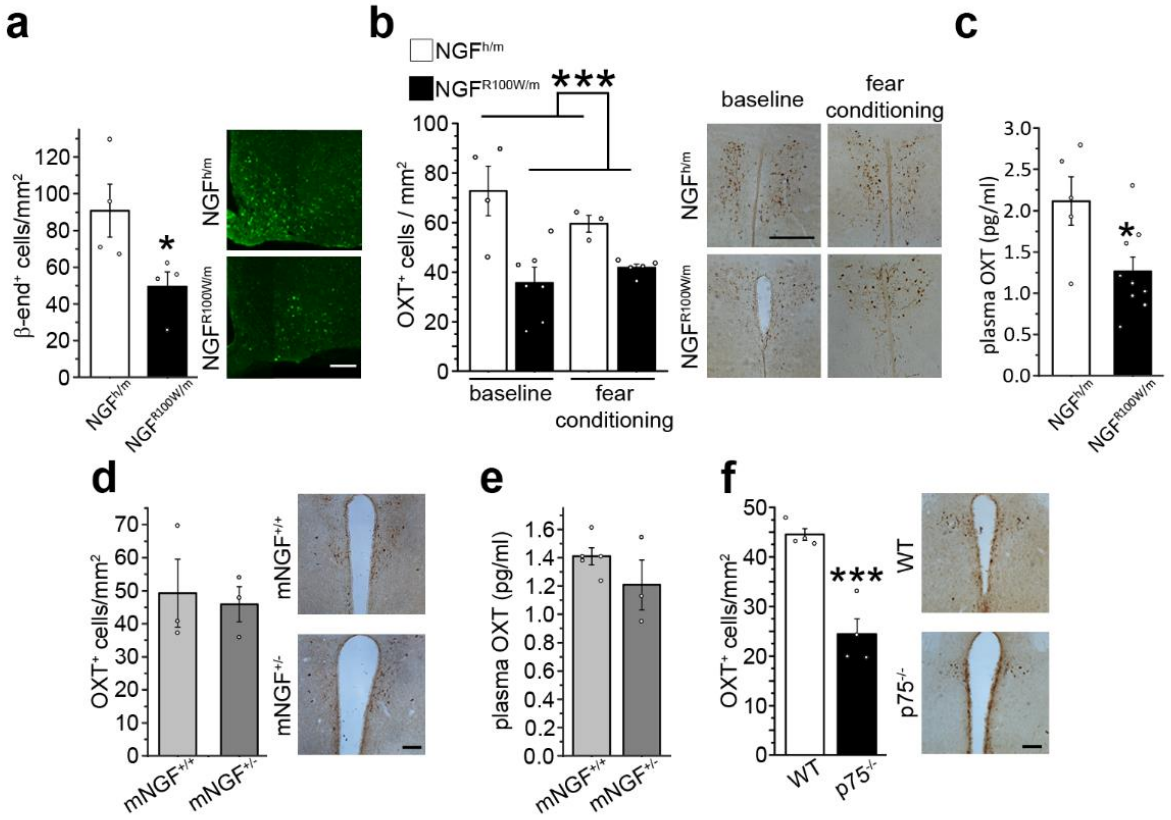

Figure 4.23 Decreased levels of endogenous analgesics in HSAN V mice. (A) Decreased density of β-endorphin-immunoreactive cells in the arcuate nucleus of the hypothalamus in $NGF^{R100W/m}$ mice (scale bar, 100 μm). **(B)** Reduced oxytocin immunoreactivity in the PVH of adult $NGF^{R100W/m}$ mice (scale bars, 200 μm). **(C)** Decreased plasmatic levels of oxytocin in $NGF^{R100W/m}$ mice. **(D)** Normal immunoreactivity and **(E)** plasmatic levels of oxytocin in $mNGF^{+/-}$ mice (scale bars, 100 μm). **(F)** Reduced oxytocin immunoreactivity in the PVA of adult $p75^{NTR-/-}$ mice (scale bar, 200 μm).

4.2.9 Altered responsiveness to painful stimuli in HSAN V human heterozygous carriers

The availability of a mouse model for HSAN V opens the opportunity to relate the mouse findings to the human heterozygous HSAN V phenotype; we collaborated with the research group led by Dr. India

Morrison, based at Linköping University (Sweden), that has been studying members of the family carrying the NGF^{R100W} mutation (Minde, 2006). Discriminative and pain thresholds for heat and cold were investigated in heterozygous R100W carriers and in healthy controls. No significant differences were found between carriers and controls in the response to thermal stimuli (**Fig. 4.24A**). However, when the subjective motivational responses to above-threshold painful thermal stimuli was assessed by means of an "urge to move" rating task (Perini et al., 2013), the R100W carrier group showed higher response latencies, exhibiting a significantly lower performance (**Fig. 4.24B**). Then, the subjects were also probed with a task requiring them to distinguish "signal" from "noise" under changing task constraints, in which sometimes painful stimulation is "signal" (requiring a behavioral response – button press) and sometimes it is "noise" (requiring to be ignored – no button press). Specifically, R100W carriers had a significantly larger bias to accept "noise" as signal (pressing the button when no response was required by task), indicating a significantly higher error frequency in a pain/no pain discrimination task (**Fig. 4.24C**).

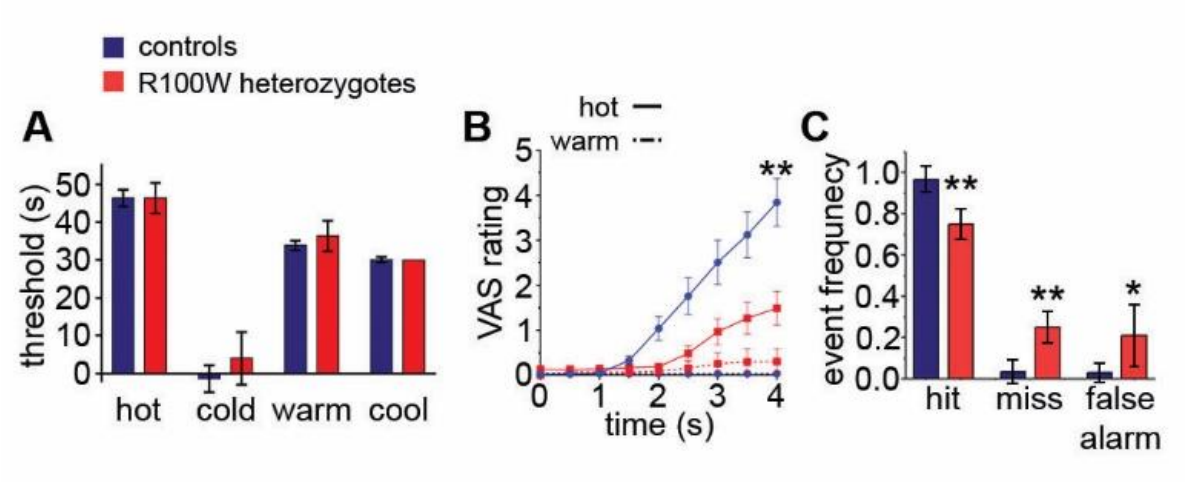

Figure 4.24 Altered motivated behavior in human R100W carriers. (A) No differences in thermal thresholds between R100W heterozygotes and controls. **(B)** Decreased urge to move in response to noxious stimulation in R100W heterozygotes. **(C)** Impaired estimation of painful situations in R100W heterozygotes.

Previous measures indicate an impact of the mutation on motivated behavior (Morrison et al., 2011). To look for a possible disruption of task-related brain activation in the human HSAN V carrier group, fMRI was used to examine the blood-oxygen-level-dependent (BOLD) response in pain-related regions of interest (ROIs). During the first seconds following the onset of the thermal stimulus, controls, but not carriers, showed a main effect of pain stimulus in rostral anterior cingulate cortex (rACC) and in pre-supplementary

motor area (pre-SMA). Time course analysis of the full 4-second trial revealed that, although this main effect did not manifest at stimulus onset in R100W carriers, these regions did show a delayed activation by the last second of the trial (**Fig. 4.25**). Moreover, unlike rACC/SMA responses in controls, this activation in heterozygous HSAN V carriers did not return to baseline at the end of the trial (**Fig. 4.25**).

Altogether, these data from R100W heterozygous carriers reveal a comparable impairment to $NGF^{R100W/m}$ mice in integrating pain-related afferent signalling with task-dependent behavioural responses, and a dysregulation of pain-triggered motor-related responses, despite normal thermal thresholds and activation of primary somatosensory cortex.

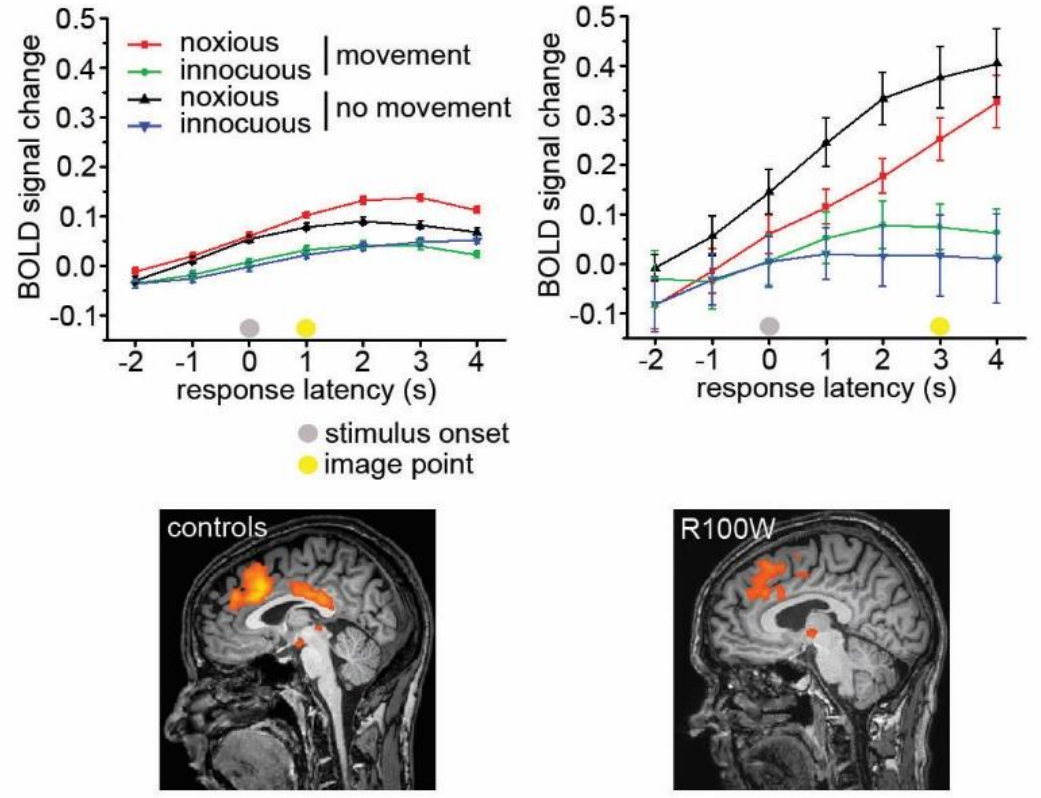

Figure 4.25 Altered cerebral pain-related modulation in heterozygous HSAN V patients. Event-related time-course plots of R100W heterozygotes pain-specific BOLD responses in rACC/SMA show higher latency and loss of baseline return compared to controls. All maps thresholded at p<0.001 uncorr.

4.3 STATISTICS SUMMARY

Figure 4.2

A. Log-rank Kaplan-Meyer survival analysis (statistical value = 767.726, DF = 3, $p < 0.001$), followed by Bonferroni post-hoc test (***$p < 0.001$).

B. Student's two-tailed t-test (t =6.730, **$p = 0.003$); $NGF^{m/m}$, n = 4; $NGF^{R100W/R100W}$, n = 2.

C. ANOVA-2 for repeated measures (treatment × time interaction, $F_{7,45} = 59.529$, $p < 0.001$) followed by Bonferroni post-hoc test (***$p < 0.001$); $NGF^{m/m}$, n = 3; $NGF^{R100W/R100W}$, n = 3.

Figure 4.3

A. Student's two-tailed t-test (t = 0.950, p = 0.386); $NGF^{m/m}$, n = 3; $NGF^{R100W/R100W}$, n = 4

B. Student's two-tailed t-test (t = -1.571, p = 0.177); $NGF^{m/m}$, n = 3; $NGF^{R100W/R100W}$, n = 4

C. Student's two-tailed t-test (t = -4.914, p = 0.002); $NGF^{m/m}$, n = 3; $NGF^{R100W/R100W}$, n = 4.

Figure 4.4

A. Capsaicin test 2 months, ANOVA-1 ($F_{2,12} = 12.869$, $p = 0.002$), followed by Bonferroni post-hoc test ($NGF^{m/m}$ *vs.* DMSO, $p = 0.002$; $NGF^{m/m}$ *vs.* $NGF^{R100W/m}$, $p = 0.017$; HT^{R100W} *vs.* DMSO, NS). DMSO, $n = 3$; $NGF^{m/m}$, $n = 5$; $NGF^{R100W/m}$, $n = 5$. Capsaicin test 6 months, ANOVA-1 ($F_{2,13} = 49.995$, $p < 0.001$), followed by Bonferroni post-hoc test ($NGF^{m/m}$ *vs.* DMSO, $p < 0.001$; $NGF^{m/m}$ *vs.* $NGF^{R100W/m}$, $p < 0.001$; $NGF^{R100W/m}$ *vs.* DMSO, $p = 0.017$). DMSO, $n = 3$; $NGF^{m/m}$, $n = 5$; $NGF^{R100W/m}$, $n = 6$.

B. Hotplate test 2 months, Student's two-tailed *t*-test (t = 0.126, p = 0.901). $NGF^{m/m}$, $n = 11$; $NGF^{R100W/m}$, $n = 15$. Hotplate test 6 months, Student's two-tailed *t*-test (t = 4.743, $p < 0.001$). $NGF^{m/m}$, $n = 4$; $NGF^{R100W/m}$, $n = 9$. Hotplate latency, 6 months, ANOVA-2 ("genotype" × "temperature" interaction, $F_{4,79} = 3.283$, $p = 0.017$), followed by Bonferroni post-hoc test, *** $p < 0.001$, ** $p = 0.003$; $NGF^{m/m}$, $n = 8$; $NGF^{R100W/m}$, $n = 8$.

C. Acetone test 2 months, Student's two-tailed *t*-test (t = 2.445, p = 0.035). $NGF^{m/m}$, $n = 6$; $NGF^{R100W/m}$, $n = 6$. Acetone test 6 months, Student's *t*-test two-tailed (t = 2.457, p = 0.026). $NGF^{m/m}$, $n = 8$; $NGF^{R100W/m}$, $n = 10$.

D. Tape removal test 2 months, Student's two-tailed *t*-test (t = 1.261, p = 0.226). $NGF^{m/m}$, *n* = 6; $NGF^{R100W/m}$, *n* = 11. Tape removal test 6 months, Student's two-tailed *t*-test (t = 2.305, p = 0.042). $NGF^{m/m}$, *n* = 5; $NGF^{R100W/m}$, *n* = 8.

E. Cotton swab test 2 months, Student's two-tailed *t*-test (t = 0.155, p = 0.879). $NGF^{m/m}$, *n* = 5; $NGF^{R100W/m}$, *n* = 11. Acetone test 6 months, Student's two-tailed *t*-test (t = 0.050, p = 0.961). $NGF^{m/m}$, *n* = 8; $NGF^{R100W/m}$, *n* = 7.

Figure 4.6

ANOVA-1 ($F_{2,17}$ = 8.621, p = 0.003), followed by Bonferroni post-hoc test, $hNGF^{WT}$ *vs.* control, p = 0.006; $hNGF^{R100W}$ *vs.* control, p = 0.01; *n* = 6 for each group.

Figure 4.8

A. ANOVA-1 ($F_{2,16}$ = 10.501, p < 0.002) followed by Student-Newman-Keuls post-hoc test, *** p < 0.001, * p = 0.03; $hNGF^{WT}$, *n* = 5; $hNGF^{R100W}$, *n* = 6; control, *n* = 6.

B. ANOVA-2 (NGF × bradykinin interaction, $F_{2,45}$ = 3.371, p = 0.044) followed by Bonferroni post-hoc test, *** p < 0.001; $hNGF^{WT}$-vehicle, *n* = 7; $hNGF^{R100W}$-vehicle, *n* = 8; control-vehicle, *n* = 8; $hNGF^{WT}$-bradykinin, *n* = 8; $hNGF^{R100W}$- bradykinin, *n* = 7; control- bradykinin, *n* = 8.

C. ANOVA-2 (NGF × bradykinin interaction, $F_{2,47}$ = 9.346, p < 0.001) followed by Bonferroni post-hoc test, *** p < 0.001, ** p = 0.008, * p = 0.02; *n* = 8 for each group.

D. ANOVA-2 repeated measures (treatment × time interaction, $F_{8,144}$ = 5.785, p < 0.001) followed by Bonferroni post-hoc test, $hNGF^{WT}$ *vs.* saline, *** p < 0.001; $hNGF^{WT}$ *vs.* $hNGF^{R100W}$, ### p < 0.001, ## p = 0.002; saline, *n* = 10; $hNGF^{WT}$, *n* = 11; $hNGF^{R100W}$, *n* = 9.

Figure 4.9

Left, Student's two-tailed *t* test (t = 6.219, p = 0.003); $NGF^{m/m}$, *n* = 3; $NGF^{R100W/m}$, *n* = 3. *Right*, Student's two-tailed *t* test (t = 12.455, p < 0.001); $NGF^{m/m}$, *n* = 4; $NGF^{R100W/m}$, *n* = 4.

Figure 4.10

Nerve conduction velocity, Aβ fiber peak, Student's two-tailed t test (t = 0.435, p = 0.669); Aδ fiber peak, Student's two-tailed t test (t = 0.737, p = 0.470); C fiber peak, Student's two-tailed t test (t = 1.629, p = 0.120); non-significant; $NGF^{m/m}$, n = 10; $NGF^{R100W/m}$, n = 11 nerves.

Figure 4.11

A. Student's two-tailed *t* test (t = 3.810 , p = 0.004); $NGF^{m/m}$, *n* = 5; $NGF^{R100W/m}$, *n* = 6).

B. Student's two-tailed *t* test (t = 0.983, p = 0.351); $NGF^{m/m}$, *n* = 5; $NGF^{R100W/m}$, *n* = 6).

C. Student's two-tailed *t* test (t = 3.295, p = 0.009); $NGF^{m/m}$, *n* = 5; $NGF^{R100W/m}$, *n* = 6).

Figure 4.12

A. 2 months, Student's two-tailed *t* test (t = 0.340, p = 0.751); $NGF^{m/m}$, *n* = 3; $NGF^{R100W/m}$, *n* = 3; 6 months, Student's two-tailed *t* test (t = 4.779, p = 0.004); $NGF^{m/m}$, *n* = 4; $NGF^{R100W/m}$, *n* = 3.

B. 2 months, Student's two-tailed *t* test (t = 0.296, p = 0.771); $NGF^{m/m}$, *n* = 6; $NGF^{R100W/m}$, *n* = 11; 6 months, Student's two-tailed *t* test (t = 1.268, p = 0.225); $NGF^{m/m}$, *n* = 8; $NGF^{R100W/m}$, *n* = 8.

Figure 4.13

A. 2 months, Student's two-tailed t test (t = 0.792, p = 0.473); n = 3 for both groups. 6 months, Student's two-tailed t test (t = 5.800, p = 0.002); $NGF^{m/m}$, n = 4; $NGF^{R100W/m}$, n = 3.

B. Student's two-tailed t test (t = 3.169, p = 0.034); n = 3 for both groups.

Figure 4.14

$NGF^{m/m}$, Student's two-tailed t-test (t = 0.323, p = 0.754), NGF, *n* = 7, saline, *n* = 5; $NGF^{R100W/m}$, Student's two-tailed t-test (t = 2.764, p = 0.033), saline, *n* = 5, NGF, *n* = 4.

Figure 4.15

A. ANOVA-1 ($F_{5,24}$ = 23.529, p < 0.001) followed by Student-Newman-Keuls post-hoc test, *** p < 0.001, ** p < 0.01, * p < 0.05; NGF, *n* = 5; $hNGF^{WT}$ 0.6 μg, *n* = 4; $hNGF^{R100W}$ 0.6 μg, *n* = 5; $hNGF^{WT}$ + $hNGF^{R100W}$ 0.3 μg/each, *n* = 3; $hNGF^{WT}$ 0.3 μg, *n* = 4;$hNGF^{R100W}$ 0.3 μg, *n* = 5; mock, *n* = 4.

B. Student's two-tailed *t* test (p =0.031); $NGF^{m/m}$, *n* = 6; $NGF^{R100W/m}$, *n* = 7.

C. Student's two-tailed *t* test (t = 2.465, p = 0.031); $NGF^{m/m}$, *n* = 6; $NGF^{R100W/m}$, *n* = 7.

Figure 4.16

A. ANOVA-2 with repeated measures (main effect of "training day", $F_{8,112}$ = 15.600, p < 0.001). $NGF^{m/m}$, *n* = 5; $NGF^{R100W/m}$, *n* = 8.

B. ANOVA-2 with repeated measures ("training day" × "genotype" interaction, $F_{8,123}$ = 2.836, p = 0.007), followed by Bonferroni post-hoc test, * p < 0.05, *** p < 0.001. $mNGF^{+/+}$, *n* = 7; $mNGF^{+/-}$, *n* = 7.

C. 2 months, Student's two-tailed *t* test (t = 0.385, p = 0.704). $NGF^{m/m}$, n = 7; $NGF^{R100W/m}$, n = 15; 6 months, Student's *t* two-tailed test (t = 1.094, p = 0.289). $NGF^{m/m}$, n = 10; $NGF^{R100W/m}$, n = 9; Student's two-tailed *t* test (t = 1.303, p = 0.215). $mNGF^{+/+}$, *n* = 6; $mNGF^{+/-}$, *n* = 9.

D. 2 months, Student's two-tailed *t* test (t = 0.282, p = 0.780). $NGF^{m/m}$, n = 7; $NGF^{R100W/m}$, n = 15; 6 months, Student's *t* two-tailed test (t = 1.453, p = 0.166). $NGF^{m/m}$, n = 10; $NGF^{R100W/m}$, n = 8; Student's two-tailed *t* test (t = 4.450, p < 0.001). $mNGF^{+/+}$, *n* = 6; $mNGF^{+/-}$, *n* = 9.

E. 2 months, Student's two-tailed *t*-test (t = 0.958, p =0.375). $NGF^{m/m}$, *n* = 4; $NGF^{R100W/m}$, *n* = 4; 6 months, Student's two-tailed *t*-test (t = 1.271, p = 0.278; $NGF^{m/m}$, *n* = 3; $NGF^{R100W/m}$, *n* = 4); Student's two-tailed *t*-test (t = 3.529, p = 0.010; $mNGF^{+/+}$, *n* = 5; $mNGF^{+/-}$, *n* = 4).

F. 2 months, Student's two-tailed *t*-test (t = 1.144, p =0.296). $NGF^{m/m}$, *n* = 4; $NGF^{R100W/m}$, *n* = 4; 6 months, Student's two-tailed *t*-test (t = 0.180, p = 0.864; $NGF^{m/m}$, *n* = 3; $NGF^{R100W/m}$, *n* = 4); Student's two-tailed *t*-test (t = 3.212, p = 0.015; $mNGF^{+/+}$, *n* = 5; $mNGF^{+/-}$, *n* = 4).

Figure 4.17

A. 2 months, Student's two-tailed *t* test (t = 2.182, p = 0.788); $NGF^{m/m}$, *n* = 4; $NGF^{R100W/m}$, *n* = 11; 6 months, Student's two-tailed *t*-test (t = 5.431, p = 0.003; $NGF^{m/m}$, *n* = 3; $NGF^{R100W/m}$, *n* = 4).

B. 2 months, Student's two-tailed *t* test (t = 1.374, p = 0.212); $NGF^{m/m}$, *n* = 4; $NGF^{R100W/m}$, *n* = 5; 6 months, Student's two-tailed *t* test (t = 2.357, p = 0.043); $NGF^{m/m}$, *n* = 4; $NGF^{R100W/m}$, *n* = 7.

C. 2 months, Student's two-tailed *t* test (t = 1.038, p = 0.334); $NGF^{m/m}$, *n* = 4; $NGF^{R100W/m}$, *n* = 5; 6 months, Student's two-tailed *t* test (t = 2.482, p = 0.035); $NGF^{m/m}$, *n* = 4; $NGF^{R100W/m}$, *n* = 7.

Figure 4.18

A. Tape removal test, Student's two-tailed *t* test (t = 0.04, p = 0.969); $NGF^{m/m}$, *n* = 8; $NGF^{h/m}$ = 7.

B. Cotton swab test, Student's two-tailed *t* test (t = 0.394, p = 0.700); $NGF^{m/m}$, *n* = 8; $NGF^{h/m}$ = 7.

C. Hot plate test, Student's two-tailed *t* test (t = 0.325, p = 0.751); $NGF^{m/m}$, *n* = 6; $NGF^{h/m}$ = 7.

D. Time spent moving, Student's two-tailed *t* test (t = 2.027, p = 0.073); $NGF^{m/m}$, *n* = 6; $NGF^{h/m}$ = 5.

E. Exploration time, Student's two-tailed *t* test (t = 5.420, p = 0.468); $NGF^{m/m}$, *n* = 5; $NGF^{h/m}$ = 5.

F. Preference index, Student's two-tailed *t* test (t = 1.368, p = 0.208); $NGF^{m/m}$, *n* = 5; $NGF^{h/m}$ = 5.

Figure 4.19

A. *Left*, ANOVA-2 ("genotype" × "response" interaction, $F_{3,57}$ = 10.113, p < 0.001), followed by Bonferroni post-hoc test, *** p < 0.001, ** p = 0.007, * p = 0.021; $NGF^{h/m}$, *n* = 11; $NGF^{R100W/m}$, *n* = 9. *Right*, ANOVA-2 ("genotype" × "response" interaction, $F_{3,77}$ = 5.892, p = 0.001), followed by Bonferroni post-hoc test, *** p < 0.001, * p = 0.014; $NGF^{h/m}$, *n* = 12; $NGF^{R100W/m}$, *n* = 7.

B. *Left*, ANOVA-2 for repeated measures (main effect of "tone", $F_{4,94}$ = 47.731, p < 0.001); $NGF^{h/m}$, *n* = 10; $NGF^{R100W/m}$, *n* = 9. *Right*, ANOVA-2 for repeated measures (main effect of "tone", $F_{4,104}$ = 32.846, p < 0.001); $NGF^{h/m}$, *n* = 11; $NGF^{R100W/m}$, *n* = 10.

C. 2 months, Student's two-tailed *t*-test (t = 0.719, p =0.482). $NGF^{m/m}$, *n* = 10; $NGF^{R100W/m}$, *n* = 9; 6 months, Student's two-tailed *t*-test (t = 0.764, p = 0.454; WT, *n* = 11; HT^{R100W}, *n* = 10).

D. 2 months, Student's two-tailed *t* test (t = 3.822, p = 0.001); $NGF^{h/m}$, *n* = 10; $NGF^{R100W/m}$, *n* = 9; 6 months, Student's two-tailed *t* test (t = 10.190, p < 0.001); $NGF^{h/m}$, *n* = 10; $NGF^{R100W/m}$, *n* = 10.

E. ANOVA-2 ("genotype" × "phase" interaction, $F_{1,22}$ = 436.453, p < 0.001) followed by Bonferroni post-hoc test, *** p < 0.001; $NGF^{h/m}$, *n* = 6; $NGF^{R100W/m}$, *n* = 5.

F. Student's two-tailed *t* test (t = 1.948, p = 0.093); $NGF^{h/m}$, *n* = 5; $NGF^{R100W/m}$ = 4.

Figure 4.20

Upper row, *left*, amygdala, Student's two-tailed *t* test (t = 4.235, p = 0.003); $NGF^{h/m}$, *n* = 4; $NGF^{R100W/m}$, *n* = 6; *middle left*, hippocampus, Student's two-tailed *t* test (t = 2.485, p = 0.038); $NGF^{h/m}$, *n* = 4; $NGF^{R100W/m}$, *n* = 6; *middle*, motor cortex, Student's two-tailed *t* test (t = 12.226, p < 0.001); $NGF^{h/m}$, *n* = 3; $NGF^{R100W/m}$, *n* = 4; *middle right*, anterior cingulate cortex (ACC), Student's two-tailed *t* test (t = 2.349, p = 0.047; $NGF^{h/m}$, *n* = 4; $NGF^{R100W/m}$, *n* = 6); *right*, caudate nucleus, Student's two-tailed *t* test (t = 3.026, p = 0.039); $NGF^{h/m}$, *n* = 3; $NGF^{R100W/m}$, *n* = 3; *lower row*; primary somatosensory cortex (S1), Student's *t* two-tailed test (t = 0.526, p = 0.621); $NGF^{h/m}$, *n* = 3; $NGF^{R100W/m}$, *n* = 4.

Figure 4.21

Student's two-tailed *t*-test (t = 2.860, p = 0.017); $NGF^{h/m}$, *n* = 5; $NGF^{R100W/m}$, *n* = 7.

Figure 4.22

A. *left*, Student's paired *t* test (t = 3.344, p = 0.012); $NGF^{h/m}$, *n* = 8; *middle left*, Student's paired *t* test (t = 21.847, p < 0.001); $NGF^{R100W/m}$, *n* = 7; *middle right*, Student's paired *t* test (t =4.117, p = 0.004); $NGF^{h/m}$, *n* = 8; *right*, Student's paired *t* test (t = 25.711, p < 0.001); $NGF^{R100W/m}$, *n* = 7.

B. Student's two-tailed *t* test (t = 0.243, p = 0.815); $NGF^{h/m}$, *n* = 4; $NGF^{R100W/m}$, *n* = 5.

Figure 4.23

A. Student's two-tailed *t*-test (t = 2.507, p = 0.046); $NGF^{h/m}$, *n* = 4; $NGF^{R100W/m}$, *n* = 4.

B. ANOVA-2 (main effect of "genotype", $F_{1,18}$ = 19.464, p < 0.001), $NGF^{h/m}$-baseline, n = 4; $NGF^{R100W/m}$-baseline, n = 7; $NGF^{h/m}$-fear conditioning, n = 3; $NGF^{R100W/m}$-fear conditioning, n = 5.

C. Student's two-tailed *t*-test (t = 2.670, p = 0.020); $NGF^{h/m}$, *n* = 5; $NGF^{R100W/m}$, *n* = 9.

D. Student's two-tailed *t*-test (t = 0.284, p = 0.790); $NGF^{m/m}$, n = 3; $NGF^{m/-}$, n = 3.

E. Student's two-tailed *t*-test (t = 1.332, p = 0.231); $NGF^{m/m}$, n = 5; $NGF^{m/-}$, n = 3.

F. Student's two-tailed *t*-test (t = 6.005, p < 0.001); $p75^{NTR+/+}$, n = 4; $p75^{NTR-/-}$, n = 4.

5. DISCUSSION

5.1 NGF as a mediator of pain

Pain is a subjective experience that can vary among individuals. It alerts us about danger, thus exerting an immediate physiological role in preserving bodily integrity, but also instructs us to learn avoiding future harmful events. It is also important to note that pain sensation is not necessarily related linearly to the nociceptive input that triggered it, neither it is solely for vital protective functions. Indeed, sensory and affective dimensions also concur to determine the final sensation. Thus, pain can be considered as the result of brain processes elicited by peripherally encoded sensory-discriminative inputs, which are integrated with affective and emotional aspects (Price, 2000), along with memories from past experiences (Sandkuhler, 2000).

One of the most important mediators of pain is NGF, which, in addition to its well-known neurotrophic role (Levi-Montalcini, 1952), is capable of powerful pro-inflammatory and sensitizing actions (Denk et al., 2017). NGF causes sensitization both *in vitro* and *in vivo*. Application of NGF to adult sensory neurons results in activation of TrkA and in the rapid sensitization of those neurons to different stimuli, including mechanical stimuli (Di Castro et al., 2006), thermal stimuli (Zhang et al., 2005) and chemical stimuli such as capsaicin (Winter et al., 1988). Cutaneous injection of NGF leads to long-lasting hyperalgesia, both in rodents and humans (Lewin et al., 1993; Lewin et al., 1994; Svensson et al., 2003). Endogenous mRNA and protein are increased in several pain disorders, for example in chronic pain conditions, and contribute to peripheral and central sensitization (Denk et al., 2014; Minnone et al., 2017). On the other hand, NGF-neutralizing molecules are effective analgesics in many model of persistent pain (McMahon et al., 1995; Ugolini et al., 2007). Indeed, the critical role of NGF in the generation and potentiation of pain has created a strong rationale for development of antibodies against NGF (i.e. Tanezumab) (Patel et al., 2018). In addition, the neurotrophic properties of NGF have led to test it as a therapeutic candidate for different conditions, such as diabetic polyneuropathy (Pittenger and Vinik, 2003) and neurodegenerative diseases (Mitra et al., 2019). However, the “algogenic” properties of NGF manifested during these trials, causing strong adverse effects, that contributed to the failure of these clinical tests (Apfel, 2002; Cattaneo and Capsoni, 2019). For all these reasons, there is a strong interest in understanding the involvement of the NGF system in the regulation of pain responses.

5.2 HSAN V and its implications for understanding pain

In this regard, Hereditary Sensory and Autonomic Neuropathies (HSANs), a group of congenital pain insensitivity diseases, offer a great opportunity to dissect the role of the NGF/TrkA system in pain. Indeed, several mutations in the genes encoding TrkA and NGF cause pain insensitivity and are responsible for the etiology of some HSAN variants (Indo, 2001; Capsoni, 2014).

In particular, to date, three mutations in the *ngf* gene have been identified in HSAN V patients: R221W, V232fs and R121W, that alter the processing of NGF, the neurotrophic activity or abolish the formation of mature NGF, respectively (Larsson et al., 2009; Carvalho et al., 2011; Shaikh et al., 2018). Of these, R121W mutation results in the R100W missense mutation in mature NGF and is not characterized by cognitive deficits, as is HSAN IV (Einarsdottir et al., 2004). R100W causes in homozygous patients a severe insensitivity to pain and frequent orthopedic fractures that significantly interfere with the quality of life (Minde et al., 2004). On the other hand, heterozygous subjects are often clinically silent, with decreased density of afferent C-fibers and attenuation of nociception (Minde et al., 2009), and with altered "pleasantness" sensation evoked by gentle tactile stimuli (Morrison et al., 2011). Given these very special sensory and cognitive features, HSAN V can represent an ideal model to investigate the interplay between nociception and construction of the pain perception.

In order to investigate the mechanism of the painlessness HSAN V mutation in the *ngf* gene, and to dissect the role of the NGF/TrkA system in pain, I generated an animal model of HSAN V, by creating a knock-in line that reproduces the NGF^{R100W} mutation in the mouse. Heterozygous $NGF^{R100W/m}$ mice show nociceptive impairment, which fully manifests in adulthood, and no cognitive deficits, in line with patients (Minde et al., 2009). The reactivity to the application of known algogens, such as capsaicin, and the sensitivity to non-noxious stimuli (i.e., application of tape to the back) were decreased, which can correlate with the reduced innervation of glabrous and hairy skin, respectively and with the reduced density of non-myelinated fibers. However, nerve conduction speed was not different from control mice, in line with similar electrophysiological findings from heterozygous patients (Minde et al., 2004). Moreover, $NGF^{R100W/m}$ mice have a lower skin NGF content, which could contribute to the reduction in cutaneous sensitivity to noxious stimuli and in glabrous skin innervation. Indeed, a long treatment with wild type NGF was able to rescue insensitivity to noxious stimuli, such as capsaicin-induce pain.

5.3 Effect of the R100W mutation on DRG neurons

NGF is a key molecule for the development and differentiation of DRG neurons and for the sensitization to painful stimuli of adult DRG (Dubin and Patapoutian, 2010). How can this mutation affect DRG in the $NGF^{R100W/m}$ HSAN V mouse model? The main neuronal populations in DRG (i.e., peptidergic and non-peptidergic neurons) were unaffected by reduced skin innervation and displayed a normal distribution in $NGF^{R100W/m}$ mice. However, the expression of key pain transduction-related molecules (i.e. TRPV1 and B2R) was altered. This finding prompted me to search for more global alterations in the gene expression profile of DRGs, by performing a transcriptomic study. The transcriptomic profile of DRGs from adult $NGF^{R100W/m}$ mice presented small alterations, with only a few hundred genes changed to a significant extent. Interestingly, transcriptomics revealed that most of the differentially expressed genes belong to the immune response category. Among them, TyroBP (TREM2) and Toll-Like Receptor 2 (TLR2). TyroBP (TREM2) is involved in bone formation and in microglia function in the brain and is associated to Nasu-Hakola disease (Shboul et al., 2018), a rare inherited leukodystrophy characterized by progressive presenile dementia (Carmona et al., 2018). The dysregulation of TyroBPexpression could contribute to the bone alterations observed in HSAN V patients (Minde, 2006). Moreover, activation of Toll-Like Receptor 2 (TLR2) modulates production of proinflammatory cytokines in neuropathic pain (Liu et al., 2012). These interesting points deserve further investigation in the future, also in view of the recent finding that microglia is a target cell for NGF (Rizzi et al., 2018).

I also analyzed DRG sensitization *in vitro*, and found that nociception-related biochemical responses to treatment with the NGF^{R100W} protein are attenuated in comparison to wild-type NGF; in particular, Substance P release and activation of TRPV1 in DRG cultures were decreased after priming with NGF^{R100W}. This is in line with the failure of NGF^{R100W} application to potentiate H^+-evoked responses in DRG cultures (Sung et al., 2018) and extends data showing that NGF^{R100W} uncouples trophic effects from nociceptive functions of NGF (Covaceuszach et al., 2010; Capsoni et al., 2011; Sung et al., 2018). NGF^{R100W} has a reduced affinity to $p75^{NTR}$ (Covaceuszach et al., 2010) and binding of NGF to this receptor is required for the upregulation of bradykinin receptors (Petersen et al., 1998). This phenotypic aspect linked to the NGF^{R100W} mutation is also observed in neurons from mice lacking $p75^{NTR}$ or in neurons from wild-type mice treated with a $p75^{NTR}$ blocking antibody (Petersen et al., 1998). These previous data suggest that the

differential engagement of TrkA and $p75^{NTR}$ receptors could explain the reduced expression of the bradykinin receptor following treatment with NGF^{R100W}, suggesting a possible molecular mechanism for the reduction in DRG priming that I observed.

5.4 Altered pain-related memory in the HSAN V model

However, the above described features of NGF^{R100W} do not completely ablate nociception and the corresponding behavioural responses in mice heterozygous for the mutation. In particular, the intensity of an electrical shock delivered to the hind paws could be adjusted to induce acute responses that were comparable to those in control mice. This gave me the opportunity to study whether higher-order, adaptive responses mediated by nociceptive inputs could be affected by the R100W mutation. For this reason, I selected the heterozygous condition to investigate the consequences of developing and living with impaired pain perception. Taking into account that painful stimuli induce robust learning and memory formation (Sandkuhler, 2000; Flor, 2002; Price and Inyang, 2015), I chose the fear conditioning test (LeDoux, 2014), a reliable Pavlovian conditioning paradigm that allows to study the ability to associate a neutral stimulus with a noxious stimulus in order to form new memories. Surprisingly, $NGF^{R100W/m}$ mice are unable to form episodic memories triggered by painful events, despite a normal capability to associate pain with an auditory tone or spatial context during fear conditioning. In contrast, predator fear is not affected; notably, this form of fear, despite representing a pain-relevant situation, is not learned, but innate. Consistently, these two forms of fear are supported by distinct neural circuits (Gross and Canteras, 2012) and, in particular, neurons in the VMH nucleus, which are normally activated by predator exposure in $NGF^{R100W/m}$ mice, appear to selectively support defensive behaviors elicited by predators (Silva et al., 2013). In addition, the age-related observed alterations of anxiety-like behaviours in $NGF^{R100W/m}$ mice are consistent with a lack of pain-related fear learning.

I can exclude that the lack of pain-memory formation is due to cognitive deficits caused by decreased NGF levels, due to the reduced secretion of NGF^{R100W} protein, because learning and memory appear to be normal in $NGF^{R100W/m}$ mice, in stark contrast with $mNGF^{+/-}$ mice. Comparison with this latter model also allowed to demonstrate that the central effects in $NGF^{R100W/m}$ mice are not simply due to NGF haploinsufficiency. In accordance with this, the R100W mutation preserves the binding of NGF^{R100W} to TrkA and the

corresponding downstream signaling (Capsoni et al., 2011; Sung et al., 2018). Normal function of TrkA is required for adequate maturation of basal forebrain cholinergic neurons, thus impacting cognitive functions such as attention, learning and memory (Fagan et al., 1997). Maturation and differentiation of NGF target neurons in the medial septum of the basal forebrain and striatum – which are involved in memory and cognitive processes – were unaffected in $NGF^{R100W/m}$ mice, thus lending further support to a normal activation of TrkA.

In addition, homozygous $NGF^{R100W/R100W}$ mice showed unaffected cholinergic neuron density in the basal forebrain and, surprisingly, a significant increase in the striatum (Testa et al., 2019). These data, once again, reflect an imbalance of NGF^{R100W} signaling via TrkA and $p75^{NTR}$; indeed, similarly to $NGF^{R100W/R100W}$ mice, $p75^{NTR-/-}$ mice show a 23% increase in the number of striatal cholinergic neurons (Van der Zee et al., 1996). On the other hand, NGF haploinsufficiency could be the cause of lethality and reduced body weight of homozygous $NGF^{R100W/R100W}$ mice (Testa et al., 2019). In fact, the mutation interferes with the processing of proNGF to mature NGF in cultured cells, leading to a decreased secretion of mature NGF ((Larsson et al., 2009) and these data). Accordingly, long-term treatment with NGF^{WT} was able to prolong the survival of $NGF^{R100W/R100W}$ mice and to restore their body weight, at least for the first two weeks (Testa et al., 2019). Another aspect that deserves to be considered is the possibility that the binding affinity of human NGF^{R100W} to mouse TrkA could be lower than wild type NGF (Paoletti et al., 2015), thus impinging on signal transduction, which could explain the lethality in homozygous condition. Notably, in the heterozygous condition, despite reduced total levels of NGF in $hNGF^{R100W/m}$ brains, this effect is attenuated by (i) the unaffected neurotrophic properties of NGF^{R100W} and (ii) by full TrkA signaling mediated by the murine NGF allele. To this regard, it is worth noting that mutations in NGF and its receptor are not completely overlapping; indeed, mutations in the *TrkA* gene cause HSAN IV, which, unlike HSAN V, is characterized by mental retardation and anhydrosis (Indo, 2018). The absence of cognitive deficits in HSAN V patients reinforces the fact that NGF^{R100W} retains its neurotrophic functions in the CNS.

5.5 The role of CGRP in mediating fear responses

CGRP neurons project to the amygdala (D'Hanis et al., 2007) and modulate learning of pain-related fear responses. Indeed, optogenetic silencing of CGRP neurons projecting to the amygdala decreases

conditioned fear responses (Campos et al., 2018), whereas optogenetic activation of these neurons or local infusion of CGRP into the amygdala elicit freezing (Palmiter, 2018). $NGF^{R100W/m}$ mice have decreased innervation of the central amygdala by CGRP-expressing fibers, which might suggest an explanation of the impaired fear response, in line with the role of CGRP in mediating the emotional aspects of pain (Palmiter, 2018). This leads to conclude that the NGF^{R100W} mutation specifically affects the expression of learned pain-related behaviours, without affecting other forms of learning.

The pain signal produced by a noxious stimulus, such as foot shock, is transmitted from sensory neurons to projection neurons in the most superficial layer (lamina I) of the spinal cord and then reaches the cortex through the spino-thalamic and the spino-parabrachial ascending pathways (Todd, 2010). To better understand the role of afferent pathways in mediating pain-induced fear behavior in the HSAN V condition, a future experiment could use adeno-associated viral vectors (AAVs) expressing channelrhodopsin (ChR). Such a construct will be bilaterally injected into the lateral subdivision of the parabrachial nucleus (PBel), to examine optogenetic activation of CGRP neurons. First, neuronal responses in the central nucleus of amygdala (CeAl) elicited by photostimulation of ChR-positive terminals from PBel will be measured by patch-clamp. According to the reduced density of CGRP terminals that I have observed, these responses could have a lower amplitude. Then, I will test if overstimulation of CGRP-positive (i) neurons in PBel or (ii) afferents in CeAl (either during the encoding or recall phases of fear conditioning) is sufficient to rescue the formation of threat memories in $NGF^{R100W/m}$ mice. This protocol could also restore a normal relationship between electric shock intensity and behavioral response, in addition to normalizing the amplitude of CeAl neuronal responses. The possible rescue will be also evaluated by measuring the response to different thermoceptive stimuli, considering that (i) CGRP neurons are able to encode stimulus intensity (Campos et al., 2018) and (ii) $NGF^{R100W/m}$ mice have a higher threshold for painful thermoceptive responses (present work). CGRP-positive neurons are also activated by non-painful noxious stimuli, such as chloroquine – which induces itch – and lipopolysaccharide (LPS) – which reproduces bacterial infection-associated inflammation. I hypothesize that these responses could be impaired in $NGF^{R100W/m}$ mice, and that optogenetic activation of CGRP-positive, PBel neurons of $NGF^{R100W/m}$ mice could rescue them.

5.6 A parallel between human and mouse brain areas activated by pain

Studies on the human heterozygote carrier group, by our Swedish collaborators, supported my findings from experiments on mice. Indeed, these subjects showed impairments in incorporating noxious stimulation into behavioral responses. The accuracy performance of this group was reduced in an experimental paradigm that required integrating task requirements with somatosensory information to produce a behavioral response (a button press, variably associated with noxious or innocuous stimulation). Despite reporting a normal thermal threshold, they exhibited a significant bias for accepting noise as signal, regardless of whether the stimulation was painful or non-painful. Subjectively, they also experienced a significantly lower urge to move the affected limb away during acute painful stimulation.

In order to look for an anatomical correlate of behavioral findings, I identified a set of mouse brain regions, such as amygdala, hippocampus, anterior cingulate cortex (ACC), caudate nucleus and motor cortex, that, after re-exposure to the conditioning stimulus (i.e., recall phase of fear conditioning), show decreased activation in $NGF^{R100W/m}$ mice with respect to controls.

I chose the amygdala and hippocampus because are directly involved in mediating the fear conditioning response (Gross and Canteras, 2012); the ACC because it is related to the affective features of pain, such as subjective feelings of unpleasantness (Tang et al., 2005), and is tightly linked to production of behavioural responses to pain (Perini et al., 2013). The inactivation of ACC prevents associative fear learning and this effect is likely to be mediated through either direct or indirect projections to the amygdala and hippocampus (Furlong et al., 2010). In addition, the primary motor (M1) cortex and the caudate nucleus show also decreased activation in $NGF^{R100W/m}$ mice. This can indicate an altered brain output in the execution of a motivated motor behaviour. This interpretation is supported by the normal activation of S1 cortex, which is primarily involved in the discriminative aspects of somatic sensation, indicating a normal processing of sensory inputs in HSAN V. Taken together, these results from mice and humans indicate that a more complex mechanism than a simple failure in nociception is at work in HSAN V. This is very different from the case of $Na_v1.7$ "pain-free" subjects, who display a normal activation of the so-called "pain matrix" (composed of brain regions such as ACC, thalamus and insula) in response to a noxious mechanical stimulus (Salomons et al., 2016). For this reason, I speculate that, in the case of mutated NGF, a higher uncertainty in discriminating potentially harmful situations from neutral ones, might result in a

failure of noxious stimulation to instruct behaviour production by activating subcortical and cortical brain regions.

5.7 HSAN V vs HSANs: the different role of endogenous analgesic peptides

In general, congenital insensitivities to pain, including HSAN V, are usually explained by defective nociceptor development and consequent loss of nociceptor function (Nahorski et al., 2015).

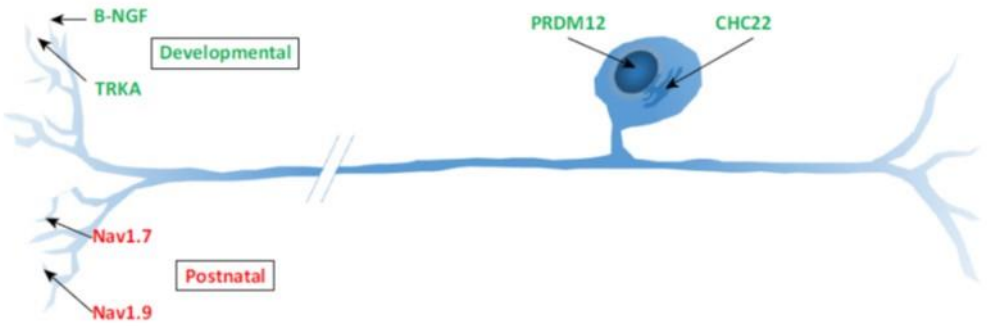

Figure 5.1 Schematic diagram detailing the location of the phenotypic effect of mutations in genes involved in nociception and their effect on nociceptor development or postnatal function (Adapted from Nahorski et al., 2015).

For instance, the "painlessness" phenotype deriving from a $Na_v1.7$ mutation causes an altered transmission of painful signals by primary nociceptors and a higher expression of endogenous analgesic peptides specifically in sensory neurons, and is reversed by the administration of the opioid antagonist naloxone in patients and mice, which potentiates the tone of noxious peripheral input to the spinal cord (Minett et al., 2015). In addition, Pereira et al. recently showed that both μ-opioid receptors and δ-opioid receptors contribute to analgesia in $Na_v1.7$-null mutant mice (Pereira et al., 2018). Hereditary painlessness can also result from a mutation in $Na_v1.9$, causing a state where nociceptors cannot generate an action potential and pain cannot be perceived by the central nervous system (Leipold et al., 2013). Moreover, deficits in the development of nociceptors are also present in hereditary painlessness caused by mutations in *PDRM12* gene, whose expression during development is restricted to DRGs (Chen et al., 2015). On the other hand, I found a normal DRG architecture in $NGF^{R100W/m}$ mice, which prompted me to focus on the central (brain) aspects of pain perception.

Unlike the painlessness phenotype caused by a $Na_v1.7$ mutation, the impairment in pain-dependent learning of $NGF^{R100W/m}$ mice cannot be simply explained by an unpregulation of endogenous analgesics, since the density of oxytocin- and β-endorphin-producing cells was reduced. Plasma levels of oxytocin were also decreased in $NGF^{R100W/m}$ mice, possibly as a consequence of tonically reduced nociception, in line with the pain-killing role of this peptide (Eliava et al., 2016). In fact, oxytocin receptor is expressed by non-peptidergic C-type sensory neurons (Moreno-Lopez et al., 2013) and *in vitro* application of oxytocin suppresses their activity (Gong et al., 2015). On the other hand, $mNGF^{+/-}$ mice do not show differences in oxytocin levels, which, thus, do not derive simply from reduced NGF levels or secretion. I interpret these data as a homeostatic response, triggered by a chronic reduction in the average intensity of nociceptive inputs to the brain, as a result of lower pain sensitivity. This leads to a reprogramming of the set-point for nociceptive responses, which manifests as a reduction in the levels of the neuropeptides (oxytocin, β-endorphin, CGRP) required to tune the brain systems dedicated to pain construction and processing. Interestingly, $p75^{NTR-/-}$ mice have reduced nociception and decreased skin innervation, despite normal DRG structure (Bergmann et al., 1997), a significantly increased risk-taking behavior (Olsen et al., 2013) and show reduced oxytocin expression in the hypothalamus (present work). Thus, $p75^{NTR-/-}$ mice show common phenotypic features with HSAN V mice, which can be explained by the reduced binding of NGF^{R100W} to $p75^{NTR}$ (Covaceuszach et al., 2010; Sung et al., 2018). To understand more in detail the role of $p75^{NTR}$ in the mechanism underlying altered pain perception in HSAN V, more experiments are needed, in order to dissect the function of this receptor in the peripheral and central nervous systems. For example, the use of a $p75^{NTR}$ agonist could improve nociception and, consequently, the ability to respond to the application of algogens (and, also, to non-noxious stimuli), with a general improvement in the skin sensitivity of $NGF^{R100W/m}$ mice. On the other hand, regarding the possible role of $p75^{NTR}$ in the failure to form pain-related memories in $NGF^{R100W/m}$ mice, I would need, first, to analyze the role of $p75^{NTR}$ in different areas involved in memory formation. In fact, reports concerning the impact of $p75^{NTR}$ deletion on cholinergic neurons, spatial memory and cognitive functions are still contradictory (Greferath et al., 2000; Catts et al., 2008; Barrett et al., 2010). For example, Dokter et al reported an impairment of memory retrieval of $p75^{NTR}$-deficient mice in the Morris Water maze, despite normal cholinergic fiber density in the subgranular and molecular layers of the dentate gyrus (Dokter et al., 2015) and increased number of cholinergic neurons in

the septum (Naumann et al., 2002). On the contrary, $p75^{NTR}$-deficient mice display enhanced spatial memory (Greferath et al., 2000) and deletion of $p75^{NTR}$ does not alter both contextual and cued fear conditioning (Busch et al., 2017), confirming what reported by Olsen et al (2013). Cholinergic neuron populations and cognitive functions are totally normal in HSAN V mice, in which $p75^{NTR}$ signaling could be reduced, whereas TrkA function is mostly unaffected. This difference could explain the absence of memory deficit in HSAN V but not in HSAN IV disease, in which the mutation directly impacts on TrkA.

5.8 A role of microglia in the HSAN V phenotype?

Finally, considering that the few modulated genes in DRG of $NGF^{R100W/m}$ were involved in immune response and phagocytosis, I have addressed microglia morphology taking to account also that these cells are a target of NGF (Rizzi et al., 2018), which modulates their activity (De Simone et al., 2007). Microglia morphology and function are closely related. In a healthy condition, microglia is described as "resting", a phenotype characterized by a branched morphology (Davis et al., 1994). Microglial cells acquire an "activated" state in inflammation or injury, with a reduction in their ramifications (Davis et al., 1994). Microglia cells are sensors of the CNS status, constantly scanning the surrounding environment (Nimmerjahn et al., 2005). The known scavenger function of microglia is also involved in neuropathic pain (Batti et al., 2016) and activation of microglia was found in the spinal cord, but not in cortical regions, following nerve injury in adult mice (Zhang et al., 2008). On the contrary, microglia in ACC and hippocampus of adult HSAN V mice appears less branched compared to controls, indicating an activated state. It will be, therefore, interesting to understand the correlated functional meaning of the morphological alterations in this model of pain insensitivity, a different condition from those considered so far. These data suggest, once again, new roles of NGF in regulating brain pathophysiology.

5.9 Applying NGF^{R100W} to pain therapy

My results demonstrate that the effects of NGF on pain go beyond its known actions on peripheral nociception (Lewin et al., 2014; Lewin and Nykjaer, 2014; Denk et al., 2017). NGF is not only a key mediator of nociception, but also a master regulator in the elaboration of pain. Studying the HSAN V

painlessness condition contributed to reveal novel aspects of the pain-sensing system and the underlying genes, protein and pathways

Indeed, the human and mouse results converge to demonstrate the disruption by the NGF^{R100W} mutation of a brain system that integrates nociceptive information with sensory cues, correlating with a defect in interpreting painful stimuli as relevant for determining adaptive behavioural responses. By exploiting the clinical features of HSAN V, I took an opposite approach with respect to the majority of studies on pain, which are based on inducing pain itself. Extending these studies to other painlessness conditions could help in isolating common molecular and cellular mechanisms. Based on the phenotype of heterozygous mice and patients, it is tempting to speculate that NGF^{R100W} could act as a dominant negative on wild type NGF. Considering the relationship between NGF and nociception, an approach based on inducing painlessness could be relevant to design much needed strategies to treat pathological pain conditions, with implications for both basic and translational research. Within this context, it will be interesting to exploit the HSAN V model and the corresponding protein NGF^{R100W} for the study of different forms of pain. For example, one could perform chronic constriction injury (CCI) of sciatic nerve, spinal nerve transection (SNT) or chemotherapeutic drug injections to analyze, in different chronic pain models, if the R100W mutation confers any resistance to the development of neuropathic pain. Conversely, these manipulations could be also performed in wild type mice and combined with NGF^{R100W} treatment in order to evaluate its efficacy in dampening acute and/or chronic pain. In addition to neuropathic pain, it will be equally interesting to evaluate, in both chronic and acute conditions, visceral pain. This could be experimentally modeled by injection of Lipopolysaccharide (LPS;(Campos et al., 2018)). Finally, itch is a clinically relevant condition that shares similarities with pain (Davidson and Giesler, 2010), which can be experimentally induced by injection of chloroquine (Aghahowa et al., 2010). The expected result is a resistance of $NGF^{R100W/m}$ mice to chloroquine treatment and, possibly, the ability of NGF^{R100W} locally delivered to wild type mice to inhibit itch. Finally, a recent paper by Dhandapani et al used a photoconvertible BDNF-SNAP to photoablate the TrkB-positive population of mechanoceptors. Also taking into account the receptor binding profile of painless NGF, a recombinant $NGF^{R100W\text{-}SNAP}$ fusion protein might be generated to induce, upon photostimulation, a selective degeneration of TrkA-positive fibers from the skin of neuropathic pain models, inducing alleviation of hyperalgesia.

Taken together, the experimental approach and the results described here can contribute in opening a new conceptual and methodological window on the generation of nociceptive signals and on the ensuing elaboration and combination with affective and mnestic components to build the "pain" sensation. This can, in turn, contribute to the advancement on knowledge on this important topic from both basic and translational points of view, and could help in defining new treatments to alleviate altered nociception conditions, such as chronic pain.

APPENDICES

APPENDIX I - Step-by-step description of the cloning strategy for the generation of targeting vectors carrying human NGF^{WT} and NGF^{R100W} coding sequences

1) An EcoRI-EcoRI DNA segment from BAC clone RP24-160F12, containing mouse NGF coding sequence flanked by left and right arms, was subcloned in the pBluescript SK$^-$ plasmid;

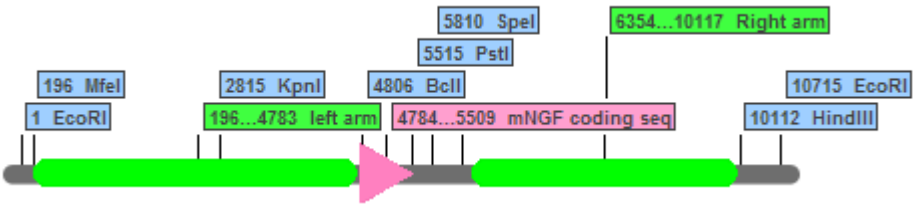

2) In parallel, a polylinker containing suitable cloning sites was synthesized and cloned in the pBluescript SK$^-$ vector;

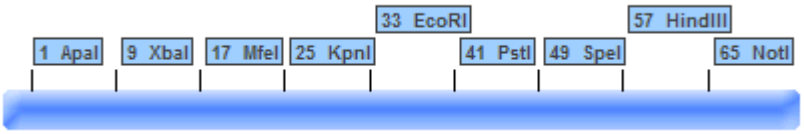

3) The C-terminal portion of human NGF coding sequence was amplified by PCR with (i) a forward primer (CCACAGGGGCGAATTCTCGGTGTGTG) covering the endogenous EcoRI site, and (ii) a reverse primer (CCTGCAGGCAAGTCAGGCTCTTCTCAC) tailed with PstI. The PCR product was cloned in (2)

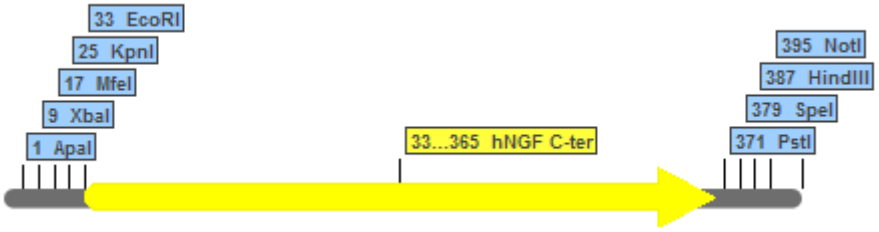

4) A KpnI-BclI DNA segment, containing the left homology arm, was cloned from (1) in a vector containing the entire human NGF coding sequence;

5) A PstI-SpeI DNA segment (295 bp) was cloned from (1) in (3)

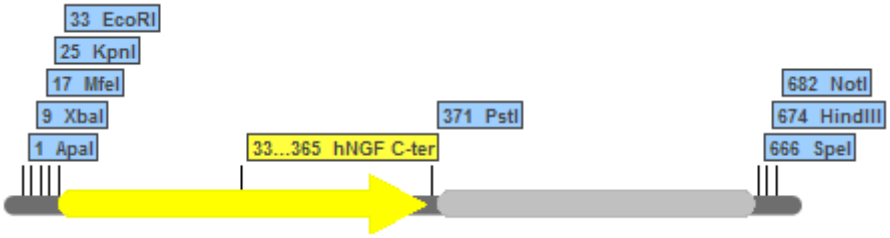

6) A SpeI-HindIII DNA segment (3662 bp) was cloned from (1) in (5) to complete the right homology arm at the 3'UTR of the hNGF coding sequence;

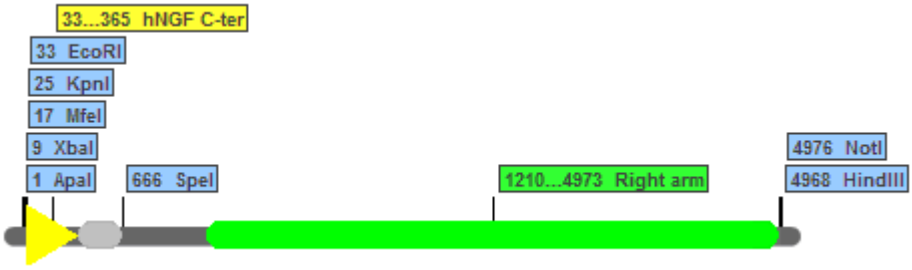

7) The Xba-NotI DNA segment from (6) was subcloned in the pKO2.1 vector, containing the Diphteria Toxin A (DTA) negative selection cassette;

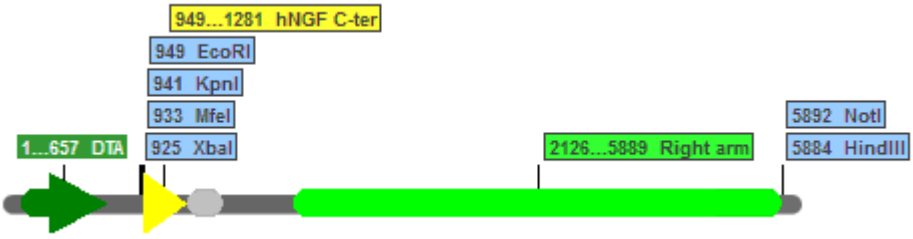

8) The KpnI-EcoRI DNA segment from (4) was cloned in (7), thus reconstituting the human NGF coding sequence;

9) The MfeI-KpnI DNA segment from (1) was cloned in (8);

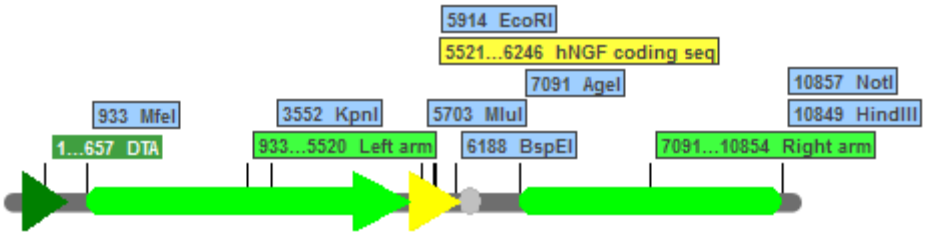

10) A MluI-BspEI DNA segment was cloned in (9) from a vector containing the human NGF sequence, previously mutagenized to obtain the R100W mutation;

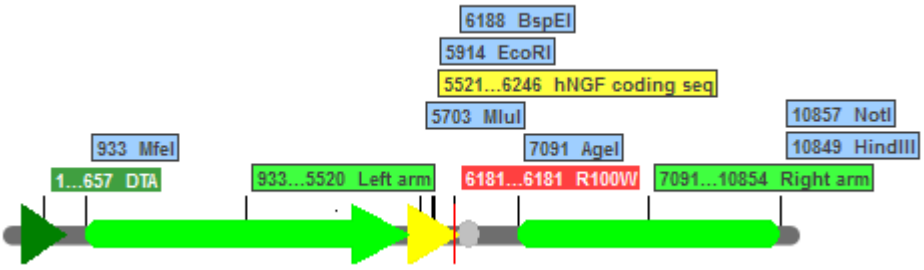

11) Finally, a Neomycin (Neo) positive selection cassette was inserted at the AgeI sites of (9) and (10) to generate the targeting vectors for human NGF^{WT} and NGF^{R100W}, respectively;

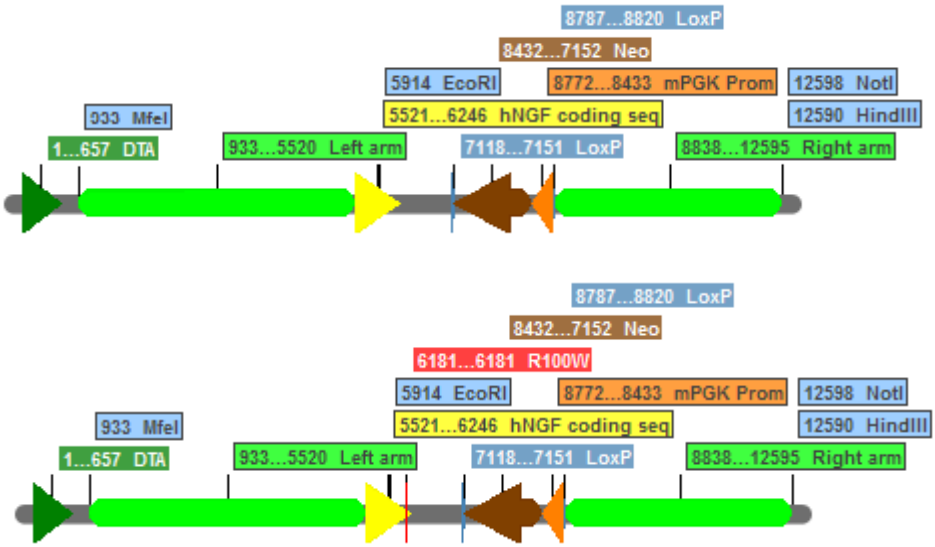

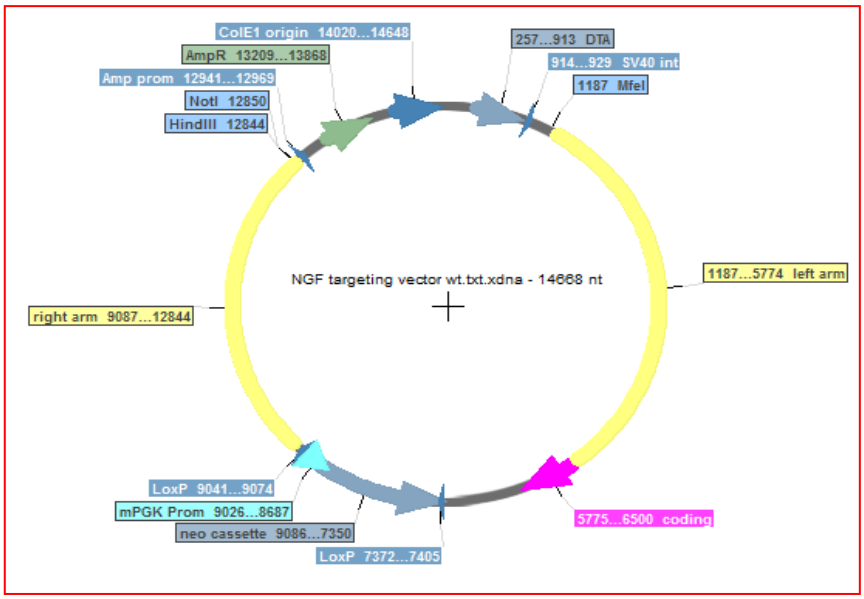

Figure I.1 Representative image of the final targeting vector, carrying the human NGF coding sequence.

APPENDIX II - Preliminary results on the altered morphology of microglia in adult HSAN V mice

Microglial cells of the spinal cord have been largely described to be sensitive to a variety of pathological conditions, including chronic pain (Milligan and Watkins, 2009). On the other hand, less is known about changes in brain microglia under pathological pain conditions. It is worth noting that microglia cells are a source of neurotrophins (Elkabes et al., 1996) and are themselves a target for NGF, expressing TrkA and $p75^{NTR}$ both *in vitro* and *ex vivo* (Rizzi et al., 2018). Consistently, microglial migratory activity is modulated by NGF (De Simone et al., 2007). For these reasons, I started to investigate the morphology of brain microglia in the context of the R100W mutation. I considered two areas that are reported to be important in the physiology of pain (see above, §4.20): ACC (involved in emotional pain) and hippocampus (involved in pain-related spatial memory). I performed immunofluorescence on mouse brain section to visualize Iba-1 (Ionized calcium-Binding Adapter molecule 1), a specific marker for microglia. To characterize in detail microglial morphology, I measured via the Imaris software, the following paremeters: area, volume and length of filaments, number of branching points per cell. The morphology of microglia in $NGF^{R100W/m}$ mice appears to be indistinguishable from controls at 2 months of age (**Fig. 1A,C)**, whereas, significant alterations were observed at 6 months of age in both areas analyzed (**Fig. 1 B,D)**. In particular, all the parameters considered showed significant reductions in $NGF^{R100W/m}$ mice compared to controls. The total density of cells in ACC and hippocampus showed no differences between HSAN V and control mice, at both ages (**Fig. 2**). These morphological differences indicate the transition from resting to activated microglial phenotype (Fernandez-Arjona et al., 2017). Thus, I would hypothesize that microglial activation in brain areas key for the elaboration of pain-related information can play a role in the fear memory deficits of HSAN V mice and, possibly, patients.

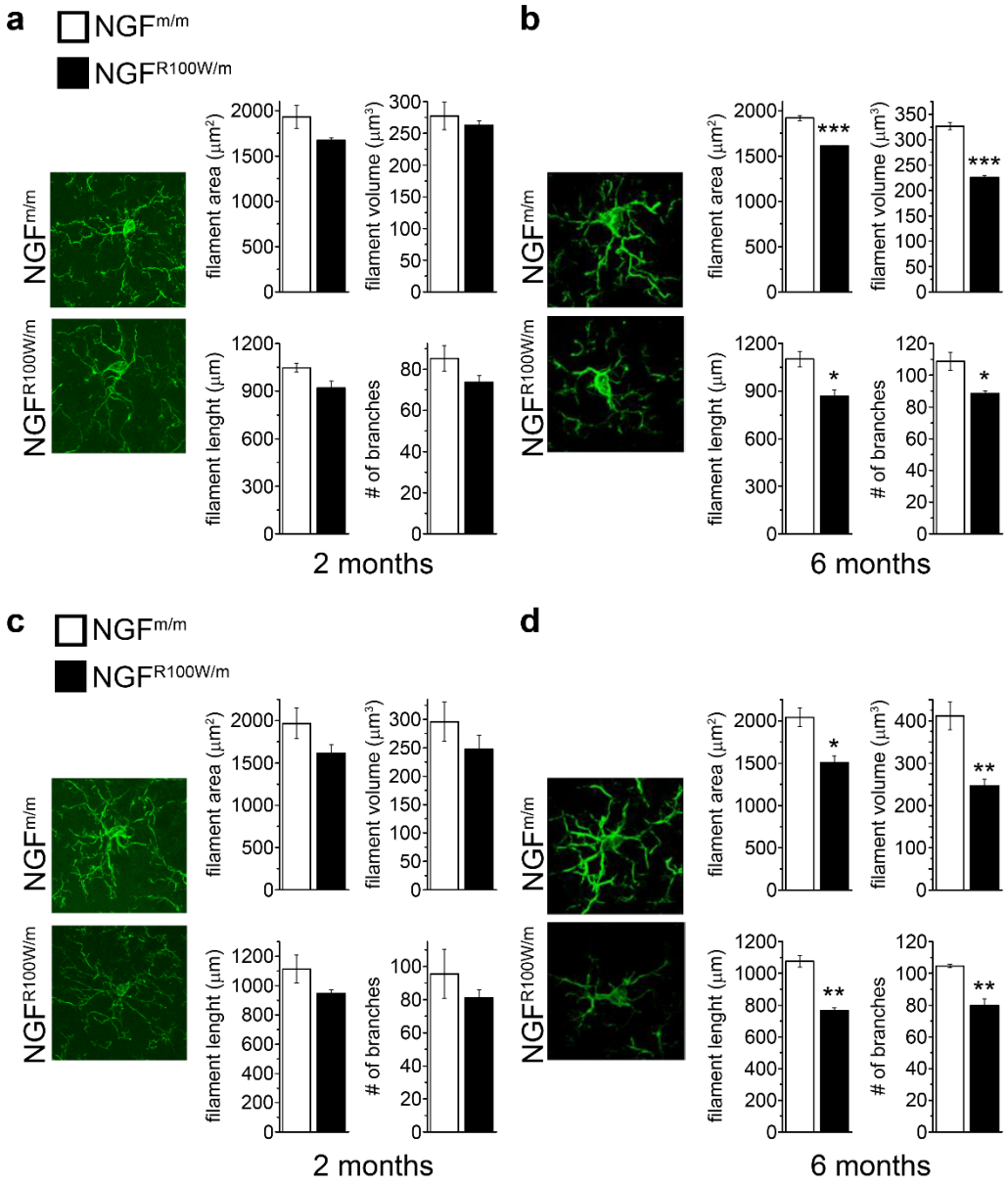

Figure II.1 Microglia morphology in HSAN V mice. No significant alterations at 2 months of age in **(A)** ACC and **(C)** hippocampus; the area, volume, length and number of branches are reduced in both areas **(B, D)** at six months.

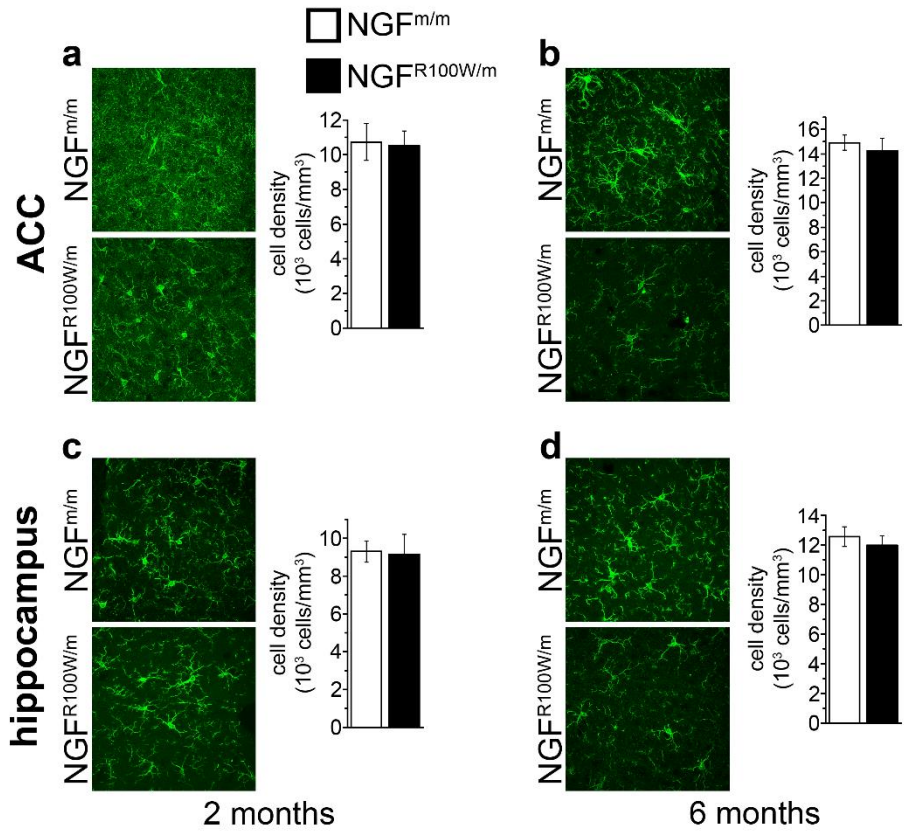

Figure II.2 Unaffected microglia density in ACC and hippocampus in HSAN V mice.

APPENDIX III - Cloning strategy for the generation of HSAN IV knock-in mouse

In addition to HSAN V, I was interested to study the HSAN IV disease. HSAN IV is, similarly to HSAN V, an autosomal recessive disorder characterized by insensitivity to pain. However, the clinical phenotype also extends to anhidrosis and mental retardation (Indo, 2001). These features be correlated with the fact that HSAN IV is caused by mutations at different sites in the *TRKA*. Thus, mutations in the ligand (i.e., NGF in HSAN V), or in its specific receptor (i.e., TrkA in HSAN IV), are not completely overlapping. For this reason, I generated a mouse knock-in line carrying the human *TRKA* coding sequence with the R649W mutation, an HSAN IV-linked mutation that has been, so far, poorly addressed in the clinical and experimental literature. A commercially available knock-in line, harboring the human wild type *TRKA* gene, was used as a control and was supplied by GenOway (Lyon, France).

The targeting construct was generated using classical cloning technologies. The plasmid AMB1-Tg-pA containing the *TRKA* coding sequence was subjected to site-specific mutagenesis PCR to introduce the pathogenic R649W mutation. Then, the AflII-FseI DNA segment of AMB1-HR, a targeting vector for the generation of mouse lines with humanized TrkA, was replaced with the mutated AflII-FseI segment from the AMB-Tg-pA vector described above (**Fig. 1**). The AMB1-Tg-pA and AMB1-HR plasmids were provided by GenOway (Lyon, France).

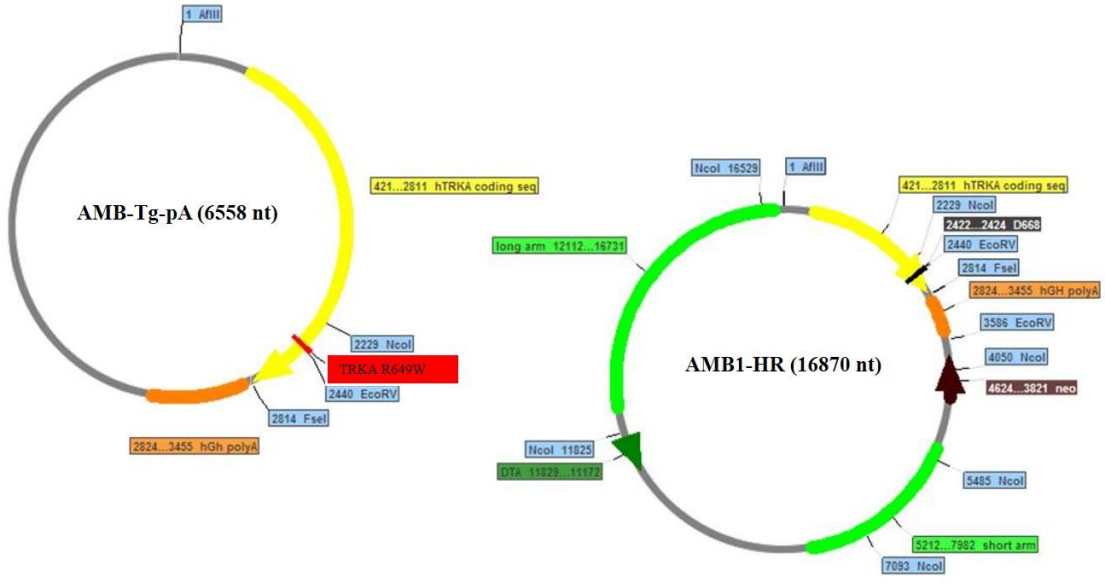

Fig. III.1 Representative image of AMB-Tg-pA and AMB1-HR plasmids, carrying the mutated *TRKA* sequence.

The final targeting vector was linearized prior to electroporation, then transfected into R1p.15 cells; positive clones were selected using neomycin resistance. The targeting strategy was based on the in-frame replacement of the exon 1 coding sequence, as well as part of intron 1, of the murine *TrkA* gene by the complete coding sequence of the human ortholog *TRKA* gene carrying the R649W point mutation. The *TRKA* cDNA cassette was followed at the 3' end by an exogenous hGH polyA cassette and a *loxP*-neomycin-*loxP* cassette (**Fig. 2**). The resulting mouse line was mated with "Cre-deleter" mice, constitutively expressing the Cre recombinase, to remove the neomycin selection cassette.

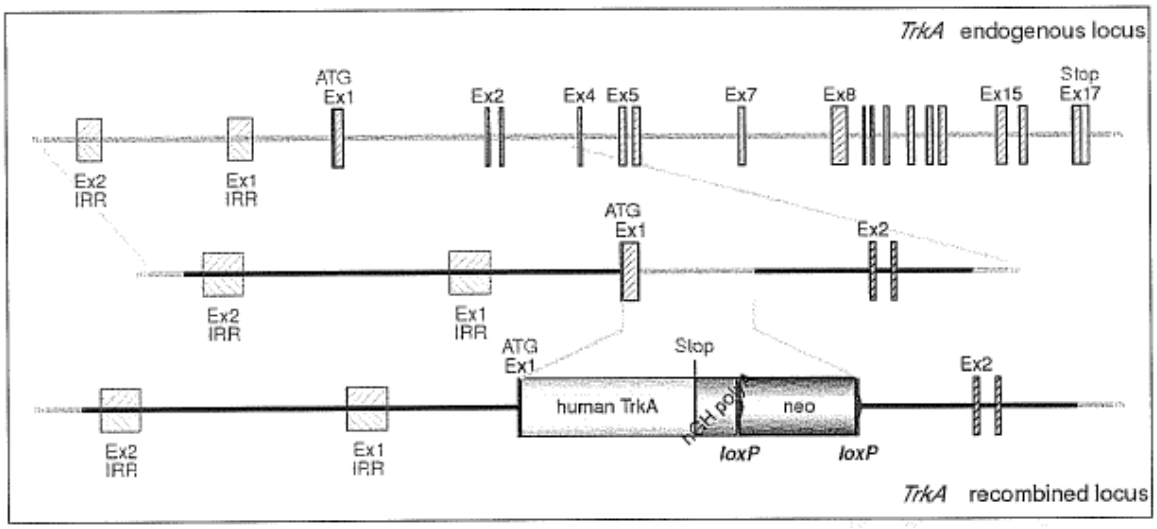

Figure III.2 Schematic representation of the *TrkA* targeting strategy, resulting in the replacement of the murine exon 1 by human *TRKA* cDNA.

Southern Blot analysis

Genomic DNA was extracted by means of phenol:chloroform:isoamyl alcohol from cell clones electroporated with $TRKA^{R649W}$ targeting vector. DNAs were first incubated with StuI (for 5' screening), then positive clones were confirmed by AflII digestion (for 3' screening). Digestions were run on a 0.8% agarose gel O/N at 50 V. After a mild depurination and denaturation, gels were blotted on nitrocellulose, and filters incubated with 5' or 3' probes. The internal 5' probe was located within the 5' homology sequence of TrkA targeting vector and detected an 11.3 kb band in the wild type allele (**Fig. 3**) and a 6.4 kb band in recombinant alleles (**Fig. 3**). The external 3' probe was located downstream the 3' homology sequence of the TrkA targeting vector, and labeled a 6.4 kb band in the wild type allele (**Fig. 4**) and a 10.9 kb band in recombinant alleles (**Fig. 4**).

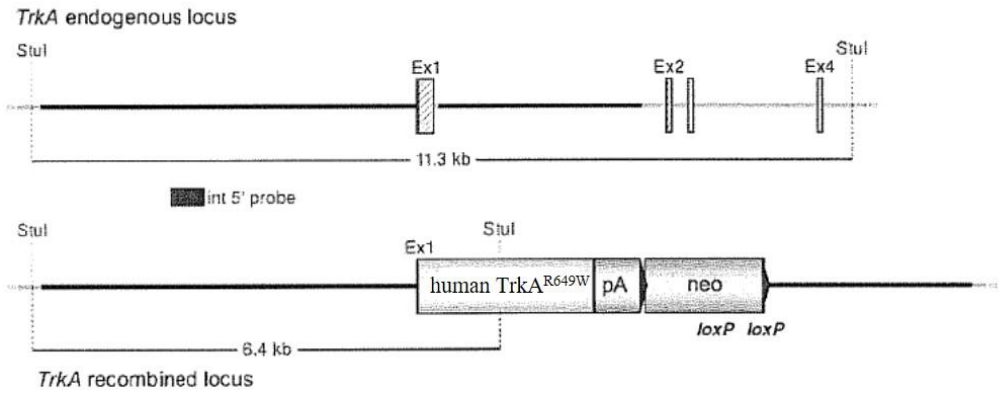

Figure III.3 Southern blot analysis for 5' homologous recombinant in ES cells.

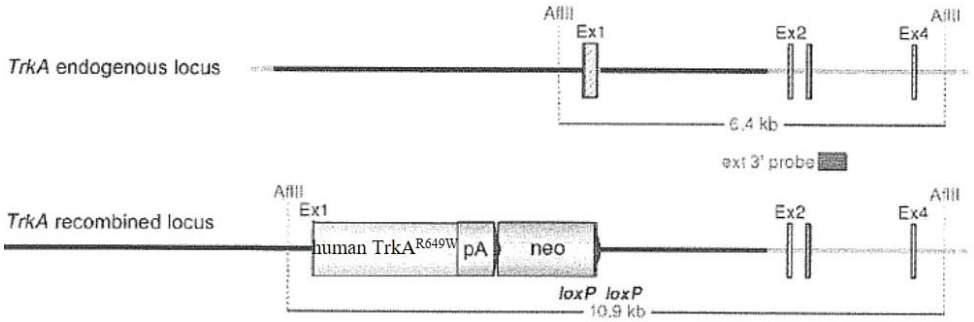

Figure III.4: Southern blot analysis for 3' homologous recombinant in ES cells.

Positive clones were injected into blastocysts from C57BL/6 mice and chimeric animals were crossed with "Cre-deleter" mice to excise the neomycin cassette, thus generating heterozygous mice carrying the humanized allele. Mice were genotyped by PCR. The following PCR primers were used:

fw_mouse: 5'-TGAGTGTGTGTCGTTCGGG- 3'

rev_mouse: 5' -ATGGGCTTAGGAACTTGGGC- 3'

fw_human: 5'-CTTGCTTGGCACTGTCCTCTCATGC- 3'

rev_human: 5' –TGCACAGCTAACCACTCCTCCATGG-3'

Band sizes are: wild-type 343 bp, mutant 442 bp.

The phenotype of these mice is currently being analyzed.

REFERENCES

Abdo H, Li L, Lallemend F, Bachy I, Xu XJ, Rice FL, Ernfors P (2011) Dependence on the transcription factor Shox2 for specification of sensory neurons conveying discriminative touch. The European journal of neuroscience 34:1529-1541.

Abrahamsen B, Zhao J, Asante CO, Cendan CM, Marsh S, Martinez-Barbera JP, Nassar MA, Dickenson AH, Wood JN (2008) The cell and molecular basis of mechanical, cold, and inflammatory pain. Science 321:702-705.

Aghahowa SE, Obianwu HO, Isah AO, Arhewoh IM (2010) Chloroquine-induced Pruritus. Indian journal of pharmaceutical sciences 72:283-289.

Akay T, Tourtellotte WG, Arber S, Jessell TM (2014) Degradation of mouse locomotor pattern in the absence of proprioceptive sensory feedback. Proceedings of the National Academy of Sciences of the United States of America 111:16877-16882.

Al-Khater KM, Todd AJ (2009) Collateral projections of neurons in laminae I, III, and IV of rat spinal cord to thalamus, periaqueductal gray matter, and lateral parabrachial area. The Journal of comparative neurology 515:629-646.

Albers KM, Wright DE, Davis BM (1994) Overexpression of nerve growth factor in epidermis of transgenic mice causes hypertrophy of the peripheral nervous system. The Journal of neuroscience : the official journal of the Society for Neuroscience 14:1422-1432.

Alessandri-Haber N, Dina OA, Yeh JJ, Parada CA, Reichling DB, Levine JD (2004) Transient receptor potential vanilloid 4 is essential in chemotherapy-induced neuropathic pain in the rat. The Journal of neuroscience : the official journal of the Society for Neuroscience 24:4444-4452.

Amano A, Akiyama S, Ikeda M, Morisaki I (1998) Oral manifestations of hereditary sensory and autonomic neuropathy type IV. Congenital insensitivity to pain with anhidrosis. Oral surgery, oral medicine, oral pathology, oral radiology, and endodontics 86:425-431.

Amanzio M, Benedetti F (1999) Neuropharmacological dissection of placebo analgesia: expectation-activated opioid systems versus conditioning-activated specific subsystems. The Journal of neuroscience : the official journal of the Society for Neuroscience 19:484-494.

Andersson JL, Lilja A, Hartvig P, Langstrom B, Gordh T, Handwerker H, Torebjork E (1997) Somatotopic organization along the central sulcus, for pain localization in humans, as revealed by positron emission tomography. Experimental brain research 117:192-199.

Andreev N, Dimitrieva N, Koltzenburg M, McMahon SB (1995) Peripheral administration of nerve growth factor in the adult rat produces a thermal hyperalgesia that requires the presence of sympathetic post-ganglionic neurones. Pain 63:109-115.

Apfel SC (2002) Nerve growth factor for the treatment of diabetic neuropathy: what went wrong, what went right, and what does the future hold? International review of neurobiology 50:393-413.

Arevalo JC, Waite J, Rajagopal R, Beyna M, Chen ZY, Lee FS, Chao MV (2006) Cell survival through Trk neurotrophin receptors is differentially regulated by ubiquitination. Neuron 50:549-559.

Ashraf S, Wibberley H, Mapp PI, Hill R, Wilson D, Walsh DA (2011) Increased vascular penetration and nerve growth in the meniscus: a potential source of pain in osteoarthritis. Annals of the rheumatic diseases 70:523-529.

Auer-Grumbach M, De Jonghe P, Verhoeven K, Timmerman V, Wagner K, Hartung HP, Nicholson GA (2003) Autosomal dominant inherited neuropathies with prominent sensory loss and mutilations: a review. Archives of neurology 60:329-334.

Axelrod FB (2002) Hereditary sensory and autonomic neuropathies. Familial dysautonomia and other HSANs. Clinical autonomic research : official journal of the Clinical Autonomic Research Society 12 Suppl 1:I2-14.

Bai L, Lehnert BP, Liu J, Neubarth NL, Dickendesher TL, Nwe PH, Cassidy C, Woodbury CJ, Ginty DD (2015) Genetic Identification of an Expansive Mechanoreceptor Sensitive to Skin Stroking. Cell 163:1783-1795.

Bandell M, Story GM, Hwang SW, Viswanath V, Eid SR, Petrus MJ, Earley TJ, Patapoutian A (2004) Noxious cold ion channel TRPA1 is activated by pungent compounds and bradykinin. Neuron 41:849-857.

Barde YA, Edgar D, Thoenen H (1982) Purification of a new neurotrophic factor from mammalian brain. The EMBO journal 1:549-553.

Barrett GL, Reid CA, Tsafoulis C, Zhu W, Williams DA, Paolini AG, Trieu J, Murphy M (2010) Enhanced spatial memory and hippocampal long-term potentiation in p75 neurotrophin receptor knockout mice. Hippocampus 20:145-152.

Basbaum AI, Bautista DM, Scherrer G, Julius D (2009) Cellular and molecular mechanisms of pain. Cell 139:267-284.

Batti L, Sundukova M, Murana E, Pimpinella S, De Castro Reis F, Pagani F, Wang H, Pellegrino E, Perlas E, Di Angelantonio S, Ragozzino D, Heppenstall PA (2016) TMEM16F Regulates Spinal Microglial Function in Neuropathic Pain States. Cell reports 15:2608-2615.

Bautista DM, Jordt SE, Nikai T, Tsuruda PR, Read AJ, Poblete J, Yamoah EN, Basbaum AI, Julius D (2006) TRPA1 mediates the inflammatory actions of environmental irritants and proalgesic agents. Cell 124:1269-1282.

Bear MF, Connors, B.W., Paradiso, M.A. (2015) Neuroscience: exploring the brain. Riverwoods: Wolters Kluwer Health.

Beattie MS, Harrington AW, Lee R, Kim JY, Boyce SL, Longo FM, Bresnahan JC, Hempstead BL, Yoon SO (2002) ProNGF induces p75-mediated death of oligodendrocytes following spinal cord injury. Neuron 36:375-386.

Beggs S, Salter MW (2013) The known knowns of microglia-neuronal signalling in neuropathic pain. Neuroscience letters 557 Pt A:37-42.

Bejaoui K, Wu C, Scheffler MD, Haan G, Ashby P, Wu L, de Jong P, Brown RH, Jr. (2001) SPTLC1 is mutated in hereditary sensory neuropathy, type 1. Nature genetics 27:261-262.

Benedetti F, Mayberg HS, Wager TD, Stohler CS, Zubieta JK (2005) Neurobiological mechanisms of the placebo effect. The Journal of neuroscience : the official journal of the Society for Neuroscience 25:10390-10402.

Bennett DL, Michael GJ, Ramachandran N, Munson JB, Averill S, Yan Q, McMahon SB, Priestley JV (1998) A distinct subgroup of small DRG cells express GDNF receptor components and GDNF is protective for these neurons after nerve injury. The Journal of neuroscience : the official journal of the Society for Neuroscience 18:3059-3072.

Berardi N, Domenici L, Parisi V, Pizzorusso T, Cellerino A, Maffei L (1993) Monocular deprivation effects in the rat visual cortex and lateral geniculate nucleus are prevented by nerve growth factor (NGF). I. Visual cortex. Proceedings Biological sciences 251:17-23.

Bergmann I, Priestley JV, McMahon SB, Brocker EB, Toyka KV, Koltzenburg M (1997) Analysis of cutaneous sensory neurons in transgenic mice lacking the low affinity neurotrophin receptor p75. The European journal of neuroscience 9:18-28.

Berkemeier LR, Winslow JW, Kaplan DR, Nikolics K, Goeddel DV, Rosenthal A (1991) Neurotrophin-5: a novel neurotrophic factor that activates trk and trkB. Neuron 7:857-866.

Berthier M, Starkstein S, Leiguarda R (1988) Asymbolia for pain: a sensory-limbic disconnection syndrome. Annals of neurology 24:41-49.

Bester H, Chapman V, Besson JM, Bernard JF (2000) Physiological properties of the lamina I spinoparabrachial neurons in the rat. Journal of neurophysiology 83:2239-2259.

Bhakar AL, Roux PP, Lachance C, Kryl D, Zeindler C, Barker PA (1999) The p75 neurotrophin receptor (p75NTR) alters tumor necrosis factor-mediated NF-kappaB activity under physiological conditions, but direct p75NTR-mediated NF-kappaB activation requires cell stress. The Journal of biological chemistry 274:21443-21449.

Blackburn-Munro G (2004) Pain-like behaviours in animals - how human are they? Trends in pharmacological sciences 25:299-305.

Blochl A, Thoenen H (1995) Characterization of nerve growth factor (NGF) release from hippocampal neurons: evidence for a constitutive and an unconventional sodium-dependent regulated pathway. The European journal of neuroscience 7:1220-1228.

Bonnington JK, McNaughton PA (2003) Signalling pathways involved in the sensitisation of mouse nociceptive neurones by nerve growth factor. The Journal of physiology 551:433-446.

Bouhouche A, Benomar A, Bouslam N, Chkili T, Yahyaoui M (2006a) Mutation in the epsilon subunit of the cytosolic chaperonin-containing t-complex peptide-1 (Cct5) gene causes autosomal recessive mutilating sensory neuropathy with spastic paraplegia. Journal of medical genetics 43:441-443.

Bouhouche A, Benomar A, Bouslam N, Ouazzani R, Chkili T, Yahyaoui M (2006b) Autosomal recessive mutilating sensory neuropathy with spastic paraplegia maps to chromosome 5p15.31-14.1. European journal of human genetics : EJHG 14:249-252.

Bradshaw RA, Blundell TL, Lapatto R, McDonald NQ, Murray-Rust J (1993) Nerve growth factor revisited. Trends in biochemical sciences 18:48-52.

Bridges D, Thompson SW, Rice AS (2001) Mechanisms of neuropathic pain. British journal of anaesthesia 87:12-26.

Busch R, Baldus M, Vogt MA, Berger SM, Bartsch D, Gass P, von Bohlen Und Halbach O (2017) Effects of p75NTR deficiency on cholinergic innervation of the amygdala and anxiety-like behavior. Journal of neurochemistry 141:461-471.

Caleo M, Lodovichi C, Maffei L (1999) Effects of nerve growth factor on visual cortical plasticity require afferent electrical activity. The European journal of neuroscience 11:2979-2984.

Campbell JN, Meyer RA (2006) Mechanisms of neuropathic pain. Neuron 52:77-92.

Campenot RB (1977) Local control of neurite development by nerve growth factor. Proceedings of the National Academy of Sciences of the United States of America 74:4516-4519.

Campos CA, Bowen AJ, Roman CW, Palmiter RD (2018) Encoding of danger by parabrachial CGRP neurons. Nature 555:617-622.

Capsoni S (2014) From genes to pain: nerve growth factor and hereditary sensory and autonomic neuropathy type V. The European journal of neuroscience 39:392-400.

Capsoni S, Ugolini G, Comparini A, Ruberti F, Berardi N, Cattaneo A (2000) Alzheimer-like neurodegeneration in aged antinerve growth factor transgenic mice. Proceedings of the National Academy of Sciences of the United States of America 97:6826-6831.

Capsoni S, Covaceuszach S, Marinelli S, Ceci M, Bernardo A, Minghetti L, Ugolini G, Pavone F, Cattaneo A (2011) Taking pain out of NGF: a "painless" NGF mutant, linked to hereditary sensory autonomic neuropathy type V, with full neurotrophic activity. PloS one 6:e17321.

Carmona S, Zahs K, Wu E, Dakin K, Bras J, Guerreiro R (2018) The role of TREM2 in Alzheimer's disease and other neurodegenerative disorders. The Lancet Neurology 17:721-730.

Carvalho OP, Thornton GK, Hertecant J, Houlden H, Nicholas AK, Cox JJ, Rielly M, Al-Gazali L, Woods CG (2011) A novel NGF mutation clarifies the molecular mechanism and extends the phenotypic spectrum of the HSAN5 neuropathy. Journal of medical genetics 48:131-135.

Caterina MJ, Julius D (2001) The vanilloid receptor: a molecular gateway to the pain pathway. Annual review of neuroscience 24:487-517.

Caterina MJ, Schumacher MA, Tominaga M, Rosen TA, Levine JD, Julius D (1997) The capsaicin receptor: a heat-activated ion channel in the pain pathway. Nature 389:816-824.

Caterina MJ, Leffler A, Malmberg AB, Martin WJ, Trafton J, Petersen-Zeitz KR, Koltzenburg M, Basbaum AI, Julius D (2000) Impaired nociception and pain sensation in mice lacking the capsaicin receptor. Science 288:306-313.

Cattaneo A, Calissano P (2012) Nerve growth factor and Alzheimer's disease: new facts for an old hypothesis. Molecular neurobiology 46:588-604.

Cattaneo A, Capsoni S (2019) Painless Nerve Growth Factor: A TrkA biased agonist mediating a broad neuroprotection via its actions on microglia cells. Pharmacological research 139:17-25.

Cattaneo A, Capsoni S, Margotti E, Righi M, Kontsekova E, Pavlik P, Filipcik P, Novak M (1999) Functional blockade of tyrosine kinase A in the rat basal forebrain by a novel antagonistic anti-receptor monoclonal antibody. The Journal of neuroscience : the official journal of the Society for Neuroscience 19:9687-9697.

Catts VS, Al-Menhali N, Burne TH, Colditz MJ, Coulson EJ (2008) The p75 neurotrophin receptor regulates hippocampal neurogenesis and related behaviours. The European journal of neuroscience 28:883-892.

Cavanaugh DJ, Lee H, Lo L, Shields SD, Zylka MJ, Basbaum AI, Anderson DJ (2009) Distinct subsets of unmyelinated primary sensory fibers mediate behavioral responses to noxious thermal and mechanical stimuli. Proceedings of the National Academy of Sciences of the United States of America 106:9075-9080.

Cervero F (2012) Understanding Pain: exploring the perception of pain. Cambridge: MIT Press.

Chao MV (1992) Neurotrophin receptors: a window into neuronal differentiation. Neuron 9:583-593.

Chao MV (2003) Neurotrophins and their receptors: a convergence point for many signalling pathways. Nature reviews Neuroscience 4:299-309.

Chen AC, Rappelsberger P (1994) Brain and human pain: topographic EEG amplitude and coherence mapping. Brain topography 7:129-140.

Chen CL, Broom DC, Liu Y, de Nooij JC, Li Z, Cen C, Samad OA, Jessell TM, Woolf CJ, Ma Q (2006) Runx1 determines nociceptive sensory neuron phenotype and is required for thermal and neuropathic pain. Neuron 49:365-377.

Chen KS, Nishimura MC, Armanini MP, Crowley C, Spencer SD, Phillips HS (1997) Disruption of a single allele of the nerve growth factor gene results in atrophy of basal forebrain cholinergic neurons and memory deficits. The Journal of neuroscience : the official journal of the Society for Neuroscience 17:7288-7296.

Chen YC et al. (2015) Transcriptional regulator PRDM12 is essential for human pain perception. Nature genetics 47:803-808.

Chuang HH, Prescott ED, Kong H, Shields S, Jordt SE, Basbaum AI, Chao MV, Julius D (2001) Bradykinin and nerve growth factor release the capsaicin receptor from PtdIns(4,5)P2-mediated inhibition. Nature 411:957-962.

Condes-Lara M, Martinez-Lorenzana G, Rodriguez-Jimenez J, Rojas-Piloni G (2008) Paraventricular hypothalamic nucleus stimulation modulates nociceptive responses in dorsal horn wide dynamic range neurons. Neuroscience letters 444:199-202.

Coste B, Mathur J, Schmidt M, Earley TJ, Ranade S, Petrus MJ, Dubin AE, Patapoutian A (2010) Piezo1 and Piezo2 are essential components of distinct mechanically activated cation channels. Science 330:55-60.

Coull JA, Beggs S, Boudreau D, Boivin D, Tsuda M, Inoue K, Gravel C, Salter MW, De Koninck Y (2005) BDNF from microglia causes the shift in neuronal anion gradient underlying neuropathic pain. Nature 438:1017-1021.

Covaceuszach S, Capsoni S, Ugolini G, Spirito F, Vignone D, Cattaneo A (2009) Development of a non invasive NGF-based therapy for Alzheimer's disease. Current Alzheimer research 6:158-170.

Covaceuszach S, Capsoni S, Marinelli S, Pavone F, Ceci M, Ugolini G, Vignone D, Amato G, Paoletti F, Lamba D, Cattaneo A (2010) In vitro receptor binding properties of a "painless" NGF mutein, linked to hereditary sensory autonomic neuropathy type V. Biochemical and biophysical research communications 391:824-829.

Cowan WM (2001) Viktor Hamburger and Rita Levi-Montalcini: the path to the discovery of nerve growth factor. Annual review of neuroscience 24:551-600.

Cox JJ, Reimann F, Nicholas AK, Thornton G, Roberts E, Springell K, Karbani G, Jafri H, Mannan J, Raashid Y, Al-Gazali L, Hamamy H, Valente EM, Gorman S, Williams R, McHale DP, Wood JN, Gribble FM, Woods CG (2006) An SCN9A channelopathy causes congenital inability to experience pain. Nature 444:894-898.

Cox LJ, Hengst U, Gurskaya NG, Lukyanov KA, Jaffrey SR (2008) Intra-axonal translation and retrograde trafficking of CREB promotes neuronal survival. Nature cell biology 10:149-159.

Cragnolini AB, Huang Y, Gokina P, Friedman WJ (2009) Nerve growth factor attenuates proliferation of astrocytes via the p75 neurotrophin receptor. Glia 57:1386-1392.

Craig AD (2002) How do you feel? Interoception: the sense of the physiological condition of the body. Nature reviews Neuroscience 3:655-666.

Craig AD (2003a) Pain mechanisms: labeled lines versus convergence in central processing. Annual review of neuroscience 26:1-30.

Craig AD (2003b) A new view of pain as a homeostatic emotion. Trends in neurosciences 26:303-307.

Crowley C, Spencer SD, Nishimura MC, Chen KS, Pitts-Meek S, Armanini MP, Ling LH, McMahon SB, Shelton DL, Levinson AD, et al. (1994) Mice lacking nerve growth factor display perinatal loss of sensory and sympathetic neurons yet develop basal forebrain cholinergic neurons. Cell 76:1001-1011.

Cui M, Feng Y, McAdoo DJ, Willis WD (1999) Periaqueductal gray stimulation-induced inhibition of nociceptive dorsal horn neurons in rats is associated with the release of norepinephrine, serotonin, and amino acids. The Journal of pharmacology and experimental therapeutics 289:868-876.

D'Hanis W, Linke R, Yilmazer-Hanke DM (2007) Topography of thalamic and parabrachial calcitonin gene-related peptide (CGRP) immunoreactive neurons projecting to subnuclei of the amygdala and extended amygdala. The Journal of comparative neurology 505:268-291.

Damann N, Voets T, Nilius B (2008) TRPs in our senses. Current biology : CB 18:R880-889.

Davidson S, Giesler GJ (2010) The multiple pathways for itch and their interactions with pain. Trends in neurosciences 33:550-558.

Davies AM, Lee KF, Jaenisch R (1993) p75-deficient trigeminal sensory neurons have an altered response to NGF but not to other neurotrophins. Neuron 11:565-574.

Davis EJ, Foster TD, Thomas WE (1994) Cellular forms and functions of brain microglia. Brain research bulletin 34:73-78.

Davis JB, Gray J, Gunthorpe MJ, Hatcher JP, Davey PT, Overend P, Harries MH, Latcham J, Clapham C, Atkinson K, Hughes SA, Rance K, Grau E, Harper AJ, Pugh PL, Rogers DC, Bingham S, Randall A, Sheardown SA (2000) Vanilloid receptor-1 is essential for inflammatory thermal hyperalgesia. Nature 405:183-187.

Dawkins JL, Hulme DJ, Brahmbhatt SB, Auer-Grumbach M, Nicholson GA (2001) Mutations in SPTLC1, encoding serine palmitoyltransferase, long chain base subunit-1, cause hereditary sensory neuropathy type I. Nature genetics 27:309-312.

De Nadai T, Marchetti L, Di Rienzo C, Calvello M, Signore G, Di Matteo P, Gobbo F, Turturro S, Meucci S, Viegi A, Beltram F, Luin S, Cattaneo A (2016) Precursor and mature NGF live tracking: one versus many at a time in the axons. Scientific reports 6:20272.

De Simone R, Ambrosini E, Carnevale D, Ajmone-Cat MA, Minghetti L (2007) NGF promotes microglial migration through the activation of its high affinity receptor: modulation by TGF-beta. Journal of neuroimmunology 190:53-60.

Deacon RM (2006) Assessing nest building in mice. Nature protocols 1:1117-1119.

Denk F, McMahon SB, Tracey I (2014) Pain vulnerability: a neurobiological perspective. Nature neuroscience 17:192-200.

Denk F, Bennett DL, McMahon SB (2017) Nerve Growth Factor and Pain Mechanisms. Annual review of neuroscience 40:307-325.

Dhandapani R, Arokiaraj CM, Taberner FJ, Pacifico P, Raja S, Nocchi L, Portulano C, Franciosa F, Maffei M, Hussain AF, de Castro Reis F, Reymond L, Perlas E, Garcovich S, Barth S, Johnsson K, Lechner SG, Heppenstall PA (2018) Control of mechanical pain hypersensitivity in mice through ligand-targeted photoablation of TrkB-positive sensory neurons. Nature communications 9:1640.

Dhawan BN, Cesselin F, Raghubir R, Reisine T, Bradley PB, Portoghese PS, Hamon M (1996) International Union of Pharmacology. XII. Classification of opioid receptors. Pharmacological reviews 48:567-592.

Di Castro A, Drew LJ, Wood JN, Cesare P (2006) Modulation of sensory neuron mechanotransduction by PKC- and nerve growth factor-dependent pathways. Proceedings of the National Academy of Sciences of the United States of America 103:4699-4704.

Dokter M, Busch R, Poser R, Vogt MA, von Bohlen Und Halbach V, Gass P, Unsicker K, von Bohlen Und Halbach O (2015) Implications of p75NTR for dentate gyrus morphology and hippocampus-related behavior revisited. Brain structure & function 220:1449-1462.

Domenici L, Cellerino A, Maffei L (1993) Monocular deprivation effects in the rat visual cortex and lateral geniculate nucleus are prevented by nerve growth factor (NGF). II. Lateral geniculate nucleus. Proceedings Biological sciences 251:25-31.

Dong X, Han S, Zylka MJ, Simon MI, Anderson DJ (2001) A diverse family of GPCRs expressed in specific subsets of nociceptive sensory neurons. Cell 106:619-632.

Drenth JP, Waxman SG (2007) Mutations in sodium-channel gene SCN9A cause a spectrum of human genetic pain disorders. The Journal of clinical investigation 117:3603-3609.

Duan B, Cheng L, Bourane S, Britz O, Padilla C, Garcia-Campmany L, Krashes M, Knowlton W, Velasquez T, Ren X, Ross S, Lowell BB, Wang Y, Goulding M, Ma Q (2014) Identification of spinal circuits transmitting and gating mechanical pain. Cell 159:1417-1432.

Dubin AE, Patapoutian A (2010) Nociceptors: the sensors of the pain pathway. The Journal of clinical investigation 120:3760-3772.

Dyck PJ, Peroutka S, Rask C, Burton E, Baker MK, Lehman KA, Gillen DA, Hokanson JL, O'Brien PC (1997) Intradermal recombinant human nerve growth factor induces pressure allodynia and lowered heat-pain threshold in humans. Neurology 48:501-505.

Dyck PJ, Mellinger JF, Reagan TJ, Horowitz SJ, McDonald JW, Litchy WJ, Daube JR, Fealey RD, Go VL, Kao PC, Brimijoin WS, Lambert EH (1983) Not 'indifference to pain' but varieties of hereditary sensory and autonomic neuropathy. Brain : a journal of neurology 106 (Pt 2):373-390.

Einarsdottir E, Carlsson A, Minde J, Toolanen G, Svensson O, Solders G, Holmgren G, Holmberg D, Holmberg M (2004) A mutation in the nerve growth factor beta gene (NGFB) causes loss of pain perception. Human molecular genetics 13:799-805.

Eliava M et al. (2016) A New Population of Parvocellular Oxytocin Neurons Controlling Magnocellular Neuron Activity and Inflammatory Pain Processing. Neuron 89:1291-1304.

Elkabes S, DiCicco-Bloom EM, Black IB (1996) Brain microglia/macrophages express neurotrophins that selectively regulate microglial proliferation and function. The Journal of neuroscience : the official journal of the Society for Neuroscience 16:2508-2521.

Fagan AM, Garber M, Barbacid M, Silos-Santiago I, Holtzman DM (1997) A role for TrkA during maturation of striatal and basal forebrain cholinergic neurons in vivo. The Journal of neuroscience : the official journal of the Society for Neuroscience 17:7644-7654.

Fagiolini M, Caleo M, Strettoi E, Maffei L (1997) Axonal transport blockade in the neonatal rat optic nerve induces limited retinal ganglion cell death. The Journal of neuroscience : the official journal of the Society for Neuroscience 17:7045-7052.

Fang X, Djouhri L, McMullan S, Berry C, Okuse K, Waxman SG, Lawson SN (2005) trkA is expressed in nociceptive neurons and influences electrophysiological properties via Nav1.8 expression in rapidly conducting nociceptors. The Journal of neuroscience : the official journal of the Society for Neuroscience 25:4868-4878.

Fernandez-Arjona MDM, Grondona JM, Granados-Duran P, Fernandez-Llebrez P, Lopez-Avalos MD (2017) Microglia Morphological Categorization in a Rat Model of Neuroinflammation by Hierarchical Cluster and Principal Components Analysis. Frontiers in cellular neuroscience 11:235.

Flor H (2002) Painful memories. Can we train chronic pain patients to 'forget' their pain? EMBO reports 3:288-291.

Fode C, Gradwohl G, Morin X, Dierich A, LeMeur M, Goridis C, Guillemot F (1998) The bHLH protein NEUROGENIN 2 is a determination factor for epibranchial placode-derived sensory neurons. Neuron 20:483-494.

Frankland PW, Bontempi B, Talton LE, Kaczmarek L, Silva AJ (2004) The involvement of the anterior cingulate cortex in remote contextual fear memory. Science 304:881-883.

Furlong TM, Cole S, Hamlin AS, McNally GP (2010) The role of prefrontal cortex in predictive fear learning. Behavioral neuroscience 124:574-586.

Gall C, Lauterborn J (1992) The dentate gyrus: a model system for studies of neurotrophin regulation. Epilepsy research Supplement 7:171-185.

Gall CM, Isackson PJ (1989) Limbic seizures increase neuronal production of messenger RNA for nerve growth factor. Science 245:758-761.

Ghilardi JR, Freeman KT, Jimenez-Andrade JM, Coughlin KA, Kaczmarska MJ, Castaneda-Corral G, Bloom AP, Kuskowski MA, Mantyh PW (2012) Neuroplasticity of sensory and sympathetic nerve fibers in a mouse model of a painful arthritic joint. Arthritis and rheumatism 64:2223-2232.

Ginty DD, Segal RA (2002) Retrograde neurotrophin signaling: Trk-ing along the axon. Current opinion in neurobiology 12:268-274.

Gogolla N (2017) The insular cortex. Current biology : CB 27:R580-R586.

Goldberg YP et al. (2007) Loss-of-function mutations in the Nav1.7 gene underlie congenital indifference to pain in multiple human populations. Clinical genetics 71:311-319.

Gong L, Gao F, Li J, Li J, Yu X, Ma X, Zheng W, Cui S, Liu K, Zhang M, Kunze W, Liu CY (2015) Oxytocin-induced membrane hyperpolarization in pain-sensitive dorsal root ganglia neurons mediated by Ca(2+)/nNOS/NO/KATP pathway. Neuroscience 289:417-428.

Greferath U, Bennie A, Kourakis A, Bartlett PF, Murphy M, Barrett GL (2000) Enlarged cholinergic forebrain neurons and improved spatial learning in p75 knockout mice. The European journal of neuroscience 12:885-893.

Grimes ML, Zhou J, Beattie EC, Yuen EC, Hall DE, Valletta JS, Topp KS, LaVail JH, Bunnett NW, Mobley WC (1996) Endocytosis of activated TrkA: evidence that nerve growth factor induces formation of signaling endosomes. The Journal of neuroscience : the official journal of the Society for Neuroscience 16:7950-7964.

Gross CT, Canteras NS (2012) The many paths to fear. Nature reviews Neuroscience 13:651-658.

Guan Z, Kuhn JA, Wang X, Colquitt B, Solorzano C, Vaman S, Guan AK, Evans-Reinsch Z, Braz J, Devor M, Abboud-Werner SL, Lanier LL, Lomvardas S, Basbaum AI (2016) Injured sensory neuron-derived CSF1 induces microglial proliferation and DAP12-dependent pain. Nature neuroscience 19:94-101.

Guler AD, Lee H, Iida T, Shimizu I, Tominaga M, Caterina M (2002) Heat-evoked activation of the ion channel, TRPV4. The Journal of neuroscience : the official journal of the Society for Neuroscience 22:6408-6414.

Hagelberg N, Jaaskelainen SK, Martikainen IK, Mansikka H, Forssell H, Scheinin H, Hietala J, Pertovaara A (2004) Striatal dopamine D2 receptors in modulation of pain in humans: a review. European journal of pharmacology 500:187-192.

Hamburger V (1993) The history of the discovery of the nerve growth factor. Journal of neurobiology 24:893-897.

Han S, Soleiman MT, Soden ME, Zweifel LS, Palmiter RD (2015) Elucidating an Affective Pain Circuit that Creates a Threat Memory. Cell 162:363-374.

Harrison SM, Davis BM, Nishimura M, Albers KM, Jones ME, Phillips HS (2004) Rescue of NGF-deficient mice I: transgenic expression of NGF in skin rescues mice lacking endogenous NGF. Brain research Molecular brain research 122:116-125.

Heerssen HM, Pazyra MF, Segal RA (2004) Dynein motors transport activated Trks to promote survival of target-dependent neurons. Nature neuroscience 7:596-604.

Hempstead BL (2002) The many faces of p75NTR. Current opinion in neurobiology 12:260-267.

Hempstead BL, Martin-Zanca D, Kaplan DR, Parada LF, Chao MV (1991) High-affinity NGF binding requires coexpression of the trk proto-oncogene and the low-affinity NGF receptor. Nature 350:678-683.

Hepburn L et al. (2014) Innate immunity. A Spaetzle-like role for nerve growth factor beta in vertebrate immunity to Staphylococcus aureus. Science 346:641-646.

Heumann R, Korsching S, Bandtlow C, Thoenen H (1987) Changes of nerve growth factor synthesis in nonneuronal cells in response to sciatic nerve transection. The Journal of cell biology 104:1623-1631.

Hjerling-Leffler J, Alqatari M, Ernfors P, Koltzenburg M (2007) Emergence of functional sensory subtypes as defined by transient receptor potential channel expression. The Journal of neuroscience : the official journal of the Society for Neuroscience 27:2435-2443.

Hohn A, Leibrock J, Bailey K, Barde YA (1990) Identification and characterization of a novel member of the nerve growth factor/brain-derived neurotrophic factor family. Nature 344:339-341.

Holtzman DM, Li Y, Chen K, Gage FH, Epstein CJ, Mobley WC (1993) Nerve growth factor reverses neuronal atrophy in a Down syndrome model of age-related neurodegeneration. Neurology 43:2668-2673.

Horigome K, Pryor JC, Bullock ED, Johnson EM, Jr. (1993) Mediator release from mast cells by nerve growth factor. Neurotrophin specificity and receptor mediation. The Journal of biological chemistry 268:14881-14887.

Howe CL, Valletta JS, Rusnak AS, Mobley WC (2001) NGF signaling from clathrin-coated vesicles: evidence that signaling endosomes serve as a platform for the Ras-MAPK pathway. Neuron 32:801-814.

Huang EJ, Reichardt LF (2001) Neurotrophins: roles in neuronal development and function. Annual review of neuroscience 24:677-736.

Huang G, Xiao P, Hung YS, Iannetti GD, Zhang ZG, Hu L (2013) A novel approach to predict subjective pain perception from single-trial laser-evoked potentials. NeuroImage 81:283-293.

Huang S, O'Donovan KJ, Turner EE, Zhong J, Ginty DD (2015) Extrinsic and intrinsic signals converge on the Runx1/CBFbeta transcription factor for nonpeptidergic nociceptor maturation. eLife 4:e10874.

Iggo A (1985) Sensory receptors in the skin of mammals and their sensory functions. Revue neurologique 141:599-613.

Iggo A, Ogawa H (1977) Correlative physiological and morphological studies of rapidly adapting mechanoreceptors in cat's glabrous skin. The Journal of physiology 266:275-296.

Indo Y (2001) Molecular basis of congenital insensitivity to pain with anhidrosis (CIPA): mutations and polymorphisms in TRKA (NTRK1) gene encoding the receptor tyrosine kinase for nerve growth factor. Human mutation 18:462-471.

Indo Y (2018) NGF-dependent neurons and neurobiology of emotions and feelings: Lessons from congenital insensitivity to pain with anhidrosis. Neuroscience and biobehavioral reviews 87:1-16.

Indo Y, Tsuruta M, Hayashida Y, Karim MA, Ohta K, Kawano T, Mitsubuchi H, Tonoki H, Awaya Y, Matsuda I (1996) Mutations in the TRKA/NGF receptor gene in patients with congenital insensitivity to pain with anhidrosis. Nature genetics 13:485-488.

Inoue K, Ozaki S, Shiga T, Ito K, Masuda T, Okado N, Iseda T, Kawaguchi S, Ogawa M, Bae SC, Yamashita N, Itohara S, Kudo N, Ito Y (2002) Runx3 controls the axonal projection of proprioceptive dorsal root ganglion neurons. Nature neuroscience 5:946-954.

Isomura Y, Takada M (2004) Neural mechanisms of versatile functions in primate anterior cingulate cortex. Reviews in the neurosciences 15:279-291.

Ito K, Enomoto H (2016) Retrograde transport of neurotrophic factor signaling: implications in neuronal development and pathogenesis. Journal of biochemistry 160:77-85.

Iulita MF, Cuello AC (2014) Nerve growth factor metabolic dysfunction in Alzheimer's disease and Down syndrome. Trends in pharmacological sciences 35:338-348.

Iwata K, Kamo H, Ogawa A, Tsuboi Y, Noma N, Mitsuhashi Y, Taira M, Koshikawa N, Kitagawa J (2005) Anterior cingulate cortical neuronal activity during perception of noxious thermal stimuli in monkeys. Journal of neurophysiology 94:1980-1991.

Jhamandas JH, Petrov T, Harris KH, Vu T, Krukoff TL (1996) Parabrachial nucleus projection to the amygdala in the rat: electrophysiological and anatomical observations. Brain research bulletin 39:115-126.

Johnson EM, Jr., Osborne PA, Taniuchi M (1989) Destruction of sympathetic and sensory neurons in the developing rat by a monoclonal antibody against the nerve growth factor (NGF) receptor. Brain research 478:166-170.

Johnston MV, Rutkowski JL, Wainer BH, Long JB, Mobley WC (1987) NGF effects on developing forebrain cholinergic neurons are regionally specific. Neurochemical research 12:985-994.

Jones KR, Reichardt LF (1990) Molecular cloning of a human gene that is a member of the nerve growth factor family. Proceedings of the National Academy of Sciences of the United States of America 87:8060-8064.

Julius D, Basbaum AI (2001) Molecular mechanisms of nociception. Nature 413:203-210.

Kandel ER, Schwartz, J.H., Jessel, T.M., Siegelbaum, S.A., Hudspeth, A.J. (2013) Principles of Neural Science, V edition. New York: McGraw-Hill.

Khodorova A, Nicol GD, Strichartz G (2013) The p75NTR signaling cascade mediates mechanical hyperalgesia induced by nerve growth factor injected into the rat hind paw. Neuroscience 254:312-323.

Kilo S, Schmelz M, Koltzenburg M, Handwerker HO (1994) Different patterns of hyperalgesia induced by experimental inflammation in human skin. Brain : a journal of neurology 117 (Pt 2):385-396.

Knobloch HS, Charlet A, Hoffmann LC, Eliava M, Khrulev S, Cetin AH, Osten P, Schwarz MK, Seeburg PH, Stoop R, Grinevich V (2012) Evoked axonal oxytocin release in the central amygdala attenuates fear response. Neuron 73:553-566.

Knowlton WM, Palkar R, Lippoldt EK, McCoy DD, Baluch F, Chen J, McKemy DD (2013) A sensory-labeled line for cold: TRPM8-expressing sensory neurons define the cellular basis for cold, cold pain, and cooling-mediated analgesia. The Journal of neuroscience : the official journal of the Society for Neuroscience 33:2837-2848.

Koerber HR, Woodbury CJ (2002) Comprehensive phenotyping of sensory neurons using an ex vivo somatosensory system. Physiology & behavior 77:589-594.

Kok C, Kennerson ML, Spring PJ, Ing AJ, Pollard JD, Nicholson GA (2003) A locus for hereditary sensory neuropathy with cough and gastroesophageal reflux on chromosome 3p22-p24. American journal of human genetics 73:632-637.

Koltzenburg M, Bennett DL, Shelton DL, McMahon SB (1999) Neutralization of endogenous NGF prevents the sensitization of nociceptors supplying inflamed skin. The European journal of neuroscience 11:1698-1704.

Koyama T, Kato K, Tanaka YZ, Mikami A (2001) Anterior cingulate activity during pain-avoidance and reward tasks in monkeys. Neuroscience research 39:421-430.

Kramer I, Sigrist M, de Nooij JC, Taniuchi I, Jessell TM, Arber S (2006) A role for Runx transcription factor signaling in dorsal root ganglion sensory neuron diversification. Neuron 49:379-393.

Kuruvilla R, Ye H, Ginty DD (2000) Spatially and functionally distinct roles of the PI3-K effector pathway during NGF signaling in sympathetic neurons. Neuron 27:499-512.

Kusumoto-Yoshida I, Liu H, Chen BT, Fontanini A, Bonci A (2015) Central role for the insular cortex in mediating conditioned responses to anticipatory cues. Proceedings of the National Academy of Sciences of the United States of America 112:1190-1195.

Lafreniere RG et al. (2004) Identification of a novel gene (HSN2) causing hereditary sensory and autonomic neuropathy type II through the Study of Canadian Genetic Isolates. American journal of human genetics 74:1064-1073.

LaMotte RH, Lundberg LE, Torebjork HE (1992) Pain, hyperalgesia and activity in nociceptive C units in humans after intradermal injection of capsaicin. The Journal of physiology 448:749-764.

Large TH, Bodary SC, Clegg DO, Weskamp G, Otten U, Reichardt LF (1986) Nerve growth factor gene expression in the developing rat brain. Science 234:352-355.

Larsson E, Kuma R, Norberg A, Minde J, Holmberg M (2009) Nerve growth factor R221W responsible for insensitivity to pain is defectively processed and accumulates as proNGF. Neurobiology of disease 33:221-228.

Laviolette SR, Grace AA (2006) The roles of cannabinoid and dopamine receptor systems in neural emotional learning circuits: implications for schizophrenia and addiction. Cellular and molecular life sciences : CMLS 63:1597-1613.

LeDoux JE (2000) Emotion circuits in the brain. Annual review of neuroscience 23:155-184.

LeDoux JE (2014) Coming to terms with fear. Proceedings of the National Academy of Sciences of the United States of America 111:2871-2878.

Lee FS, Rajagopal R, Kim AH, Chang PC, Chao MV (2002) Activation of Trk neurotrophin receptor signaling by pituitary adenylate cyclase-activating polypeptides. The Journal of biological chemistry 277:9096-9102.

Lee KF, Li E, Huber LJ, Landis SC, Sharpe AH, Chao MV, Jaenisch R (1992) Targeted mutation of the gene encoding the low affinity NGF receptor p75 leads to deficits in the peripheral sensory nervous system. Cell 69:737-749.

Lee R, Kermani P, Teng KK, Hempstead BL (2001) Regulation of cell survival by secreted proneurotrophins. Science 294:1945-1948.

Lei L, Laub F, Lush M, Romero M, Zhou J, Luikart B, Klesse L, Ramirez F, Parada LF (2005) The zinc finger transcription factor Klf7 is required for TrkA gene expression and development of nociceptive sensory neurons. Genes & development 19:1354-1364.

Leipold E et al. (2013) A de novo gain-of-function mutation in SCN11A causes loss of pain perception. Nature genetics 45:1399-1404.

Levanon D, Bettoun D, Harris-Cerruti C, Woolf E, Negreanu V, Eilam R, Bernstein Y, Goldenberg D, Xiao C, Fliegauf M, Kremer E, Otto F, Brenner O, Lev-Tov A, Groner Y (2002) The Runx3 transcription factor regulates development and survival of TrkC dorsal root ganglia neurons. The EMBO journal 21:3454-3463.

Lever IJ, Bradbury EJ, Cunningham JR, Adelson DW, Jones MG, McMahon SB, Marvizon JC, Malcangio M (2001) Brain-derived neurotrophic factor is released in the dorsal horn by distinctive patterns of afferent fiber stimulation. The Journal of neuroscience : the official journal of the Society for Neuroscience 21:4469-4477.

Levi-Montalcini R (1952) Effects of mouse tumor transplantation on the nervous system. Annals of the New York Academy of Sciences 55:330-344.

Levi-Montalcini R (1987) The nerve growth factor 35 years later. Science 237:1154-1162.

Levi-Montalcini R, Angeletti PU (1966) Second symposium on catecholamines. Modification of sympathetic function. Immunosympathectomy. Pharmacological reviews 18:619-628.

Lewin GR, Mendell LM (1994) Regulation of cutaneous C-fiber heat nociceptors by nerve growth factor in the developing rat. Journal of neurophysiology 71:941-949.

Lewin GR, Nykjaer A (2014) Pro-neurotrophins, sortilin, and nociception. The European journal of neuroscience 39:363-374.

Lewin GR, Lisney SJ, Mendell LM (1992) Neonatal Anti-NGF Treatment Reduces the Adelta- and C-Fibre Evoked Vasodilator Responses in Rat Skin: Evidence That Nociceptor Afferents Mediate Antidromic Vasodilatation. The European journal of neuroscience 4:1213-1218.

Lewin GR, Ritter AM, Mendell LM (1993) Nerve growth factor-induced hyperalgesia in the neonatal and adult rat. The Journal of neuroscience : the official journal of the Society for Neuroscience 13:2136-2148.

Lewin GR, Rueff A, Mendell LM (1994) Peripheral and central mechanisms of NGF-induced hyperalgesia. The European journal of neuroscience 6:1903-1912.

Lewin GR, Lechner SG, Smith ES (2014) Nerve growth factor and nociception: from experimental embryology to new analgesic therapy. Handbook of experimental pharmacology 220:251-282.

Li L, Rutlin M, Abraira VE, Cassidy C, Kus L, Gong S, Jankowski MP, Luo W, Heintz N, Koerber HR, Woodbury CJ, Ginty DD (2011) The functional organization of cutaneous low-threshold mechanosensory neurons. Cell 147:1615-1627.

Light AR, Perl ER (1979) Spinal termination of functionally identified primary afferent neurons with slowly conducting myelinated fibers. The Journal of comparative neurology 186:133-150.

Lindholm D, Heumann R, Meyer M, Thoenen H (1987) Interleukin-1 regulates synthesis of nerve growth factor in non-neuronal cells of rat sciatic nerve. Nature 330:658-659.

Lingueglia E (2007) Acid-sensing ion channels in sensory perception. The Journal of biological chemistry 282:17325-17329.

Liu T, Gao YJ, Ji RR (2012) Emerging role of Toll-like receptors in the control of pain and itch. Neuroscience bulletin 28:131-144.

Liu Y, Latremoliere A, Li X, Zhang Z, Chen M, Wang X, Fang C, Zhu J, Alexandre C, Gao Z, Chen B, Ding X, Zhou JY, Zhang Y, Chen C, Wang KH, Woolf CJ, He Z (2018) Touch and tactile neuropathic pain sensitivity are set by corticospinal projections. Nature 561:547-550.

Lolignier S, Eijkelkamp N, Wood JN (2015) Mechanical allodynia. Pflugers Archiv : European journal of physiology 467:133-139.

Lonze BE, Ginty DD (2002) Function and regulation of CREB family transcription factors in the nervous system. Neuron 35:605-623.

Low PA, Burke WJ, McLeod JG (1978) Congenital sensory neuropathy with selective loss of small myelinated fibers. Annals of neurology 3:179-182.

Lu YC, Chen YZ, Wei YY, He XT, Li X, Hu W, Yanagawa Y, Wang W, Wu SX, Dong YL (2015) Neurochemical properties of the synapses between the parabrachial nucleus-derived CGRP-positive axonal terminals and the GABAergic neurons in the lateral capsular division of central nucleus of amygdala. Molecular neurobiology 51:105-118.

Luo W, Wickramasinghe SR, Savitt JM, Griffin JW, Dawson TM, Ginty DD (2007) A hierarchical NGF signaling cascade controls Ret-dependent and Ret-independent events during development of nonpeptidergic DRG neurons. Neuron 54:739-754.

Ma L, Lei L, Eng SR, Turner E, Parada LF (2003) Brn3a regulation of TrkA/NGF receptor expression in developing sensory neurons. Development 130:3525-3534.

Ma Q, Fode C, Guillemot F, Anderson DJ (1999) Neurogenin1 and neurogenin2 control two distinct waves of neurogenesis in developing dorsal root ganglia. Genes & development 13:1717-1728.

MacInnis BL, Campenot RB (2002) Retrograde support of neuronal survival without retrograde transport of nerve growth factor. Science 295:1536-1539.

Maffei L, Berardi N, Domenici L, Parisi V, Pizzorusso T (1992) Nerve growth factor (NGF) prevents the shift in ocular dominance distribution of visual cortical neurons in monocularly deprived rats. The Journal of neuroscience : the official journal of the Society for Neuroscience 12:4651-4662.

Majdan M, Miller FD (1999) Neuronal life and death decisions functional antagonism between the Trk and p75 neurotrophin receptors. International journal of developmental neuroscience : the official journal of the International Society for Developmental Neuroscience 17:153-161.

Mamet J, Baron A, Lazdunski M, Voilley N (2002) Proinflammatory mediators, stimulators of sensory neuron excitability via the expression of acid-sensing ion channels. The Journal of neuroscience : the official journal of the Society for Neuroscience 22:10662-10670.

Margolis EB, Hjelmstad GO, Bonci A, Fields HL (2005) Both kappa and mu opioid agonists inhibit glutamatergic input to ventral tegmental area neurons. Journal of neurophysiology 93:3086-3093.

Marmigere F, Ernfors P (2007) Specification and connectivity of neuronal subtypes in the sensory lineage. Nature reviews Neuroscience 8:114-127.

Maro GS, Vermeren M, Voiculescu O, Melton L, Cohen J, Charnay P, Topilko P (2004) Neural crest boundary cap cells constitute a source of neuronal and glial cells of the PNS. Nature neuroscience 7:930-938.

Martikainen IK, Nuechterlein EB, Pecina M, Love TM, Cummiford CM, Green CR, Stohler CS, Zubieta JK (2015) Chronic Back Pain Is Associated with Alterations in Dopamine Neurotransmission in the Ventral Striatum. The Journal of neuroscience : the official journal of the Society for Neuroscience 35:9957-9965.

McAllister AK, Katz LC, Lo DC (1999) Neurotrophins and synaptic plasticity. Annual review of neuroscience 22:295-318.

McEvilly RJ, Erkman L, Luo L, Sawchenko PE, Ryan AF, Rosenfeld MG (1996) Requirement for Brn-3.0 in differentiation and survival of sensory and motor neurons. Nature 384:574-577.

McGaugh JL (2004) The amygdala modulates the consolidation of memories of emotionally arousing experiences. Annual review of neuroscience 27:1-28.

McKemy DD, Neuhausser WM, Julius D (2002) Identification of a cold receptor reveals a general role for TRP channels in thermosensation. Nature 416:52-58.

McMahon SB, Bennett DL, Priestley JV, Shelton DL (1995) The biological effects of endogenous nerve growth factor on adult sensory neurons revealed by a trkA-IgG fusion molecule. Nature medicine 1:774-780.

Melzack R (1975) The McGill Pain Questionnaire: major properties and scoring methods. Pain 1:277-299.

Melzack R (1999) From the gate to the neuromatrix. Pain Suppl 6:S121-126.

Melzack R, Wall PD (1965) Pain mechanisms: a new theory. Science 150:971-979.

Metsis M (2001) Genes for neurotrophic factors and their receptors: structure and regulation. Cellular and molecular life sciences : CMLS 58:1014-1020.

Michael GJ, Averill S, Nitkunan A, Rattray M, Bennett DL, Yan Q, Priestley JV (1997) Nerve growth factor treatment increases brain-derived neurotrophic factor selectively in TrkA-expressing dorsal root ganglion cells and in their central terminations within the spinal cord. The Journal of neuroscience : the official journal of the Society for Neuroscience 17:8476-8490.

Middlemas A, Delcroix JD, Sayers NM, Tomlinson DR, Fernyhough P (2003) Enhanced activation of axonally transported stress-activated protein kinases in peripheral nerve in diabetic neuropathy is prevented by neurotrophin-3. Brain : a journal of neurology 126:1671-1682.

Milligan ED, Watkins LR (2009) Pathological and protective roles of glia in chronic pain. Nature reviews Neuroscience 10:23-36.

Minde J, Toolanen G, Andersson T, Nennesmo I, Remahl IN, Svensson O, Solders G (2004) Familial insensitivity to pain (HSAN V) and a mutation in the NGFB gene. A neurophysiological and pathological study. Muscle & nerve 30:752-760.

Minde J, Andersson T, Fulford M, Aguirre M, Nennesmo I, Remahl IN, Svensson O, Holmberg M, Toolanen G, Solders G (2009) A novel NGFB point mutation: a phenotype study of heterozygous patients. Journal of neurology, neurosurgery, and psychiatry 80:188-195.

Minde JK (2006) Norrbottnian congenital insensitivity to pain. Acta orthopaedica Supplementum 77:2-32.

Minett MS, Pereira V, Sikandar S, Matsuyama A, Lolignier S, Kanellopoulos AH, Mancini F, Iannetti GD, Bogdanov YD, Santana-Varela S, Millet Q, Baskozos G, MacAllister R, Cox JJ, Zhao J, Wood JN (2015) Endogenous opioids contribute to insensitivity to pain in humans and mice lacking sodium channel Nav1.7. Nature communications 6:8967.

Ming G, Song H, Berninger B, Inagaki N, Tessier-Lavigne M, Poo M (1999) Phospholipase C-gamma and phosphoinositide 3-kinase mediate cytoplasmic signaling in nerve growth cone guidance. Neuron 23:139-148.

Minnone G, De Benedetti F, Bracci-Laudiero L (2017) NGF and Its Receptors in the Regulation of Inflammatory Response. International journal of molecular sciences 18.

Mitra S, Behbahani H, Eriksdotter M (2019) Innovative Therapy for Alzheimer's Disease-With Focus on Biodelivery of NGF. Frontiers in neuroscience 13:38.

Moayedi M, Davis KD (2013) Theories of pain: from specificity to gate control. Journal of neurophysiology 109:5-12.

Mogil JS, Belknap JK (1997) Sex and genotype determine the selective activation of neurochemically-distinct mechanisms of swim stress-induced analgesia. Pharmacology, biochemistry, and behavior 56:61-66.

Mogil JS, Breese NM, Witty MF, Ritchie J, Rainville ML, Ase A, Abbadi N, Stucky CL, Seguela P (2005) Transgenic expression of a dominant-negative ASIC3 subunit leads to increased sensitivity to mechanical and inflammatory stimuli. The Journal of neuroscience : the official journal of the Society for Neuroscience 25:9893-9901.

Molliver DC, Snider WD (1997) Nerve growth factor receptor TrkA is down-regulated during postnatal development by a subset of dorsal root ganglion neurons. The Journal of comparative neurology 381:428-438.

Molliver DC, Wright DE, Leitner ML, Parsadanian AS, Doster K, Wen D, Yan Q, Snider WD (1997) IB4-binding DRG neurons switch from NGF to GDNF dependence in early postnatal life. Neuron 19:849-861.

Moqrich A, Hwang SW, Earley TJ, Petrus MJ, Murray AN, Spencer KS, Andahazy M, Story GM, Patapoutian A (2005) Impaired thermosensation in mice lacking TRPV3, a heat and camphor sensor in the skin. Science 307:1468-1472.

Moreno-Lopez Y, Martinez-Lorenzana G, Condes-Lara M, Rojas-Piloni G (2013) Identification of oxytocin receptor in the dorsal horn and nociceptive dorsal root ganglion neurons. Neuropeptides 47:117-123.

Morrison I, Loken LS, Minde J, Wessberg J, Perini I, Nennesmo I, Olausson H (2011) Reduced C-afferent fibre density affects perceived pleasantness and empathy for touch. Brain : a journal of neurology 134:1116-1126.

Morton DL, Sandhu JS, Jones AK (2016) Brain imaging of pain: state of the art. Journal of pain research 9:613-624.

Moshourab RA, Wetzel C, Martinez-Salgado C, Lewin GR (2013) Stomatin-domain protein interactions with acid-sensing ion channels modulate nociceptor mechanosensitivity. The Journal of physiology 591:5555-5574.

Mountcastle VB (1957) Modality and topographic properties of single neurons of cat's somatic sensory cortex. Journal of neurophysiology 20:408-434.

Mufson EJ, Conner JM, Varon S, Kordower JH (1994) Nerve growth factor-like immunoreactive profiles in the primate basal forebrain and hippocampal formation. The Journal of comparative neurology 341:507-519.

Nader K, Schafe GE, Le Doux JE (2000) Fear memories require protein synthesis in the amygdala for reconsolidation after retrieval. Nature 406:722-726.

Nahorski MS, Chen YC, Woods CG (2015) New Mendelian Disorders of Painlessness. Trends in neurosciences 38:712-724.

Naser PV, Kuner R (2018) Molecular, Cellular and Circuit Basis of Cholinergic Modulation of Pain. Neuroscience 387:135-148.

Naumann T, Casademunt E, Hollerbach E, Hofmann J, Dechant G, Frotscher M, Barde YA (2002) Complete deletion of the neurotrophin receptor p75NTR leads to long-lasting increases in the number of basal forebrain cholinergic neurons. The Journal of neuroscience : the official journal of the Society for Neuroscience 22:2409-2418.

Nersesyan H, Slavin KV (2007) Current aproach to cancer pain management: Availability and implications of different treatment options. Therapeutics and clinical risk management 3:381-400.

Nersesyan Y, Demirkhanyan L, Cabezas-Bratesco D, Oakes V, Kusuda R, Dawson T, Sun X, Cao C, Cohen AM, Chelluboina B, Veeravalli KK, Zimmermann K, Domene C, Brauchi S, Zakharian E (2017) Oxytocin Modulates Nociception as an Agonist of Pain-Sensing TRPV1. Cell reports 21:1681-1691.

Neugebauer V, Li W (2002) Processing of nociceptive mechanical and thermal information in central amygdala neurons with knee-joint input. Journal of neurophysiology 87:103-112.

Neugebauer V, Li W, Bird GC, Han JS (2004) The amygdala and persistent pain. The Neuroscientist : a review journal bringing neurobiology, neurology and psychiatry 10:221-234.

Nicol GD, Vasko MR (2007) Unraveling the story of NGF-mediated sensitization of nociceptive sensory neurons: ON or OFF the Trks? Molecular interventions 7:26-41.

Nimmerjahn A, Kirchhoff F, Helmchen F (2005) Resting microglial cells are highly dynamic surveillants of brain parenchyma in vivo. Science 308:1314-1318.

Norrsell U, Finger S, Lajonchere C (1999) Cutaneous sensory spots and the "law of specific nerve energies": history and development of ideas. Brain research bulletin 48:457-465.

Nykjaer A, Lee R, Teng KK, Jansen P, Madsen P, Nielsen MS, Jacobsen C, Kliemannel M, Schwarz E, Willnow TE, Hempstead BL, Petersen CM (2004) Sortilin is essential for proNGF-induced neuronal cell death. Nature 427:843-848.

Obata K, Katsura H, Sakurai J, Kobayashi K, Yamanaka H, Dai Y, Fukuoka T, Noguchi K (2006) Suppression of the p75 neurotrophin receptor in uninjured sensory neurons reduces neuropathic pain after nerve injury. The Journal of neuroscience : the official journal of the Society for Neuroscience 26:11974-11986.

Obata K, Yamanaka H, Kobayashi K, Dai Y, Mizushima T, Katsura H, Fukuoka T, Tokunaga A, Noguchi K (2004) Role of mitogen-activated protein kinase activation in injured and intact primary afferent neurons for mechanical and heat hypersensitivity after spinal nerve ligation. The Journal of neuroscience : the official journal of the Society for Neuroscience 24:10211-10222.

Olsen D, Kaas M, Schwartz O, Nykjaer A, Glerup S (2013) Loss of BDNF or its receptors in three mouse models has unpredictable consequences for anxiety and fear acquisition. Learning & memory 20:499-504.

Omerbasic D, Smith ES, Moroni M, Homfeld J, Eigenbrod O, Bennett NC, Reznick J, Faulkes CG, Selbach M, Lewin GR (2016) Hypofunctional TrkA Accounts for the Absence of Pain Sensitization in the African Naked Mole-Rat. Cell reports 17:748-758.

Ostrowsky K, Magnin M, Ryvlin P, Isnard J, Guenot M, Mauguiere F (2002) Representation of pain and somatic sensation in the human insula: a study of responses to direct electrical cortical stimulation. Cerebral cortex 12:376-385.

Palmiter RD (2018) The Parabrachial Nucleus: CGRP Neurons Function as a General Alarm. Trends in neurosciences 41:280-293.

Paoletti F, Malerba F, Ercole BB, Lamba D, Cattaneo A (2015) A comparative analysis of the structural, functional and biological differences between Mouse and Human Nerve Growth Factor. Biochimica et biophysica acta 1854:187-197.

Pare M, Smith AM, Rice FL (2002) Distribution and terminal arborizations of cutaneous mechanoreceptors in the glabrous finger pads of the monkey. The Journal of comparative neurology 445:347-359.

Patel MK, Kaye AD, Urman RD (2018) Tanezumab: Therapy targeting nerve growth factor in pain pathogenesis. Journal of anaesthesiology, clinical pharmacology 34:111-116.

Patel TD, Jackman A, Rice FL, Kucera J, Snider WD (2000) Development of sensory neurons in the absence of NGF/TrkA signaling in vivo. Neuron 25:345-357.

Pathak A, Carter Bruce D (2017) Retrograde apoptotic signaling by the p75 neurotrophin receptor. Neuronal Signaling 1:NS20160007.

Peier AM, Moqrich A, Hergarden AC, Reeve AJ, Andersson DA, Story GM, Earley TJ, Dragoni I, McIntyre P, Bevan S, Patapoutian A (2002) A TRP channel that senses cold stimuli and menthol. Cell 108:705-715.

Peirs C, Williams SP, Zhao X, Walsh CE, Gedeon JY, Cagle NE, Goldring AC, Hioki H, Liu Z, Marell PS, Seal RP (2015) Dorsal Horn Circuits for Persistent Mechanical Pain. Neuron 87:797-812.

Pereira V, Millet Q, Aramburu J, Lopez-Rodriguez C, Gaveriaux-Ruff C, Wood JN (2018) Analgesia linked to Nav1.7 loss of function requires micro- and delta-opioid receptors. Wellcome open research 3:101.

Perini I, Bergstrand S, Morrison I (2013) Where pain meets action in the human brain. The Journal of neuroscience : the official journal of the Society for Neuroscience 33:15930-15939.

Perini I, Tavakoli M, Marshall A, Minde J, Morrison I (2016) Rare human nerve growth factor-beta mutation reveals relationship between C-afferent density and acute pain evaluation. Journal of neurophysiology 116:425-430.

Perl ER (2007) Ideas about pain, a historical view. Nature reviews Neuroscience 8:71-80.

Petersen M, Segond von Banchet G, Heppelmann B, Koltzenburg M (1998) Nerve growth factor regulates the expression of bradykinin binding sites on adult sensory neurons via the neurotrophin receptor p75. Neuroscience 83:161-168.

Pittenger G, Vinik A (2003) Nerve growth factor and diabetic neuropathy. Experimental diabesity research 4:271-285.

Pitts AF, Miller MW (2000) Expression of nerve growth factor, brain-derived neurotrophic factor, and neurotrophin-3 in the somatosensory cortex of the mature rat: coexpression with high-affinity neurotrophin receptors. The Journal of comparative neurology 418:241-254.

Ploner M, Sorg C, Gross J (2017) Brain Rhythms of Pain. Trends in cognitive sciences 21:100-110.

Prato V, Taberner FJ, Hockley JRF, Callejo G, Arcourt A, Tazir B, Hammer L, Schad P, Heppenstall PA, Smith ES, Lechner SG (2017) Functional and Molecular Characterization of Mechanoinsensitive "Silent" Nociceptors. Cell reports 21:3102-3115.

Price DD (2000) Psychological and neural mechanisms of the affective dimension of pain. Science 288:1769-1772.

Price MP, McIlwrath SL, Xie J, Cheng C, Qiao J, Tarr DE, Sluka KA, Brennan TJ, Lewin GR, Welsh MJ (2001) The DRASIC cation channel contributes to the detection of cutaneous touch and acid stimuli in mice. Neuron 32:1071-1083.

Price MP, Lewin GR, McIlwrath SL, Cheng C, Xie J, Heppenstall PA, Stucky CL, Mannsfeldt AG, Brennan TJ, Drummond HA, Qiao J, Benson CJ, Tarr DE, Hrstka RF, Yang B, Williamson RA, Welsh MJ

(2000) The mammalian sodium channel BNC1 is required for normal touch sensation. Nature 407:1007-1011.
Price TJ, Inyang KE (2015) Commonalities between pain and memory mechanisms and their meaning for understanding chronic pain. Progress in molecular biology and translational science 131:409-434.
Purves D (1975) Functional and structural changes in mammalian sympathetic neurones following interruption of their axons. The Journal of physiology 252:429-463.
Purves D, Snider WD, Voyvodic JT (1988) Trophic regulation of nerve cell morphology and innervation in the autonomic nervous system. Nature 336:123-128.
Purves D, Augustine G.J., Fitzpatrick D., Hall W.C., LaMantia A.-S., Mooney R.D., Platt M.L., White L.E. (2017) Neuroscience, VI edition. Sunderland: Sinauer Associates.
Rainville P, Duncan GH, Price DD, Carrier B, Bushnell MC (1997) Pain affect encoded in human anterior cingulate but not somatosensory cortex. Science 277:968-971.
Raju TN (1999) The Nobel chronicles. 1944: Joseph Erlanger (1874-1965); and Herbert Spencer Gasser (1888-1963). Lancet 353:851.
Ranade SS, Woo SH, Dubin AE, Moshourab RA, Wetzel C, Petrus M, Mathur J, Begay V, Coste B, Mainquist J, Wilson AJ, Francisco AG, Reddy K, Qiu Z, Wood JN, Lewin GR, Patapoutian A (2014) Piezo2 is the major transducer of mechanical forces for touch sensation in mice. Nature 516:121-125.
Renganathan M, Cummins TR, Waxman SG (2001) Contribution of Na(v)1.8 sodium channels to action potential electrogenesis in DRG neurons. Journal of neurophysiology 86:629-640.
Riccio A, Pierchala BA, Ciarallo CL, Ginty DD (1997) An NGF-TrkA-mediated retrograde signal to transcription factor CREB in sympathetic neurons. Science 277:1097-1100.
Rich KM, Yip HK, Osborne PA, Schmidt RE, Johnson EM, Jr. (1984) Role of nerve growth factor in the adult dorsal root ganglia neuron and its response to injury. The Journal of comparative neurology 230:110-118.
Ritchie ME, Phipson B, Wu D, Hu Y, Law CW, Shi W, Smyth GK (2015) limma powers differential expression analyses for RNA-sequencing and microarray studies. Nucleic acids research 43:e47.
Ritter AM, Lewin GR, Kremer NE, Mendell LM (1991) Requirement for nerve growth factor in the development of myelinated nociceptors in vivo. Nature 350:500-502.
Rizzi C, Tiberi A, Giustizieri M, Marrone MC, Gobbo F, Carucci NM, Meli G, Arisi I, D'Onofrio M, Marinelli S, Capsoni S, Cattaneo A (2018) NGF steers microglia toward a neuroprotective phenotype. Glia 66:1395-1416.
Rosenbaum T, Simon SA (2007) TRPV1 Receptors and Signal Transduction. In: TRP Ion Channel Function in Sensory Transduction and Cellular Signaling Cascades (Liedtke WB, Heller S, eds). Boca Raton (FL).
Rosenthal A, Goeddel DV, Nguyen T, Lewis M, Shih A, Laramee GR, Nikolics K, Winslow JW (1990) Primary structure and biological activity of a novel human neurotrophic factor. Neuron 4:767-773.
Roux PP, Barker PA (2002) Neurotrophin signaling through the p75 neurotrophin receptor. Progress in neurobiology 67:203-233.
Roux PP, Colicos MA, Barker PA, Kennedy TE (1999) p75 neurotrophin receptor expression is induced in apoptotic neurons after seizure. The Journal of neuroscience : the official journal of the Society for Neuroscience 19:6887-6896.
Royce GJ, Bromley S, Gracco C, Beckstead RM (1989) Thalamocortical connections of the rostral intralaminar nuclei: an autoradiographic analysis in the cat. The Journal of comparative neurology 288:555-582.
Ruberti F, Capsoni S, Comparini A, Di Daniel E, Franzot J, Gonfloni S, Rossi G, Berardi N, Cattaneo A (2000) Phenotypic knockout of nerve growth factor in adult transgenic mice reveals severe deficits in basal forebrain cholinergic neurons, cell death in the spleen, and skeletal muscle dystrophy. The Journal of neuroscience : the official journal of the Society for Neuroscience 20:2589-2601.
Sabsovich I, Wei T, Guo TZ, Zhao R, Shi X, Li X, Yeomans DC, Klyukinov M, Kingery WS, Clark JD (2008) Effect of anti-NGF antibodies in a rat tibia fracture model of complex regional pain syndrome type I. Pain 138:47-60.
Sah P, Faber ES, Lopez De Armentia M, Power J (2003) The amygdaloid complex: anatomy and physiology. Physiological reviews 83:803-834.
Salomons TV, Iannetti GD, Liang M, Wood JN (2016) The "Pain Matrix" in Pain-Free Individuals. JAMA neurology 73:755-756.

Sandkuhler J (2000) Learning and memory in pain pathways. Pain 88:113-118.
Schwartz JP, Pearson J, Johnson EM (1982) Effect of exposure to anti-NGF on sensory neurons of adult rats and guinea pigs. Brain research 244:378-381.
Schwei MJ, Honore P, Rogers SD, Salak-Johnson JL, Finke MP, Ramnaraine ML, Clohisy DR, Mantyh PW (1999) Neurochemical and cellular reorganization of the spinal cord in a murine model of bone cancer pain. The Journal of neuroscience : the official journal of the Society for Neuroscience 19:10886-10897.
Scott A, Hasegawa H, Sakurai K, Yaron A, Cobb J, Wang F (2011) Transcription factor short stature homeobox 2 is required for proper development of tropomyosin-related kinase B-expressing mechanosensory neurons. The Journal of neuroscience : the official journal of the Society for Neuroscience 31:6741-6749.
Senger DL, Campenot RB (1997) Rapid retrograde tyrosine phosphorylation of trkA and other proteins in rat sympathetic neurons in compartmented cultures. The Journal of cell biology 138:411-421.
Sevcik MA, Ghilardi JR, Halvorson KG, Lindsay TH, Kubota K, Mantyh PW (2005) Analgesic efficacy of bradykinin B1 antagonists in a murine bone cancer pain model. The journal of pain : official journal of the American Pain Society 6:771-775.
Shackman AJ, Salomons TV, Slagter HA, Fox AS, Winter JJ, Davidson RJ (2011) The integration of negative affect, pain and cognitive control in the cingulate cortex. Nature reviews Neuroscience 12:154-167.
Shaikh SS, Nahorski MS, Woods CG (2018) A third HSAN5 mutation disrupts the nerve growth factor furin cleavage site. Molecular pain 14:1744806918809223.
Shao Y, Akmentin W, Toledo-Aral JJ, Rosenbaum J, Valdez G, Cabot JB, Hilbush BS, Halegoua S (2002) Pincher, a pinocytic chaperone for nerve growth factor/TrkA signaling endosomes. The Journal of cell biology 157:679-691.
Sharma N, Deppmann CD, Harrington AW, St Hillaire C, Chen ZY, Lee FS, Ginty DD (2010) Long-distance control of synapse assembly by target-derived NGF. Neuron 67:422-434.
Shboul M, Roschger P, Ganger R, Paschalis L, Rokidi S, Zandieh S, Behunova J, Muschitz C, Fahrleitner-Pammer A, Ng AYJ, Tohari S, Venkatesh B, Bonnard C, Reversade B, Klaushofer K, Al Kaissi A (2018) Bone matrix hypermineralization associated with low bone turnover in a case of Nasu-Hakola disease. Bone.
Shelton DL, Zeller J, Ho WH, Pons J, Rosenthal A (2005) Nerve growth factor mediates hyperalgesia and cachexia in auto-immune arthritis. Pain 116:8-16.
Sherrington CS (1906) The Integrative Action of the Nervous System. New York: Charles Scribner's Sons.
Shi C, Davis M (1999) Pain pathways involved in fear conditioning measured with fear-potentiated startle: lesion studies. The Journal of neuroscience : the official journal of the Society for Neuroscience 19:420-430.
Shu X, Mendell LM (1999) Nerve growth factor acutely sensitizes the response of adult rat sensory neurons to capsaicin. Neuroscience letters 274:159-162.
Shyu BC, Lin CY, Sun JJ, Sylantyev S, Chang C (2004) A method for direct thalamic stimulation in fMRI studies using a glass-coated carbon fiber electrode. Journal of neuroscience methods 137:123-131.
Silva BA, Mattucci C, Krzywkowski P, Murana E, Illarionova A, Grinevich V, Canteras NS, Ragozzino D, Gross CT (2013) Independent hypothalamic circuits for social and predator fear. Nature neuroscience 16:1731-1733.
Simons LE, Moulton EA, Linnman C, Carpino E, Becerra L, Borsook D (2014) The human amygdala and pain: evidence from neuroimaging. Human brain mapping 35:527-538.
Skaper SD (2001) Nerve growth factor: a neurokine orchestrating neuroimmune-endocrine functions. Molecular neurobiology 24:183-199.
Slaugenhaupt SA, Blumenfeld A, Gill SP, Leyne M, Mull J, Cuajungco MP, Liebert CB, Chadwick B, Idelson M, Reznik L, Robbins C, Makalowska I, Brownstein M, Krappmann D, Scheidereit C, Maayan C, Axelrod FB, Gusella JF (2001) Tissue-specific expression of a splicing mutation in the IKBKAP gene causes familial dysautonomia. American journal of human genetics 68:598-605.
Smeyne RJ, Klein R, Schnapp A, Long LK, Bryant S, Lewin A, Lira SA, Barbacid M (1994) Severe sensory and sympathetic neuropathies in mice carrying a disrupted Trk/NGF receptor gene. Nature 368:246-249.

Smith GD, Gunthorpe MJ, Kelsell RE, Hayes PD, Reilly P, Facer P, Wright JE, Jerman JC, Walhin JP, Ooi L, Egerton J, Charles KJ, Smart D, Randall AD, Anand P, Davis JB (2002) TRPV3 is a temperature-sensitive vanilloid receptor-like protein. Nature 418:186-190.

Sofroniew MV, Howe CL, Mobley WC (2001) Nerve growth factor signaling, neuroprotection, and neural repair. Annual review of neuroscience 24:1217-1281.

Sora I, Takahashi N, Funada M, Ujike H, Revay RS, Donovan DM, Miner LL, Uhl GR (1997) Opiate receptor knockout mice define mu receptor roles in endogenous nociceptive responses and morphine-induced analgesia. Proceedings of the National Academy of Sciences of the United States of America 94:1544-1549.

Sousa-Valente J, Calvo L, Vacca V, Simeoli R, Arevalo JC, Malcangio M (2018) Role of TrkA signalling and mast cells in the initiation of osteoarthritis pain in the monoiodoacetate model. Osteoarthritis and cartilage 26:84-94.

Story GM, Peier AM, Reeve AJ, Eid SR, Mosbacher J, Hricik TR, Earley TJ, Hergarden AC, Andersson DA, Hwang SW, McIntyre P, Jegla T, Bevan S, Patapoutian A (2003) ANKTM1, a TRP-like channel expressed in nociceptive neurons, is activated by cold temperatures. Cell 112:819-829.

Sung K, Ferrari LF, Yang W, Chung C, Zhao X, Gu Y, Lin S, Zhang K, Cui B, Pearn ML, Maloney MT, Mobley WC, Levine JD, Wu C (2018) Swedish Nerve Growth Factor Mutation (NGF(R100W)) Defines a Role for TrkA and p75(NTR) in Nociception. The Journal of neuroscience : the official journal of the Society for Neuroscience 38:3394-3413.

Suzuki M, Mizuno A, Kodaira K, Imai M (2003) Impaired pressure sensation in mice lacking TRPV4. The Journal of biological chemistry 278:22664-22668.

Svensson P, Cairns BE, Wang K, Arendt-Nielsen L (2003) Injection of nerve growth factor into human masseter muscle evokes long-lasting mechanical allodynia and hyperalgesia. Pain 104:241-247.

Szklarczyk D, Franceschini A, Wyder S, Forslund K, Heller D, Huerta-Cepas J, Simonovic M, Roth A, Santos A, Tsafou KP, Kuhn M, Bork P, Jensen LJ, von Mering C (2015) STRING v10: protein-protein interaction networks, integrated over the tree of life. Nucleic acids research 43:D447-452.

Tanaka Y, Niwa S, Dong M, Farkhondeh A, Wang L, Zhou R, Hirokawa N (2016) The Molecular Motor KIF1A Transports the TrkA Neurotrophin Receptor and Is Essential for Sensory Neuron Survival and Function. Neuron 90:1215-1229.

Taneda K, Tominaga M, Tengara S, Ogawa H, Takamori K (2010) Neurotropin inhibits both capsaicin-induced substance P release and nerve growth factor-induced neurite outgrowth in cultured rat dorsal root ganglion neurones. Clinical and experimental dermatology 35:73-77.

Tang HB, Inoue A, Oshita K, Nakata Y (2004) Sensitization of vanilloid receptor 1 induced by bradykinin via the activation of second messenger signaling cascades in rat primary afferent neurons. European journal of pharmacology 498:37-43.

Tang J, Ko S, Ding HK, Qiu CS, Calejesan AA, Zhuo M (2005) Pavlovian fear memory induced by activation in the anterior cingulate cortex. Molecular pain 1:6.

Testa G, Calvello M, Cattaneo A, Capsoni S (2019) Cholinergic striatal neurons are increased in HSAN V homozygous mice despite reduced NGF bioavailability. Biochemical and biophysical research communications 509:763-766.

Todd AJ (2010) Neuronal circuitry for pain processing in the dorsal horn. Nature reviews Neuroscience 11:823-836.

Tominaga M, Caterina MJ (2004) Thermosensation and pain. Journal of neurobiology 61:3-12.

Tominaga M, Numazaki M, Iida T, Tominaga T (2003) [Molecular mechanisms of nociception]. Nihon shinkei seishin yakurigaku zasshi = Japanese journal of psychopharmacology 23:139-147.

Tonra JR, Curtis R, Wong V, Cliffer KD, Park JS, Timmes A, Nguyen T, Lindsay RM, Acheson A, DiStefano PS (1998) Axotomy upregulates the anterograde transport and expression of brain-derived neurotrophic factor by sensory neurons. The Journal of neuroscience : the official journal of the Society for Neuroscience 18:4374-4383.

Torebjork HE, Lundberg LE, LaMotte RH (1992) Central changes in processing of mechanoreceptive input in capsaicin-induced secondary hyperalgesia in humans. The Journal of physiology 448:765-780.

Tracey I, Mantyh PW (2007) The cerebral signature for pain perception and its modulation. Neuron 55:377-391.

Treede RD (1995) Peripheral acute pain mechanisms. Annals of medicine 27:213-216.

Treede RD (2018) The International Association for the Study of Pain definition of pain: as valid in 2018 as in 1979, but in need of regularly updated footnotes. Pain reports 3:e643.

Treede RD, Meyer RA, Raja SN, Campbell JN (1992) Peripheral and central mechanisms of cutaneous hyperalgesia. Progress in neurobiology 38:397-421.

Treede RD, Jensen TS, Campbell JN, Cruccu G, Dostrovsky JO, Griffin JW, Hansson P, Hughes R, Nurmikko T, Serra J (2008) Neuropathic pain: redefinition and a grading system for clinical and research purposes. Neurology 70:1630-1635.

Ugolini G, Marinelli S, Covaceuszach S, Cattaneo A, Pavone F (2007) The function neutralizing anti-TrkA antibody MNAC13 reduces inflammatory and neuropathic pain. Proceedings of the National Academy of Sciences of the United States of America 104:2985-2990.

Usoskin D, Furlan A, Islam S, Abdo H, Lonnerberg P, Lou D, Hjerling-Leffler J, Haeggstrom J, Kharchenko O, Kharchenko PV, Linnarsson S, Ernfors P (2015) Unbiased classification of sensory neuron types by large-scale single-cell RNA sequencing. Nature neuroscience 18:145-153.

Vaccarino AL, Olson GA, Olson RD, Kastin AJ (1999) Endogenous opiates: 1998. Peptides 20:1527-1574.

Vaegter CB, Jansen P, Fjorback AW, Glerup S, Skeldal S, Kjolby M, Richner M, Erdmann B, Nyengaard JR, Tessarollo L, Lewin GR, Willnow TE, Chao MV, Nykjaer A (2011) Sortilin associates with Trk receptors to enhance anterograde transport and neurotrophin signaling. Nature neuroscience 14:54-61.

Valdes-Sanchez T, Kirstein M, Perez-Villalba A, Vega JA, Farinas I (2010) BDNF is essentially required for the early postnatal survival of nociceptors. Developmental biology 339:465-476.

Valet M, Sprenger T, Boecker H, Willoch F, Rummeny E, Conrad B, Erhard P, Tolle TR (2004) Distraction modulates connectivity of the cingulo-frontal cortex and the midbrain during pain--an fMRI analysis. Pain 109:399-408.

Van der Zee CE, Ross GM, Riopelle RJ, Hagg T (1996) Survival of cholinergic forebrain neurons in developing p75NGFR-deficient mice. Science 274:1729-1732.

Verhoeven K, De Jonghe P, Coen K, Verpoorten N, Auer-Grumbach M, Kwon JM, FitzPatrick D, Schmedding E, De Vriendt E, Jacobs A, Van Gerwen V, Wagner K, Hartung HP, Timmerman V (2003) Mutations in the small GTP-ase late endosomal protein RAB7 cause Charcot-Marie-Tooth type 2B neuropathy. American journal of human genetics 72:722-727.

Verpoorten N, De Jonghe P, Timmerman V (2006) Disease mechanisms in hereditary sensory and autonomic neuropathies. Neurobiology of disease 21:247-255.

Wager TD, Atlas LY, Lindquist MA, Roy M, Woo CW, Kross E (2013) An fMRI-based neurologic signature of physical pain. The New England journal of medicine 368:1388-1397.

Wang X, Berninger B, Poo M (1998) Localized synaptic actions of neurotrophin-4. The Journal of neuroscience : the official journal of the Society for Neuroscience 18:4985-4992.

Wang X, Ratnam J, Zou B, England PM, Basbaum AI (2009) TrkB signaling is required for both the induction and maintenance of tissue and nerve injury-induced persistent pain. The Journal of neuroscience : the official journal of the Society for Neuroscience 29:5508-5515.

Watanabe T, Ito T, Inoue G, Ohtori S, Kitajo K, Doya H, Takahashi K, Yamashita T (2008) The p75 receptor is associated with inflammatory thermal hypersensitivity. Journal of neuroscience research 86:3566-3574.

White FA, Silos-Santiago I, Molliver DC, Nishimura M, Phillips H, Barbacid M, Snider WD (1996) Synchronous onset of NGF and TrkA survival dependence in developing dorsal root ganglia. The Journal of neuroscience : the official journal of the Society for Neuroscience 16:4662-4672.

Williams KS, Killebrew DA, Clary GP, Seawell JA, Meeker RB (2015) Differential regulation of macrophage phenotype by mature and pro-nerve growth factor. Journal of neuroimmunology 285:76-93.

Winter J, Forbes CA, Sternberg J, Lindsay RM (1988) Nerve growth factor (NGF) regulates adult rat cultured dorsal root ganglion neuron responses to the excitotoxin capsaicin. Neuron 1:973-981.

Woo SH, Lukacs V, de Nooij JC, Zaytseva D, Criddle CR, Francisco A, Jessell TM, Wilkinson KA, Patapoutian A (2015) Piezo2 is the principal mechanotransduction channel for proprioception. Nature neuroscience 18:1756-1762.

Woolf CJ, Ma Q (2007) Nociceptors--noxious stimulus detectors. Neuron 55:353-364.

Woolf CJ, Ma QP, Allchorne A, Poole S (1996) Peripheral cell types contributing to the hyperalgesic action of nerve growth factor in inflammation. The Journal of neuroscience : the official journal of the Society for Neuroscience 16:2716-2723.

Woolf CJ, Safieh-Garabedian B, Ma QP, Crilly P, Winter J (1994) Nerve growth factor contributes to the generation of inflammatory sensory hypersensitivity. Neuroscience 62:327-331.

Wu Z, Nagata K, Iijima T (2002) Involvement of sensory nerves and immune cells in osteophyte formation in the ankle joint of adjuvant arthritic rats. Histochemistry and cell biology 118:213-220.

Xu H, Ramsey IS, Kotecha SA, Moran MM, Chong JA, Lawson D, Ge P, Lilly J, Silos-Santiago I, Xie Y, DiStefano PS, Curtis R, Clapham DE (2002) TRPV3 is a calcium-permeable temperature-sensitive cation channel. Nature 418:181-186.

Yamashita T, Tucker KL, Barde YA (1999) Neurotrophin binding to the p75 receptor modulates Rho activity and axonal outgrowth. Neuron 24:585-593.

Yano H, Torkin R, Martin LA, Chao MV, Teng KK (2009) Proneurotrophin-3 is a neuronal apoptotic ligand: evidence for retrograde-directed cell killing. The Journal of neuroscience : the official journal of the Society for Neuroscience 29:14790-14802.

Yano H, Lee FS, Kong H, Chuang J, Arevalo J, Perez P, Sung C, Chao MV (2001) Association of Trk neurotrophin receptors with components of the cytoplasmic dynein motor. The Journal of neuroscience : the official journal of the Society for Neuroscience 21:RC125.

Yoshikawa M, Senzaki K, Yokomizo T, Takahashi S, Ozaki S, Shiga T (2007) Runx1 selectively regulates cell fate specification and axonal projections of dorsal root ganglion neurons. Developmental biology 303:663-674.

Yu T, Calvo L, Anta B, Lopez-Benito S, Southon E, Chao MV, Tessarollo L, Arevalo JC (2011) Regulation of trafficking of activated TrkA is critical for NGF-mediated functions. Traffic 12:521-534.

Zahn PK, Subieta A, Park SS, Brennan TJ (2004) Effect of blockade of nerve growth factor and tumor necrosis factor on pain behaviors after plantar incision. The journal of pain : official journal of the American Pain Society 5:157-163.

Zhang F, Vadakkan KI, Kim SS, Wu LJ, Shang Y, Zhuo M (2008) Selective activation of microglia in spinal cord but not higher cortical regions following nerve injury in adult mouse. Molecular pain 4:15.

Zhang X, Huang J, McNaughton PA (2005) NGF rapidly increases membrane expression of TRPV1 heat-gated ion channels. The EMBO journal 24:4211-4223.

Zhang YH, Nicol GD (2004) NGF-mediated sensitization of the excitability of rat sensory neurons is prevented by a blocking antibody to the p75 neurotrophin receptor. Neuroscience letters 366:187-192.

Zimmerman A, Bai L, Ginty DD (2014) The gentle touch receptors of mammalian skin. Science 346:950-954.

Zimmermann K, Hein A, Hager U, Kaczmarek JS, Turnquist BP, Clapham DE, Reeh PW (2009) Phenotyping sensory nerve endings in vitro in the mouse. Nature protocols 4:174-196.

Zimmermann K, Leffler A, Babes A, Cendan CM, Carr RW, Kobayashi J, Nau C, Wood JN, Reeh PW (2007) Sensory neuron sodium channel Nav1.8 is essential for pain at low temperatures. Nature 447:855-858.

Zirlinger M, Lo L, McMahon J, McMahon AP, Anderson DJ (2002) Transient expression of the bHLH factor neurogenin-2 marks a subpopulation of neural crest cells biased for a sensory but not a neuronal fate. Proceedings of the National Academy of Sciences of the United States of America 99:8084-8089.

Zotterman Y (1939) Touch, pain and tickling: an electro-physiological investigation on cutaneous sensory nerves. The Journal of physiology 95:1-28.

Zubieta JK, Ketter TA, Bueller JA, Xu Y, Kilbourn MR, Young EA, Koeppe RA (2003) Regulation of human affective responses by anterior cingulate and limbic mu-opioid neurotransmission. Archives of general psychiatry 60:1145-1153.

Zylka MJ, Rice FL, Anderson DJ (2005) Topographically distinct epidermal nociceptive circuits revealed by axonal tracers targeted to Mrgprd. Neuron 45:17-25.